

DECOMPOSITION STUDIES OF OIL SHALE

by

Duane John Johnson

A Thesis submitted to the Faculty of the University
of Utah in Partial Fulfillment of the Requirements
For the Degree of

DOCTOR OF PHILOSOPHY

Department of Fuels Engineering

University of Utah
June, 1966

This Thesis for the Doctor of Philosophy Degree

by

Duane John Johnson

Has Been Approved
May, 1966

Chairman Supervisory Committee

Reader Supervisory Committee

Reader, Supervisory Committee

Reader, Supervisory Committee

Reader, Supervisory ~~C~~ommittee

Head, Fuels Engineering

Dean, Graduate School ✓

ACKNOWLEDGMENTS

I wish to express my gratitude to Dr. George Richard Hill for his advice and assistance on this work and throughout my graduate program.

Thanks are also extended to Dr. Larry Anderson for his suggestions on the manuscript.

Appreciation is especially expressed to Mr. J. L. Dougan for his financial assistance on this project and on my graduate studies.

I wish to thank Mr. Keith Dickson and Mr. Benjamin Hsieh for their gas chromatographic analytical work and Mr. Forrester Betts for his analyses of the shale oil.

My special thanks to my wife, Kathy, for her patience and understanding.

UNIVERSITY OF UTAH LIBRARIES

TABLE OF CONTENTS

	<u>Page</u>
ACKNOWLEDGMENTS	iii
LIST OF FIGURES	vii
LIST OF TABLES	ix
ABSTRACT	xi
INTRODUCTION	1
LITERATURE SURVEY	3
Nature of Oil Shale	3
Origin of Oil Shale	4
Inorganic Constituents	4
Nature of Kerogen	6
Nature of Shale Oil	6
Kinetics and Mechanism	7
SAMPLE INFORMATION	10
KINETIC STUDY AND BATCH STUDIES	10a
Equipment	10a
Experimental Procedure	12
Results and Discussion	14
First Order Kinetics	17
Zero Order Kinetics	26
General Kinetics and Mechanisms	28
Oil Quality and Yields	43
Pressure Effects	50
BATCH LOW PRESSURE STUDIES	52

TABLE OF CONTENTS (Continued)

	<u>Page</u>
Equipment	52
Experimental Procedure	52
Results and Discussion	53
Shales Very Rich in Kerogen	55
STUDY OF THE GAS COMPOSITION	59
Equipment	59
Procedure	59
Results and Discussion	60
Second Stage	68
FLOW STUDIES	70
Equipment for Low Pressure Flow Study	70
Experimental Procedure	71
Equipment for High Pressure Flow Study	72
Experimental Procedure	73
Results and Discussion for the Flow Experiments	74
Shale Oil Properties	83
Comparison of Low and High Pressure Flow Studies	85
Penetration of Heated Natural Gas Into Sample	87
Summary of Flow Tests	93
IN SITU STUDY	96
SUMMARY	100
Kinetics and Mechanisms	100

TABLE OF CONTENTS (Continued)

	<u>Page</u>
Natural Gas as a Heating Medium For Oil Shale	102
Effect of Heating Rate on Appearance of Oil	103
Oil Quality and Oil Yields	103
Nature of the Shale Oil.....	104
Effect of Water in the Retort	104
Rubberoid Stage in Kerogen Decomposition	104
LIST OF REFERENCES	105
APPENDIX	110
RESEARCH PROPOSALS	147
VITA	157

LIST OF FIGURES

<u>Figure</u>		<u>Page</u>
1	- (a) Photograph of equipment (b) Flow diagram of equipment	11
2	- Sample container and sample	13
3	- Volume of gas evolved versus time	15
4	- Volume of gas evolved versus time	16
4a	- Volume of gas evolved versus time	16a
5	- Gas evolution curve and difference curve	18
6	- $\ln \frac{a}{a-x}$ versus time	20
7	- $\ln \frac{a}{a-x}$ versus time	21
8	- $\ln \frac{a}{a-x}$ versus time	22
9	- Arrhenius plot for first order decomposition in temperature range of 331-427°C	24
10	- Arrhenius plot for zero order decomposition in temperature range 331-427°C	27
11	- Oil shale kerogen decomposition	35
12	- Volume of gas evolved versus time for 331°C	46
13	- Chromatograms (a) of shale oil (b) of shale oil with standards added	48
14	- Percent carbon dioxide in product gas versus temperature	62
15	- Percent hydrogen sulfide in product gas versus temperature	63

LIST OF FIGURES (Continued)

<u>Figure</u>		<u>Page</u>
16	- Percent methane in product gas versus temperature	64
17	- Percent ethane in product gas versus temperature	64
18	- Percent propane in product gas versus temperature	65
19	- Mass spectrographic peak height for hydrogen versus temperature	66
20	- Retort and sample temperatures versus time	78
21	- Retort and sample temperatures versus time	79
22	- Oil yield versus time	81
23	- Unheated oil shale. Photomicrograph taken parallel to main drill core axis	89
24	- Heated oil shale. Photomicrograph taken parallel to main drill core axis	90
25	- Unheated oil shale. Photomicrograph taken perpen- dicular to main drill core axis	91
26	- Heated oil shale. Photomicrograph taken perpendicular to main drill core axis	92
27	- Chromatograms (a) of shale oil (b) of shale oil with standards added	98
28	- Chromatograms (a) of Pennsylvania petroleum and shale oil mixture (b) of Pennsylvania petroleum	99

LIST OF TABLES

<u>Table</u>	<u>Page</u>
1	Calculated Mineral Composition of a 28-Gallon-Per-Ton Green River Oil Shale 5
2	Activation Energies of Decomposition of Oil Shale 29
3	Activation Energies for the Appearance of Products From the Data of Hubbard and Robinson 30
4	Bitumen Concentrations When Bitumen Reaches Maximum . . . 32
5	Energies of Decomposition of Oil Shale Kerogen 36
6	Effect of Temperature on Oil Quality 40
7	Properties of Crude Shale Oils from Various Processes . . 41
8	Effect of Temperature on Oil and Gas Yields 45
9	Effect of Pressure on Oil Yield and Quality 51
10	Effect of Temperature and Pressure on Oil Yield and Quality 54
11	Temperature Effect on Gas Yield, Product Gas Analysis, Gas Heating Value 61
12	Effect of Temperature on Yield of Oil 75
13	Effect of Natural Gas Flow Rate on Heating Rate 76
14	Effect of Heating Rates on Temperature of Oil Appearance . 82
15	Effect of Temperature on Shale Oil Properties 83
16	Comparative Oil Yields and Qualities for the Flow Tests . 86
17	Porosity and Permeability of Oil Shale 88
18	Shale Oil Analyses 97
19	Properties of Crude Shale Oils 97

LIST OF TABLES (Continued)

<u>Table</u>		<u>Page</u>
20	U. S. Bureau of Mines Fischer Assay Results	111
21	Data From D-OS Series of Experiments	112
22	Gas Sample Analysis	116
23	Gas Evolution Kinetic Data	117
24	Data for B-OS Series of Experiments	130
25	Gas Analysis for C-OS Experiments	132
26	Data For Flow Studies	134
27	Yield Data For Flow Studies	135
28	Properties of Oil Samples	137

ABSTRACT

A kinetic study was made on the decomposition of oil shale kerogen. This was done by heating the sample in a closed retort and monitoring the gaseous products of decomposition.

Based on the kinetic study and also on the information made available by earlier investigators a new two step model for kerogen pyrolysis was proposed which more adequately fits all the evidence.

A series of batch and flow studies were made to determine if heated natural gas could be successfully used to bring about decomposition of kerogen. The effects of temperature, pressure, heating rate, and natural gas flow rate were also determined.

It was found that heated natural gas could be used to produce adequate quantities of a high API gravity, low pour point oil. The treatment of the oil shale with heated natural gas caused a considerable increase in the porosity and permeability of the sample and therefore opened the underlying material for thermal treatment. The use of a higher heating rate caused a delay in the appearance of the oil. High natural gas flow rates resulted in increased oil yields and an increase in the quality of the oil. The effect of high pressures was to promote extensive polymerization. The product oils were found to be primarily paraffinic in nature and were low in sulfur, nitrogen, and oxygen.

INTRODUCTION

There has been a considerable amount of investigation into the kinetics and mechanisms of oil shale decomposition and into the effects of various experimental parameters on the nature of the product oils.

There is a need, however, for further kinetic study of Colorado oil shales. Also the methods used by most of the past investigators place considerable doubt on the validity of their kinetic interpretations.

Studies of the in situ method of retorting oil shale have been carried out for many years but a method suggested by Mr. J. L. Dougan, the use of heated natural gas in an in situ decomposition is untested.

The purpose of the study reported in this thesis was two-fold. First an attempt was made to learn more about the basic nature of the pyrolysis of oil shale kerogen. There were indications that the kinetic and mechanistic treatments given to the decomposition of oil shale by early investigators did not fit the actual situation. A re-examination of the kinetics of kerogen decomposition by monitoring the gaseous products as a function of time was attempted. Also it was hoped that a model could be proposed which would better explain the data collected by earlier investigators.

Secondly, the intent was to learn more about the parameters involved in the in situ removal of kerogen from oil shale using natural gas as the heating medium. In the in situ method the heating medium is directed into the oil shale bed and its sensible heat is utilized to bring the bed to the decomposition temperature of the kerogen. Part of the organic material is broken away from the parent structure and removed in the gas phase. The purpose of this phase of the research was to

design several groups of experiments whereby the effects of pressure, temperature, heating rate, and natural gas flow rate on the decomposition of oil shale kerogen and the nature of the products could be determined. It was hoped that by studying the effects of the various parameters operating conditions for the in situ process could be suggested.

LITERATURE SURVEY

Nature of Oil Shale

The oil shale utilized in this study was essentially an organic rich Marlestone from the Green River formation in western Colorado.

In its natural state the "oil" in oil shale is a high molecular weight organic solid called kerogen and the "shale" matrix is a mixture of inorganic carbonates, clays, and other minor constituents. Due to the heterogeneous nature of oil shale its classification is necessarily somewhat arbitrary. It is generally agreed, however, that a material may be termed an oil shale when the rock base is compact and of sedimentary origin, the kerogen yields a liquid hydrocarbon when thermally decomposed, and only negligible quantities of kerogen are extracted from the rock with common solvents for petroleum.

Throughout this paper the term oil shale will be used in its general sense, that is, a mixture of kerogen and shale-like rock which satisfies the above criteria. The term kerogen will be used to denote the organic material in the rock as it occurs naturally and shale oil will be used to denote the liquid hydrocarbon produced when the rock is distilled. The term bitumen will be used to designate the heavy solid or semi-solid hydrocarbon which forms in the oil shale early in the heating stage and is soluble in the common solvents for petroleum, such as benzene. The gaseous products of the thermal decomposition of oil shale are those products which do not condense to a liquid in a dry ice/acetone bath.

Origin of Oil Shale

It is generally believed that oil shale is the result of a process beginning with the deposition of primarily vegetable matter, together with silt and mud, at the bottom of shallow fresh or saline lakes, followed by the decay of the organic constituents as initial compaction takes place, and concluding with the complete lithification of the inorganic sediment (51,10,21,27,58,56,38,8,53).

More specifically, kerogen probably owes its origin to the fatty acids contained in algae, the decay of which produced free acids. The process of decay and the overburden pressure raised the temperature of the mixture and brought about polymerization of the free or partly free acids. Heat and pressure, resulting from the subsequent sandstone overburden, brought about expulsion of excess water, elimination of oxygen in the form of carbon dioxide (by decarboxylation), and molecular rearrangements. This formed a more rigid high polymer and resulted in further lithification (51,60,10,21).

Oxygen, and probably to a lesser extent sulfur, possibly acted as a linking agent between polymer molecules. Nitrogen and sulfur probably originated in the protein matter of the algae and were imprisoned during polymerization. Additional sources of nitrogen were most likely the various species of marine, animal, and bird life, the remains of insects, and the spores of fungus and higher plant life often found in the formation (51,10,30,7).

Inorganic Constituents

The inorganic content of oil shales is generally 20-50 per cent carbonates, 20-40 per cent silicate

and other trace minerals. Table 1 shows a breakdown of the inorganic matter in a typical shale.

Table 1⁽¹⁶⁾

Calculated Mineral Composition of a 28-Gallon-Per-Ton
Green River oil shale.

<u>Mineral</u>	<u>Formula</u>	<u>Weight %</u>
Dolomite	$(\text{CaMg})(\text{CO}_3)_2$	33
Calcite	CaCO_3	20
Plagioclase	$\text{NaAlSi}_3\text{O}_8$ and $\text{CaAl}_2\text{Si}_2\text{O}_8$	12
Illite	$\text{K}_2\text{O} \cdot 3\text{Al}_2\text{O}_3 \cdot 6\text{SiO}_2 \cdot 2\text{H}_2\text{O}$	11
Quartz	SiO_2	10
Analcite	$\text{NaAlSi}_2\text{O}_6 \cdot \text{H}_2\text{O}$	7
Orthoclase	KAlSi_3O_8	4
Iron	Fe	2
Pyrite (or marcasite)	FeS_2	1
Total		100 %

Nature of Kerogen

Probably the most widely accepted theory as to the nature of the kerogen "molecule" is essentially that of Jones and Dickert⁽³⁹⁾. They propose a kerogen molecule that is polymer weighing well above 3000. It is highly naphthenic, with aromatics, and nitrogen and sulfur heterocyclic ring systems randomly distributed throughout and closely associated with the naphthenes.

The hydrocarbons are present primarily as saturated ring systems directly connected or separated only by means of short alkyl groups. Short alkyl groups also are substituted on these rings. The aromatic rings amount to no more than 10% of the hydrocarbon structures, and prefer bonding to naphthenes rather than paraffins.

Twenty to thirty per cent of the hydrocarbon material is paraffinic, predominately isoparaffinic, and approaching saturated isoprene in structure.

Nature of Shale Oil

The composition of shale oil is a direct function of the process by which it was obtained. Variables such as temperature, rate of heating, pressure, the atmosphere surrounding the oil shale, the solvent used in solvent extraction, the residence time of the shale oil vapors in the retort cell have an effect on the nature of the oil produced from the oil shale. Robinson and Stanfield⁽⁵³⁾ have given a summary of studies into the type of materials found in shale oils derived in various ways.

In general shale oils are mixtures of paraffins, olefins, diolefins, naphthenes and some aromatics. The olefins are probably

predominantly straight chain, and a loss of hydrogen during retorting.

causes an increase in the aromaticity of the material over that of the parent kerogen molecule.

Kinetics and Mechanism

Prior to 1931 it was thought that the direct products of oil shale pyrolysis were shale oil, spent shale, and gases. In 1913 Engler⁽²²⁾ recognized that heating oil shale changed its solubility in organic solvents and therefore the simple one-stage decomposition must be incorrect.

McKee and Lyder⁽⁴⁷⁾ proposed that kerogen, rather than decomposing to form petroleum-like materials as the primary decomposition products, gave a heavy solid or semi-solid bitumen as an intermediate step to the formation of the oil and gas. The oil and gas were formed by thermal cracking of the bitumen. They placed a sharp limit on the temperature of decomposition of kerogen, between 400°C and 410°C.

Franks and Goodier⁽²⁴⁾ discovered that McKee and Lyder's temperature for kerogen decomposition (400-410°C) was in error and that primary bitumen could be produced at 300°C. Cane⁽¹¹⁾ demonstrated that measurable torbanite decomposition occurred at 200°C.

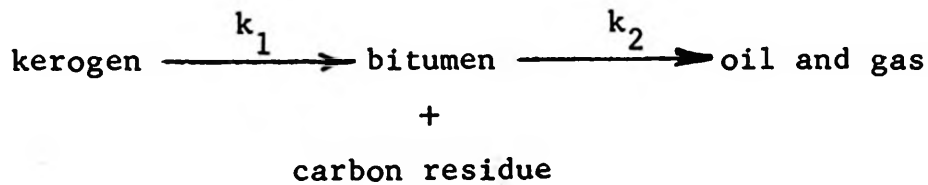
In 1923 Zimmerly⁽⁶⁷⁾ studied the rate of formation of bitumen in closed tubes over the range of 275°-365°C (527° to 668°F). The material studied was an oil shale from Soldier Summit, Utah, having a yield of 40 gallons/ton of shale. He found that the formation of bitumen was first order in relation to the initial kerogen concentration. The transformation of kerogen to bitumen did not begin at a definite temperature.

Hubbard and Robinson⁽³⁴⁾ studied the kinetics of decomposition of Colorado oil shales having Fischer assays of 26.7, 52.6, and 75.0 gallon per ton over the temperature range of 350° to 525°C (662° to 977°F) by heating samples of ground shale in a tubular electric furnace for varying lengths of time in a helium atmosphere and extracting the samples with dry benzene. This work suggested a first order mechanism which could best be explained by two different Arrhenius equations, depending upon the temperature range employed.

Diricco and Barrick⁽¹⁹⁾ studied the decomposition kinetics of a Colorado oil shale bearing 24.2 gallons per ton of oil. They conducted their experiments in the pressure range of from 50 to 625 mm. of Hg and concluded that the pressure had no effect on the rate of reaction. In the range 250° - 465°C (482° - 867°F) they found the kerogen decomposition to be first order.

Allred⁽¹⁾ used a thermogravimetric method in which the weight loss of the heated sample was determined directly using a sensitive weighing device. He used a temperature range of 176° - 704°C (350 - 1300°F) and a Colorado oil shale having a Fischer assay of 26.7 gallons per ton. He found that the rate determining reaction did not follow simple first order kinetics but was better fit by a "logistic" function and that "the weight fraction of the total kerogen appearing as bitumen plus oil and gas becomes constant at the time the bitumen concentration reaches a maximum." This means that little or no carbonaceous matter is formed after that time and that all of the kerogen has been converted to bitumen, gas, and carbonaceous residue.

Based on those conclusions he proposed the following mechanism:



The rate determining step up to 900°F was the bitumen decomposition.

He divided the reaction kinetics into three segments. The first was identified by k_x and corresponded to the portion of the reaction up to the point at which the products were fifty per cent formed. The activation energy for this portion he found to be 13.6 kcal/gm-mole in the temperature range of 477-616°C.

The second segment covered the portion of the reaction from the point where the products were about fifty per cent formed to the portion where $\ln\left(\frac{1-R}{R}\right) \approx \ln(1-R)$. He designated this region by the rate constant k_2 and he found three separate slopes of his Arrhenius plot. The activation energies for the three were 40.5 kcal/gm-mole from 429-277°C (this portion he determined using the data of Hubbard and Robinson), 25.8 kcal/gm-mole from 477 to 531°C, and 13.6 kcal/gm-mole from 531 to 616°C.

The final portion in which $\ln\left(\frac{1-R}{R}\right) \approx \ln(1-R)$, and which he designated by the rate constant k_3 , gave an activation energy of 4.58 kcal/gm-mole from 566 to 616°C.

SAMPLE INFORMATION

The oil shale used in this investigation consisted of a series of drill-core samples supplied by Equity Oil Company and taken from their properties on Sulfur Creek in the Piceance Creek Basin of Colorado.

All of the drill cores were split along their major axis into two or three segments. One of the segments at each drill core depth was assayed by the United States Bureau of Mines Petroleum Center at Laramie, Wyoming, using the modified Fischer Retort method.

In the modified Fischer Retort method the sample is ground to -8 mesh and 50 to 100 grams are placed in a cast aluminum retort fitted with several aluminum plates. The plates and sample are in several alternating layers. The sample is then heated to $500 \pm 10^{\circ}\text{C}$ in about forty minutes. The retort is then held at 500°C until retorting is completed; usually about sixty minutes is all the time required.

The results of the Fischer assays are listed in Table 20, Appendix A along with the series and experiment in which the individual samples were used. The analyses consisted of the weight percentages of oil, water, residue, and gas plus losses produced as each sample was heated.

The samples were crushed and sized as described in the individual sections discussing the materials and procedures used in each series of experiments.

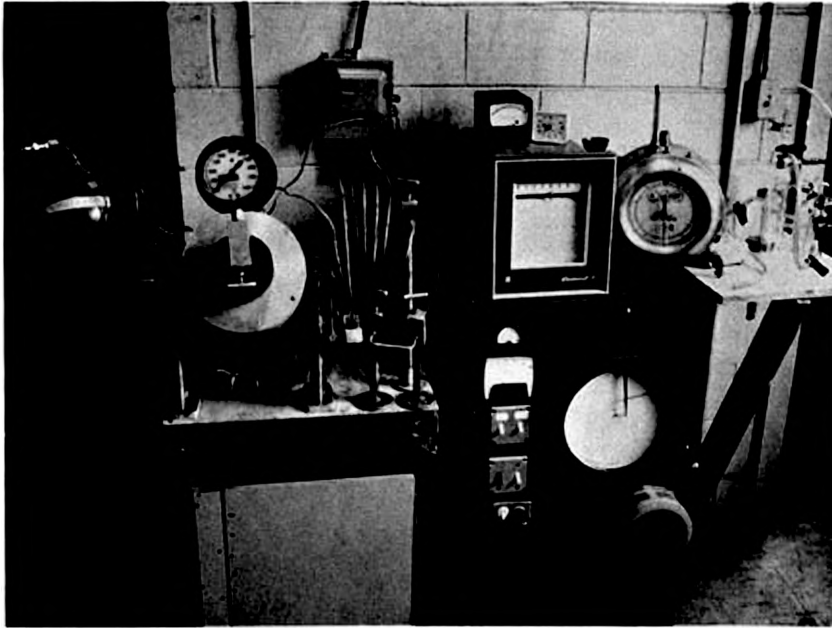
KINETIC STUDY AND BATCH STUDIES

Equipment

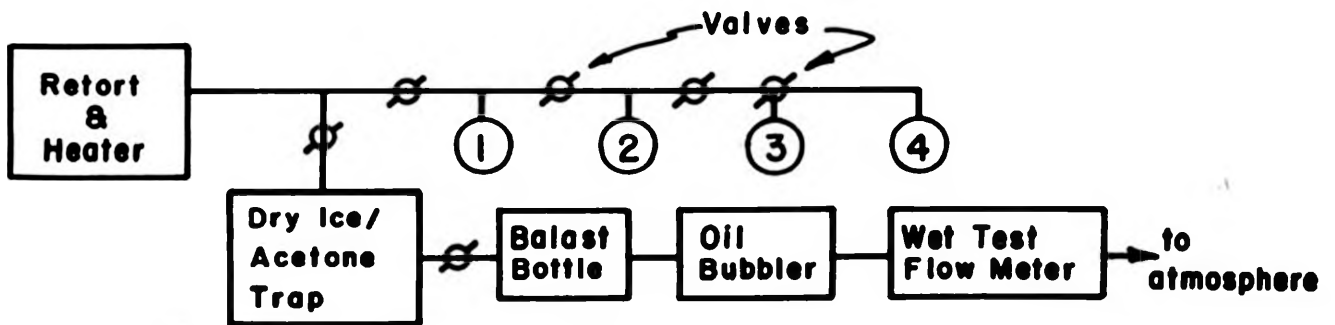
In the kinetic study a Parr model 4011 high pressure rocker-type bomb equipped with an external heating jacket was fitted with a short exit tube to allow a continuous monitoring of the off-gases and collection of oil. Although the study was carried out at atmospheric pressure the high pressure autoclave was employed in order to accomodate several experiments requiring a closed retort capable of withstanding high internal pressures.

The retort was connected in series with a dry ice-acetone cold-finger type liquid trap and a wet-test gas flow meter. Their relative positions are shown in Figure 1. The helium and vacuum lines were used in cleansing the retort of air prior to each run and in taking gas samples. They were installed in such a way that both the retort and gas sampling flasks could be flushed with helium and then evacuated, flushed with helium again, etc.

Thermocouples in the heater jacket were connected to a Sym-Ply-Trol temperature controller. The controller was used in conjunction with a variable transformer and a mercury relay and allowed temperature control within $\pm 3^{\circ}\text{C}$ and temperature accuracy within $\pm 5^{\circ}\text{C}$. There was some temperature gradient from the bottom to the top of the retort, with the bottom of the retort (the thermocouple location) being approximately 100°C higher in temperature than the outside retort cap and the gas exit stem. The top of the sample column was about six inches below the level of the exit stem, but there is no doubt that the top of the sample column was at a slightly lower temperature than at the bottom. The effect of this will be explored in a later section.



(a)



1. Pressure Gauge
2. Gas Sampling Port
3. Inlet for Gas Atmospheres
4. Vacuum Pump

(b)

Figure 1. (a) Photograph of equipment (b) Flow diagram of equipment

Experimental Procedure

The kinetic series of experiments was identified by the designation D-OS- and the index number identified the particular experiment in the series.

The core samples used in the experiments were hand crushed with a hammer and cold chisel. The particles utilized were randomly chosen from those fragments passing through a 1.05 inch mesh screen and remaining on a .525 inch mesh screen.

The sample material was placed in a glass liner with a side vent and a ground glass cap as shown in Figure 2. The liner was then placed in the retort, the retort cap was sealed, and the entire assembly was fitted into the retort jacket heater.

The retort was brought up to temperature as quickly as possible and the evolution of gas was monitored with a wet-test flow meter which indicated the total gas volume passing through it. The atmospheric pressure and gas flow meter temperature were recorded and the gas volume was corrected to standard conditions.

In order that a material balance could be kept the following items were weighed during the course of each run:

1. the glass liner (empty)
2. the glass liner plus the sample
3. the glass liner plus the residue remaining at the end of the run
4. the cold-finger trap (empty)
5. the cold-finger trap after the liquids were collected

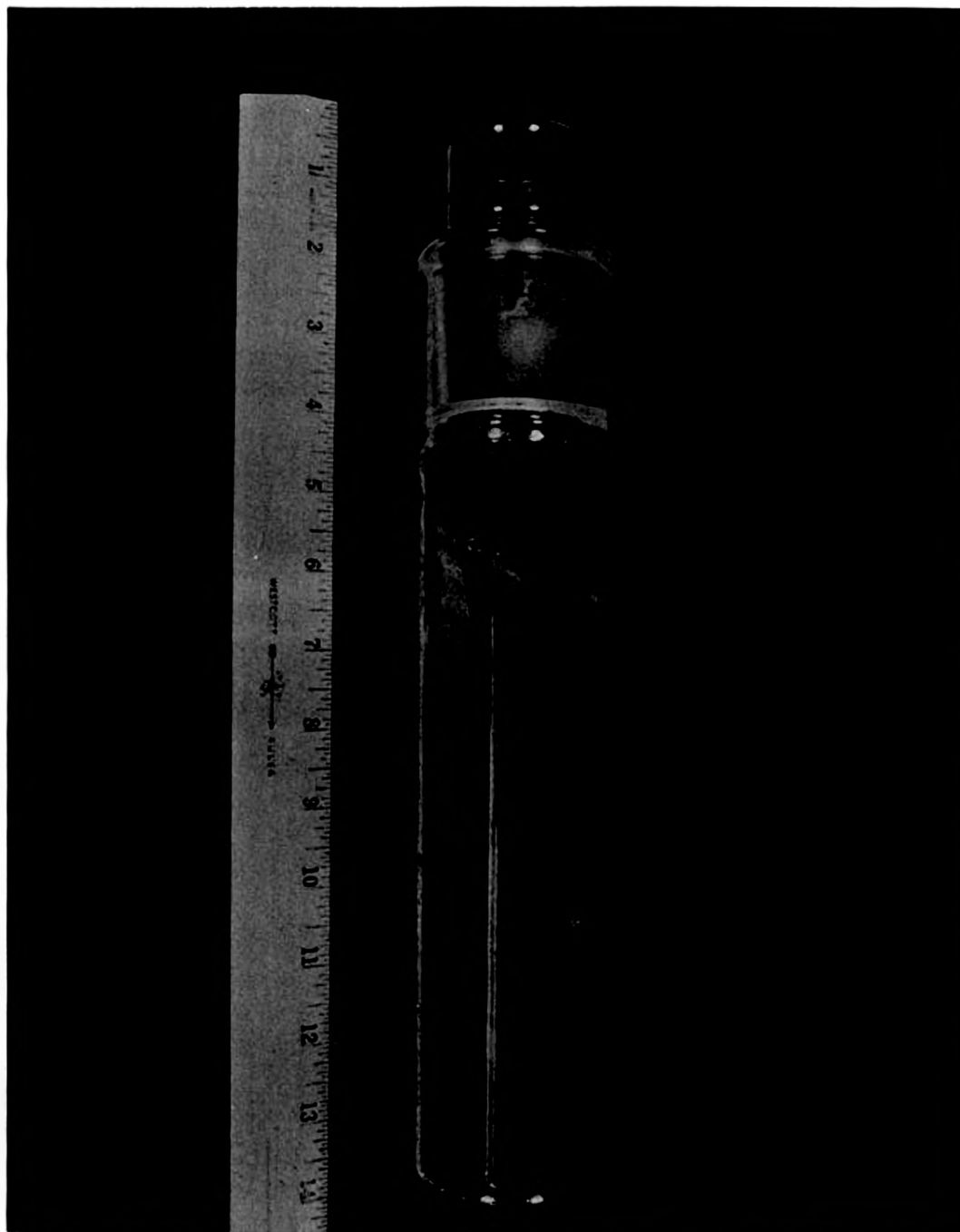


Figure 2. Sample container and sample

The weight of gas plus loss was determined by difference using the experimental data for the amount of residue and liquids collected. All liquids and gases were measured volumetrically and the oils were tested for specific gravity, API gravity, and pour points according to standard ASTM methods.

Results and Discussion

The data are summarized in Tables 21-23, Appendix A. The total gas evolved as a function of time in the respective experiments is given in Figures 3 - 4a. In each case the total volume of gas evolved at any time, t , was corrected to standard temperature and pressure and normalized by dividing by the original sample weight.

In Figures 3 - 4a it was assumed that the zero order part of the reaction contributed to the entire gas evolution curve and that the zero order portion of the curve (the linear portion) would have extended back until it intercepted the ordinate at $t = 0$ if it were not obscured by the non-linear portion of the curve. Therefore the zero order contribution to the non-linear part of the experimental curve had to be removed before a kinetic treatment of this part could be attempted.

The zero order contribution to the non-linear part of the gas evolution curve was accounted for by extrapolating the final, linear part of the curve until it intersected the ordinate at $t = 0$. The zero order curve was then deducted from the experimental gas evolution curve and the resultant curve was used as the data curve for kinetic calculations. This resultant curve was called the difference curve.

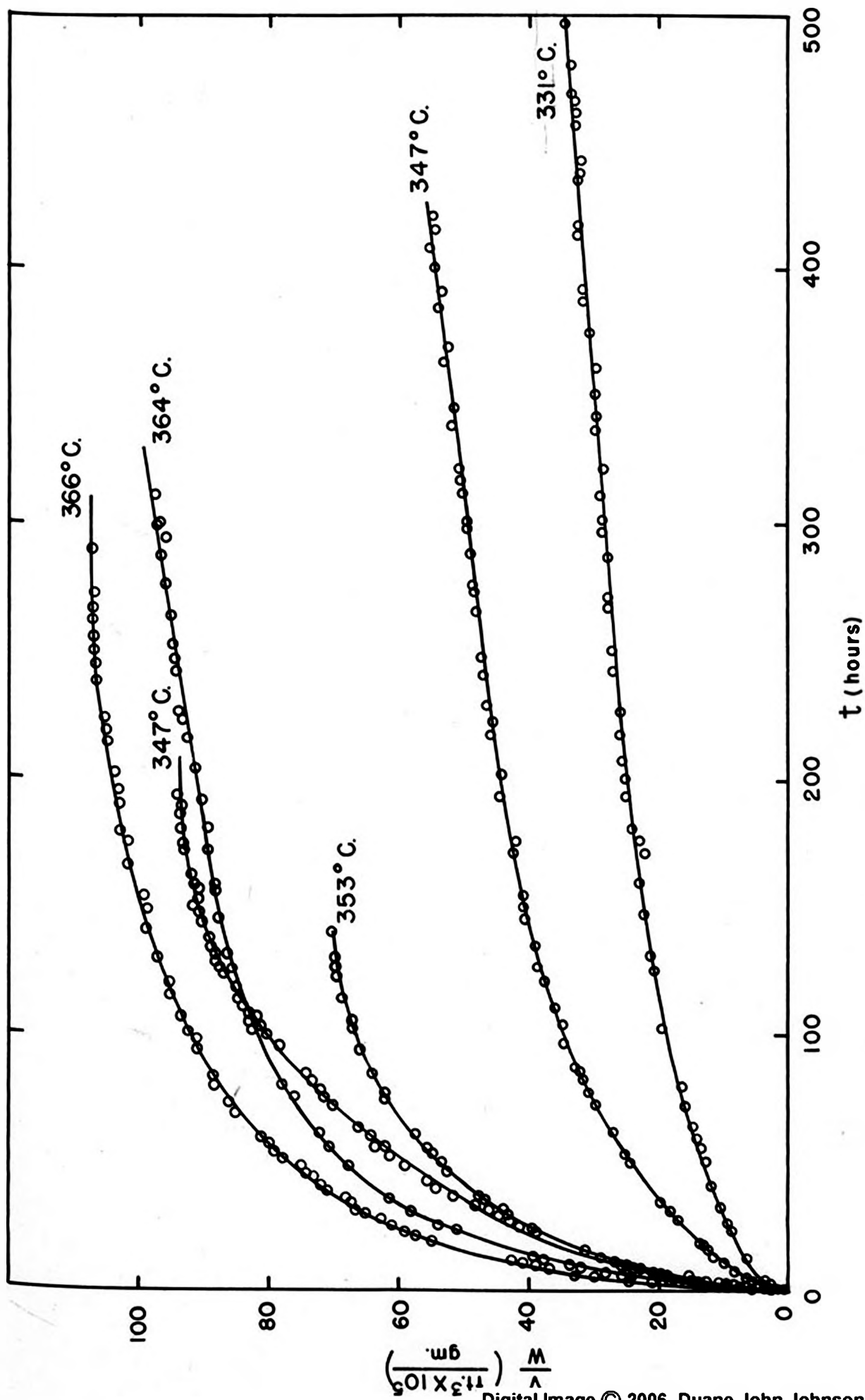


Figure 3. Volume of gas evolved verses time.

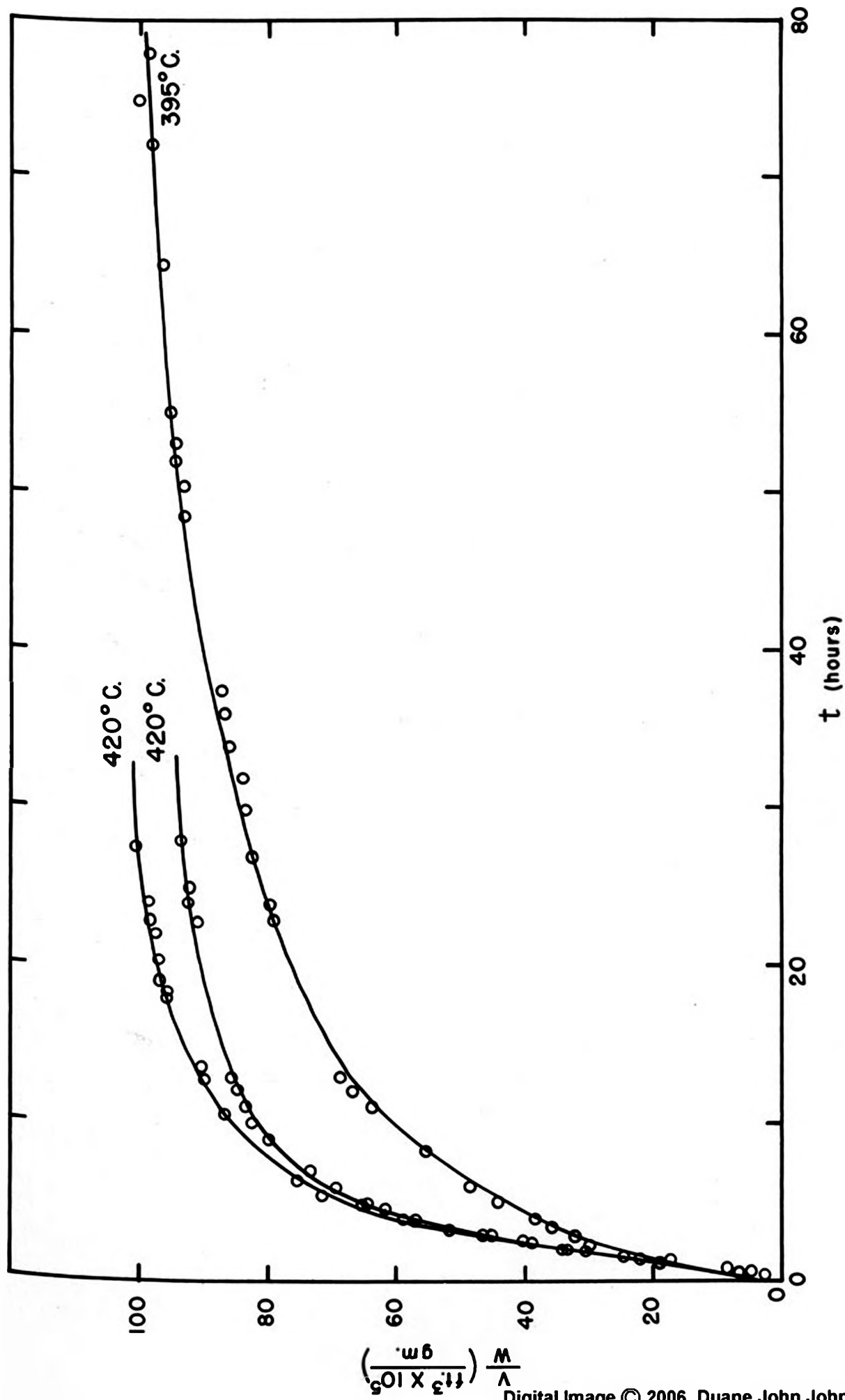


Figure 4. Volume of gas evolved verses time.

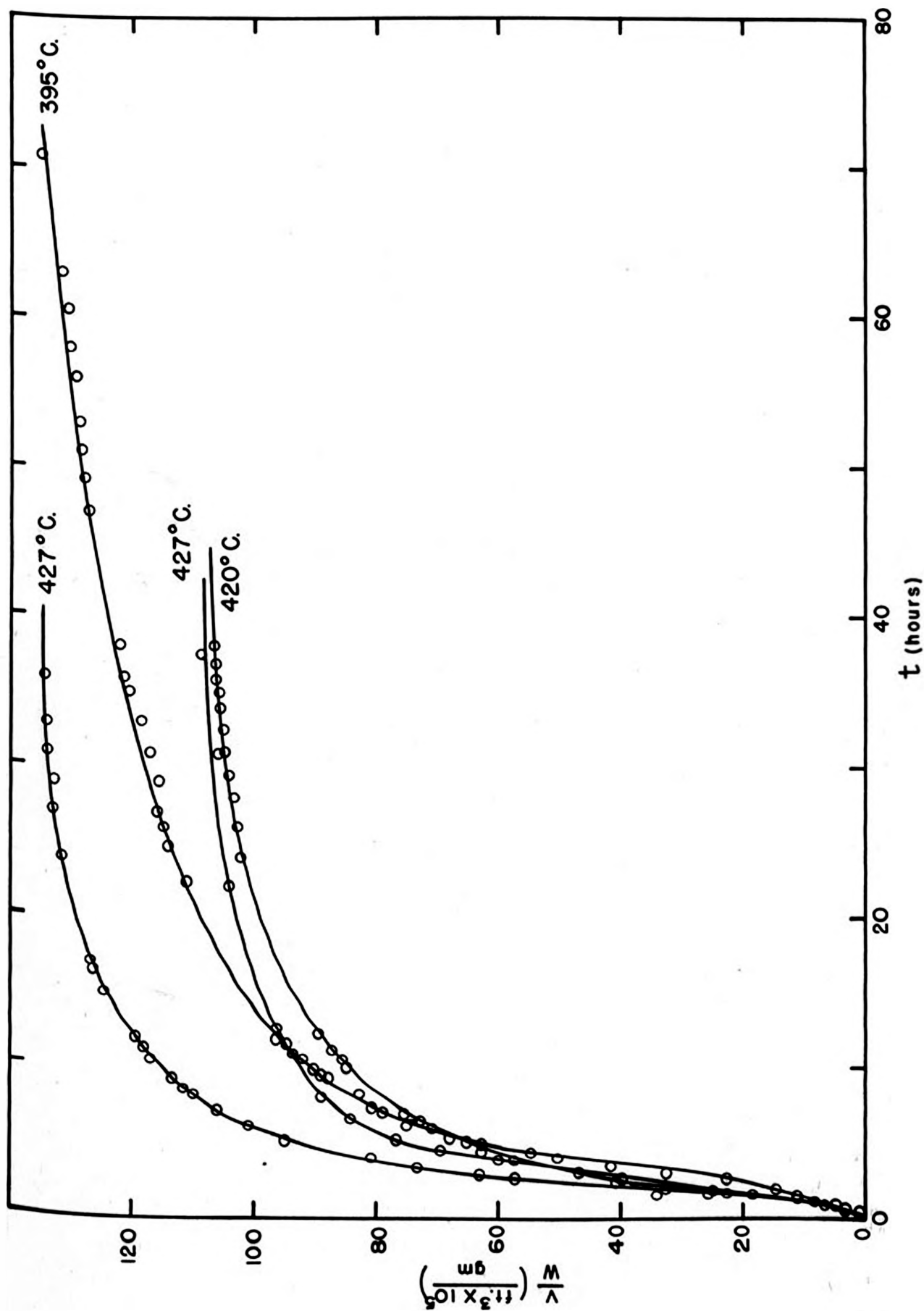


Figure 4a. Volume of gas evolved verses time.

When the slope of the difference curve became zero the distance along the ordinate at that point was called a , the initial concentration of the gas-producing species in the kerogen. When the kerogen was decomposed these species remained in the gas phase after passing through the cold finger trap. The symbol a , therefore, corresponded to the total volume of gas which was evolved at the point where the decomposition became completely zero order minus the zero order contribution at that point.

In Figure 5 is reproduced the experimental curve for D-OS-22 showing the zero order portion of the curve extrapolated to $t = 0$ and the difference curve resulting when the zero order contribution to the curve was deducted.

First Order Kinetics

For a reaction of the n^{th} order the general differential equation is defined as:

$$\frac{dx}{dt} = k(a-x)^n$$

where k is the rate constant, t is the time, n is the over-all order of the reaction, a is the initial concentration of the species in question, and x is the fraction of the species reacted at any time, t .

If a decomposition were to follow first order kinetics $n = 1$ and the general expression for the rate of appearance of the products is

$$\frac{dx}{dt} = k(a-x)$$

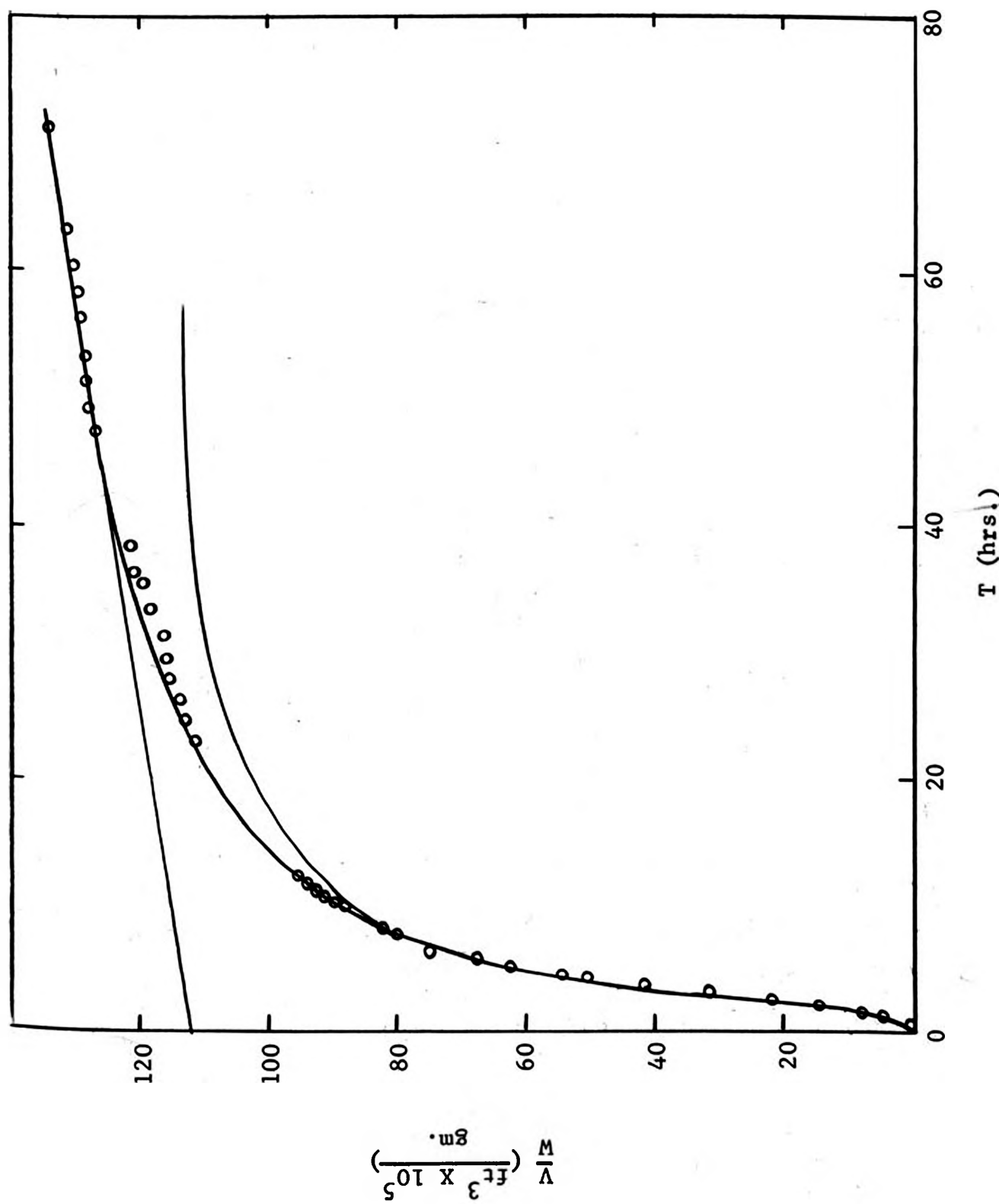


Figure 5. Gas evolution curve and difference curve
for 395°C

In the study of the decomposition of kerogen by monitoring the off-gases rather than the loss in weight of the oil shale sample "a" becomes the total amount of non-condensable gas evolved in the first order part of the reaction, x becomes the volume of gas evolved at any time t, and a-x becomes the unreacted portion of the species which produces the off-gases. The units for both a and x are cubic feet of evolved gas per gram of sample and t is in hours.

In the integrated form the first order expression for the appearance of the gaseous products becomes:

$$\ln(a-x) = -kt + \text{const}$$

when $t = 0$, $x = 0$ and the constant becomes $\ln a$. The final integrated forms of the equation then are:

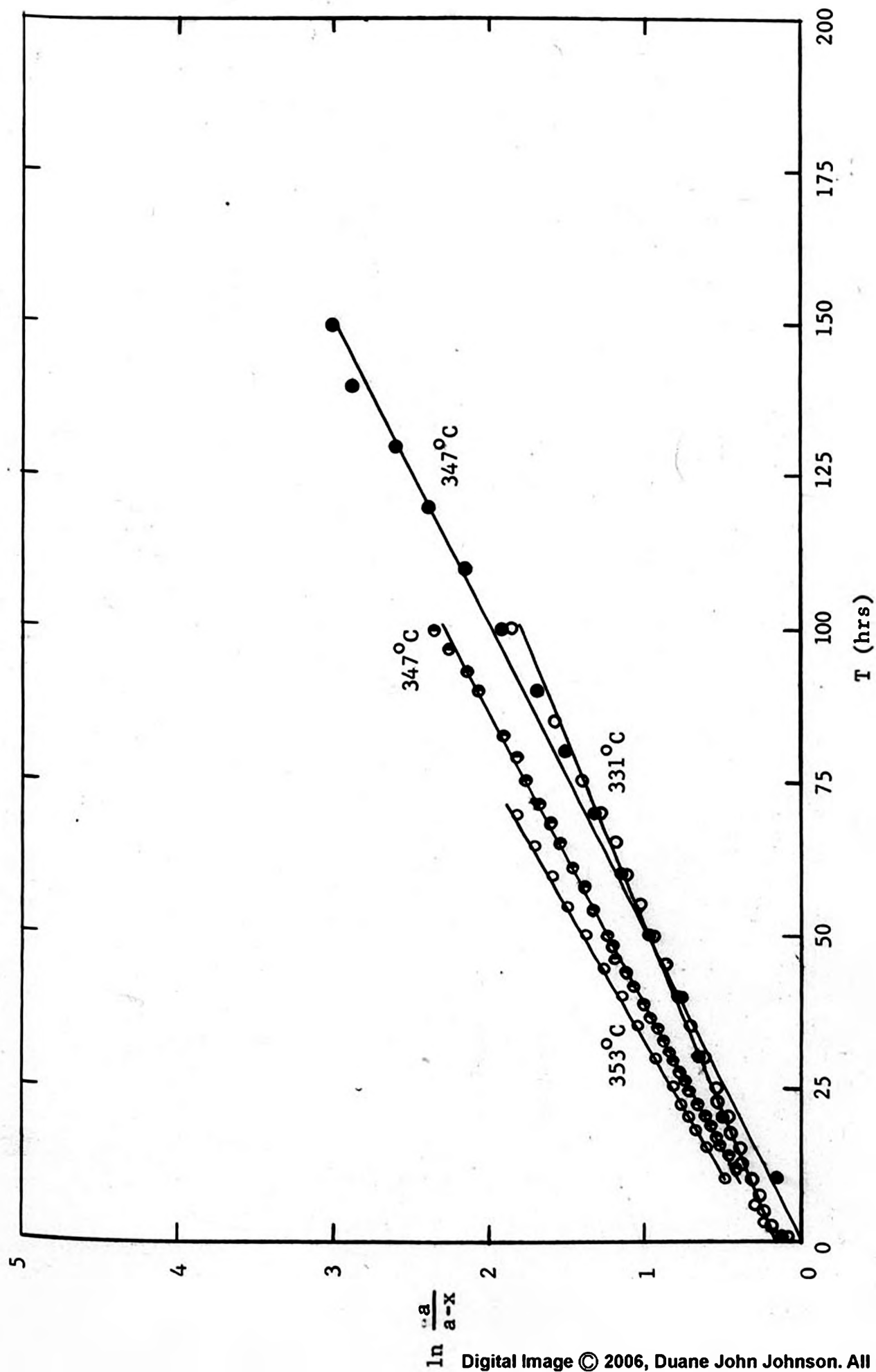
$$\ln\left(\frac{a}{a-x}\right) = kt$$

or

$$x = a(1 - e^{-kt})$$

If first order kinetics were obeyed a straight line should result when $\ln \frac{a}{a-x}$ is plotted against t. In Figures 6-8 the $\ln\left(\frac{a}{a-x}\right)$ was plotted against t for the experimental data, i.e. for the difference curves.

The least squares lines through the points representing each temperature showed good linearity resulting from a first order treatment of the data. The deviations from linearity appeared in the initial induction period and in the period when the decomposition was changing from the initial reaction to the final or zero order reaction. The

Figure 6. $\ln \frac{a}{a-x}$ versus time

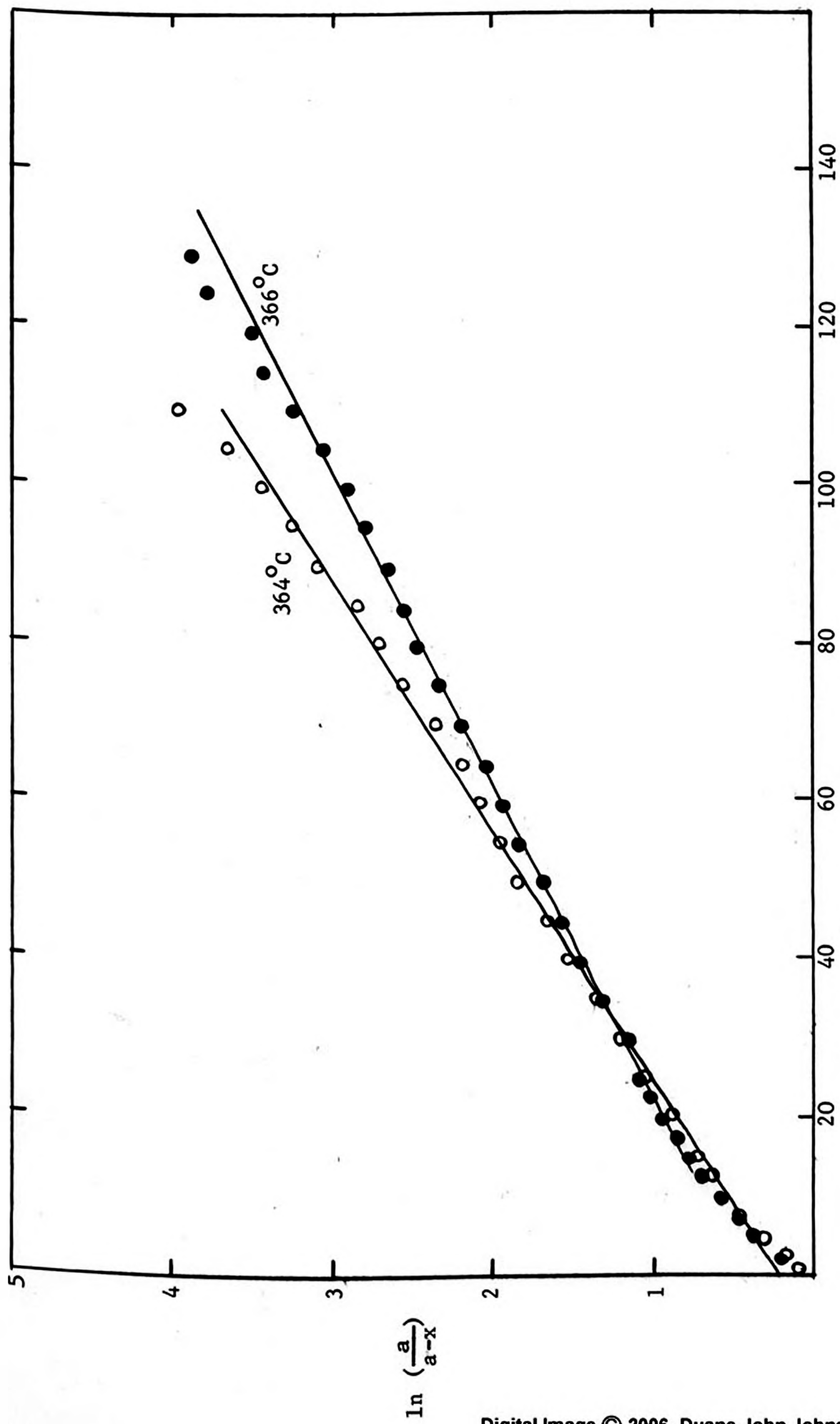


Figure 7. $\ln\left(\frac{a}{a-x}\right)$ versus time

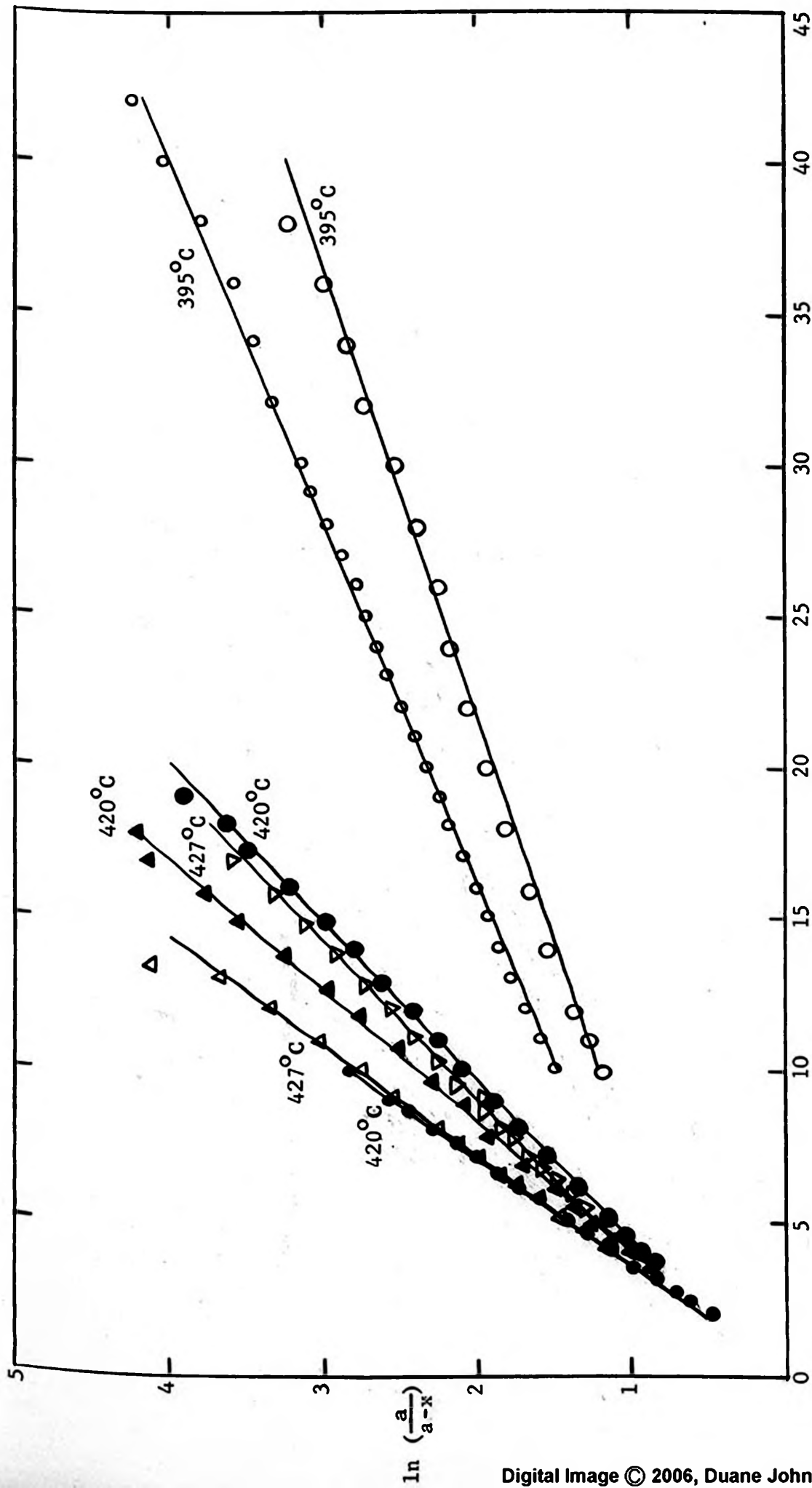


Figure 8. $\ln\left(\frac{a}{a-x}\right)$ versus time

slopes of the lines in Figure 6-8 will be defined as k_1 , or the rate constant for that portion of the decomposition reaction which follows first order kinetics.

For valid first order kinetics the line representing the plot of $\ln\left(\frac{a}{a-x}\right)$ vs. time should pass through the origin. The experimental first order plots all passed through the ordinate at a positive value, with one, D-OS-15, having a slightly negative intercept. The experimental first order plots all showed an initial induction period where linearity was not obeyed. It became more prolonged and pronounced as the temperature increased. The length of this region at the higher temperatures may be some indication that an additional reaction mechanism was becoming recognizable at about 375-390°C and becoming more important as the temperature was raised. There were not sufficient data available here to treat this region rigorously, however, and a more careful examination of the induction period and/or initial reaction must come at a later date.

The least squares determination of the best straight line was applied only to those points after the induction period which satisfied visual linearity. Therefore, the points comprising the induction period were not considered and the origin of the line actually was shifted to that point where linearity began.

The Arrhenius plot for the first order segment of the reaction is given in Figure 9. There was some scatter but a least squares line could be drawn without difficulty. The equation for the best line representing the experimental data was:

$$\ln k = \frac{-13,093}{T^{\circ}\text{K}} + 17.228$$

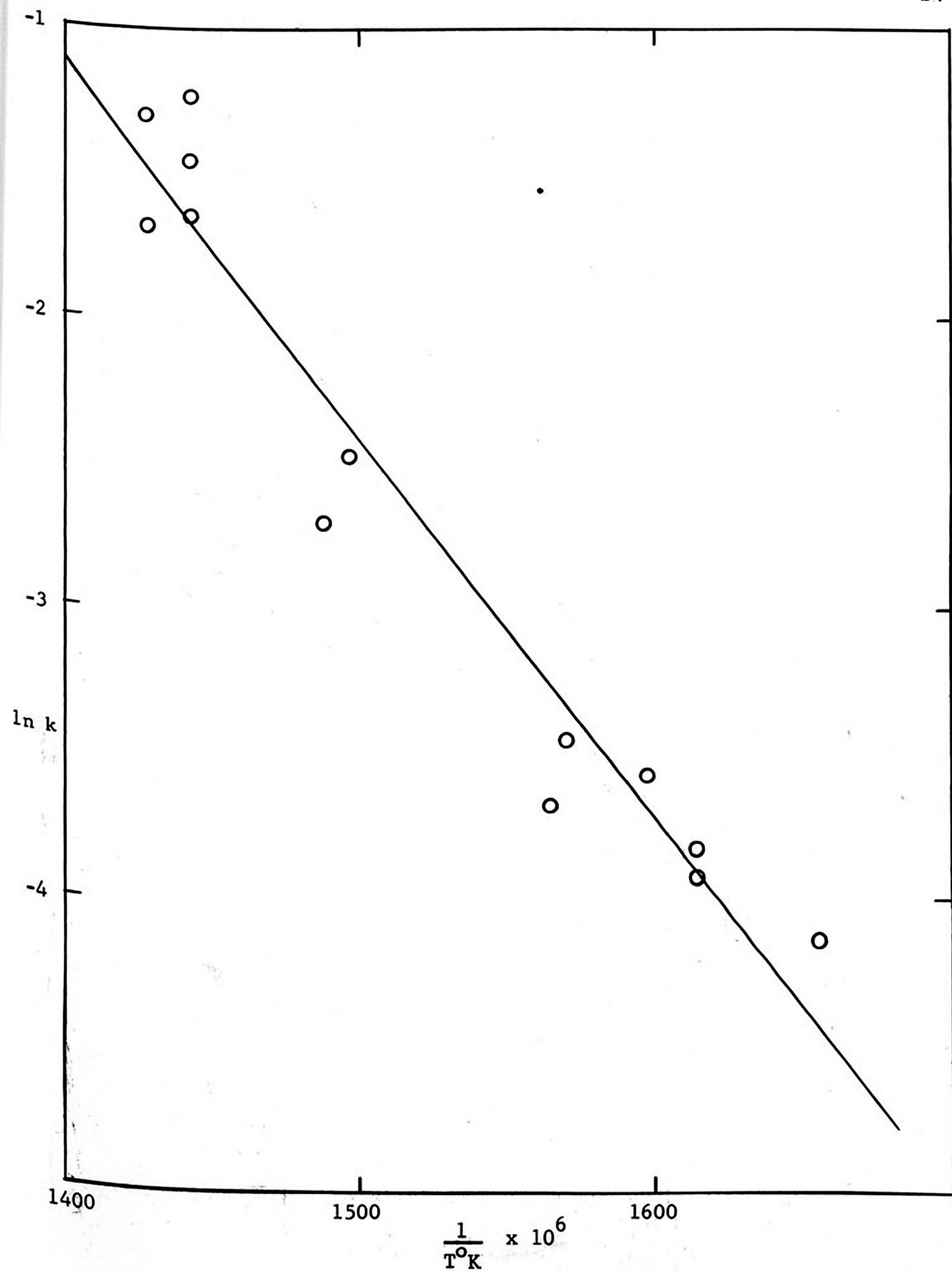


Figure 9. Arrhenius plot for first order decomposition in

where k is the rate constant and T is the temperature in degrees Kelvin. The activation energy was 26.2 kcal/gm-mole of oil shale. An Eyring plot of the k values gave an enthalpy of 24.9 kcal/gm-mole of oil shale.

Several of the gas evolution curves in Figures 3-4a are completely out of place when compared to the others. One of the curves at 347°C, and one at 395°C do not appear to fit into the series of curves.

An examination of Figures 6-8 suggests several additional conclusions. The $\ln\left(\frac{a}{a-x}\right)$ versus time plots for 331°C and the lower one for 347°C cross at about 45 hours. This should not take place in the normal situation. The line for 366°C also passes through those for 353 and 364°C.

The differences in slopes for the curves at 364 and 366°C are greater than either differs from that at 353°C. In several cases the slopes of the plots at 427 and 420°C show better agreement than do the two lines for 427°C. The slopes for the 366°C and one of the 347°C plots are nearly identical.

It is doubtful if the temperatures could have been in error to such a degree as to bring about the above inconsistencies. As reported earlier the accuracy of the temperatures measurements was at least $\pm 5^\circ\text{C}$.

It is more likely that either the heterogeneous nature of the oil shale samples or an inherent weakness in the method of monitoring the volume of off gases was responsible for the scatter of the data. There was not sufficient sample available from any single location so it was necessary to use samples taken from Digital Image © 2006, Duane John Johnson. All rights reserved.

same oil shale bed. Samples having the same content of organic matter were chosen, the assumption being that they would exhibit identical behavior when heated. Perhaps this assumption is invalid and two oil shales with identical values for the kerogen content can exhibit widely differing rates of gas evolution.

Zero Order Kinetics

The final portion of the gas evolution curve was linear, thus demonstrating no dependence of reaction rate upon the concentration of unreacted species. The Arrhenius plot for this portion is given in Figure 10. There is again a good deal of scatter but a straight line definition of the points is not unreasonable. The equation of the best line through the points was:

$$\ln k = \frac{-10,416}{T^{\circ}\text{K}} + 13.876$$

where k is the rate constant at T , the temperature in degrees Kelvin. The activation energy was 20.8 kcal/gm-mole of oil shale and the enthalpy of activation was 19.4 kcal/gm-mole.

When this kinetic study was initiated the two step mechanism proposed by McKee and Lyder was assumed to be correct and the intermediate product in the kerogen pyrolysis reaction, the bitumen, was assumed to be in a steady state in the temperature range studied. As is pointed out in the discussion following, the intermediate product was not in a steady state and also a new mechanism for the second step in the pyrolysis was needed. As a result the values for the activation

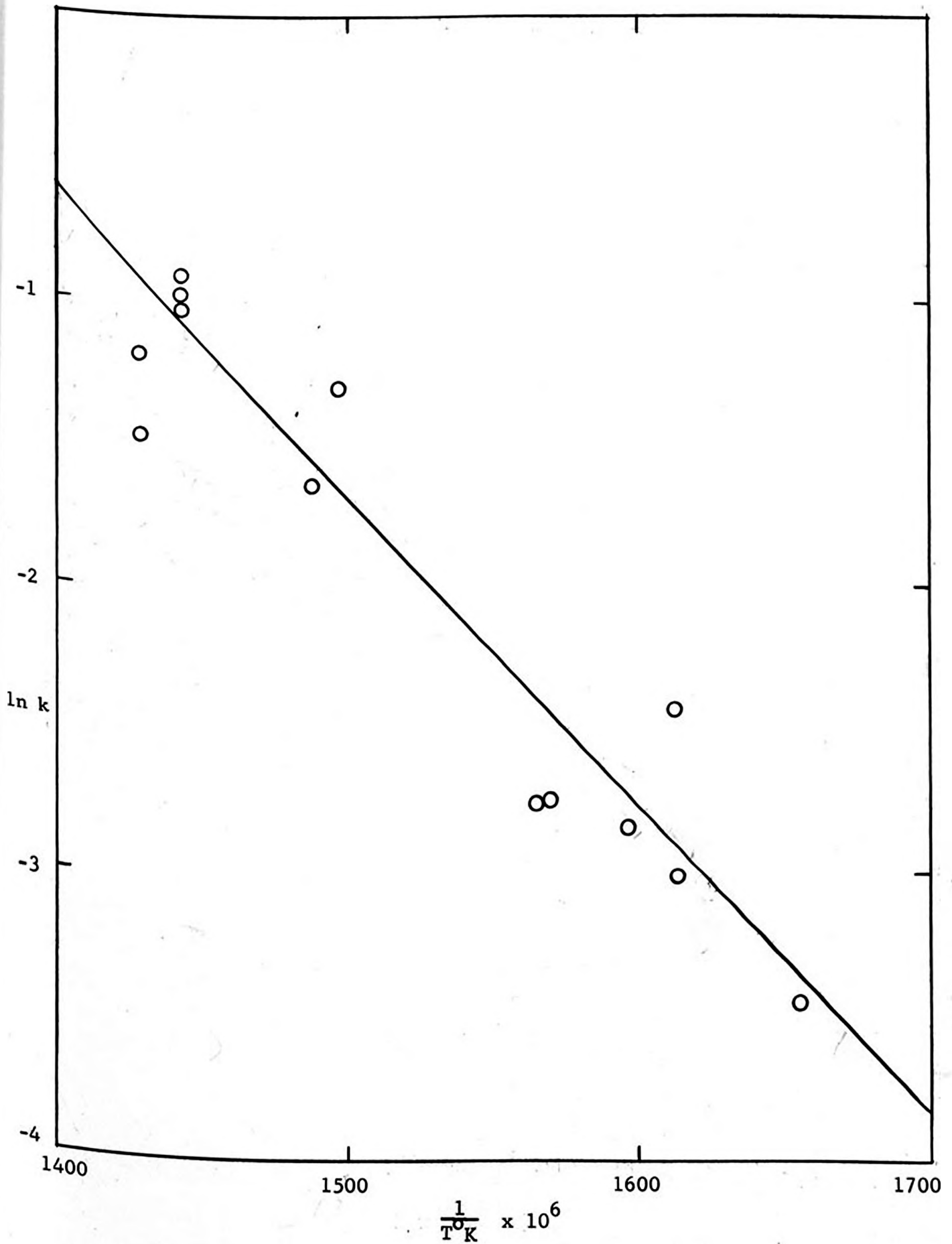


Figure 10. Arrhenius plot for zero order decomposition in temperature range 331-427°C

energies as determined in the kinetic study done by the monitoring of the off-gases were invalid. There was also some doubt as to the accuracy of kinetic data as was discussed earlier.

The data and the results were included, however, and in Table 5 the resultant activation energy of the first order portion of the reaction was compared with the activation energy derived from a treatment of Hubbard and Robinson's data in the same manner.

General Kinetics and Mechanisms

At the present time the mechanism for oil shale pyrolysis which was first suggested by McKee and Lyder is considered the definitive one. In this mechanism the kerogen does not decompose directly to the final products of oil, gas, and coke, but first passes through an intermediate called bitumen. The kerogen is insoluble in common organic solvents for petroleum, but the bitumen is readily soluble. The mechanism is commonly written in equation form;



The kinetic studies to date have generally been done by following the increase in weight of oil, gas, and bitumen as a function of time. The first order kinetics concluded by the various investigators must therefore be an overall order for the entire reaction.

In Table 2 the results of the kinetic work on oil shale to date are given.

Table 2

Activation Energies of Decomposition of Oil Shale

<u>Author</u>	<u>R</u>	<u>Temp. Range °C</u>	<u>Ea kcal/gm-mole</u>
Zimmerly (67)	bitumen	275-365	41.7
Cane (12)	bitumen + gas + oil	350-400	48.5
Diricco (19)	bitumen + gas + oil	250-465	45.5
Hubbard and Robinson (34)	bitumen + gas + oil	350-437	62.4
		437-525	25.3
Allred (1)*	oil + gas	477-531	25.8
	oil + gas	531-616	k_2 13.6
	oil + gas	477-616	k_x 13.6
	oil + gas	566-616	k_3
Allred, using Hubbard's data	oil + gas	429-477	k_2 40.5

$$* \ln\left(\frac{1-R}{R}\right) = -kt, \text{ all others } \ln(1-R) = -kt; \text{ where } R = \frac{x}{\text{kerogen}}$$

If the weights of the gas, oil, and bitumen products which were given by Hubbard and Robinson (34) for a 26.7 gal/ton oil shale are substituted for R in the equation $\ln(1-R) = -kt$ for various temperatures some interesting results are obtained. A straight line can be drawn through the data points in each case and Table 3 gives the resulting activation energies. P in each case represents the

weight of product divided by the weight of initial kerogen. The temperature range given is that over which the $\ln(1-R)$ vs. kt plot is linear.

Table 3

Activation Energies for the Appearance of Products
from the data of Hubbard and Robinson⁽³⁴⁾

R	Temperature Range °C	Ea kcal/gm-mole
bitumen	400 - 475	40.0
oil	400 - 475	36.0
gas	400 - 525	21.8
oil + gas	350 - 450 (52.6 gal/ton)	46.2
oil + gas	450 - 525	27.0
oil + gas	400 - 450 (26.7 gal/ton)	42.4
oil + gas	475 - 525	19.0

Hubbard and Robinson plotted the weight percentages of gas, oil, and bitumen produced in the thermal decomposition of oil shale as a function of time⁽³⁴⁾. As pointed out by Allred the concentration

of oil plus gas produced, when the bitumen reaches its maximum, is equal to about 50 percent of the total oil plus gas yield. It is also apparent that at the bitumen maxima the amount of bitumen formed is equal to the amount decomposing.

If Zimmerly's Arrhenius plot is used the specific reaction rate constants for the production of bitumen can be predicted for any temperature within the temperature range used. The rate constants can then be used to determine the amount of bitumen present at any time.

This was done using the temperatures chosen by Hubbard and Robinson for their kinetic study. In each case the time chosen was the time when their bitumen yield curves reached the maximum. Therefore the concentrations predicted were the amounts of bitumen that should have appeared at the times Hubbard and Robinson found their maximum bitumen concentrations. The results are shown in Table 4. The difference between the predicted values and those of Hubbard and Robinson are the fraction of bitumen which has decomposed up to that time.

When the information in Tables 2 through 4 is examined several conclusions can be drawn.

First of all, Table 4 indicates that at the time when the maximum bitumen concentration is formed at each temperature there is a considerable time lag before the bitumen that has formed decomposes into products. As shown in column 4 of Table 4 the major part of the bitumen has been formed at the time when the bitumen maximum appears in Hubbard's concentration curves, but after that time 50 per cent or more of the products of the bitumen decomposition are still to be formed. This

Table 4

Bitumen Concentrations When Bitumen Reaches Maximum

Temp.	k	Time For Bitumen To Reach Maximum	Theoretical Bitumen at Maximum	Actual Bitumen at Maximum	R Remaining at Maximum	R' Decomposed at Maximum
400°C	.944/hr	70 min	71.4%	22%	31%	69
425°C	2.8	20	61.3	37	60	39
450°C	8.11	11	77.4	33	43	57
475°C	21.4	6.5	90.2	33	37	63
500°C	52.5	4.5	98.4	27	27	71

R is percentage of theoretical bitumen formed at maximum which still remains.

R' is percentage of theoretical bitumen which has decomposed.

suggests that the decomposition of bitumen into its products is the kinetic slow step, although the order of magnitude of this step is not much smaller than that of the bitumen formation.

Zimmerly has done an excellent job of determining the activation energy of the first step in the pyrolysis of kerogen, namely the decomposition of kerogen into bitumen. Table 2 shows his activation energy of 42 kcal/gm-mole for a first order process from 275 - 365°C and Table 3 shows that Hubbard and Robinson's data give an energy of 40 kcal/gm-mole in the range of 400 - 475°C.

In their kinetic studies at temperatures 475 - 500°C the earlier investigators all utilized the weight of gas + oil + bitumen as their R denoting the amount of weight loss of kerogen. This would be meaningful if they were following a single process but the information above indicates that they did not have steady state conditions. They were measuring the formation of both the intermediate and end products of a two step consecutive reaction.

A better approach would have been to choose a temperature at which the bitumen formation was complete and monitor the gas and oil weight loss after that time. This would allow the determination of the rate constants for the second stage of the process, namely the decomposition of bitumen into gaseous and liquid products.

By choosing a temperature range of 477 - 615°C (and 427 - 477°C from Hubbard's data) Allred essentially eliminated the first step in the kerogen pyrolysis, the formation of the bitumen. The rate constants which represented that portion of the bitumen decomposition which occurred after the bitumen maxima were reached he identified as $k_{..}$.

As was mentioned earlier the bitumen maximum was the point at which $(1-R/R) \approx 1$ and Table 4 shows that at that point virtually all of the bitumen has been formed in the temperature range used by Allred.

At this point it is apparent that a new mechanism is needed to explain the energies obtained in past investigations and the new evidence representing the work of Allred and additional treatment of Hubbard's data.

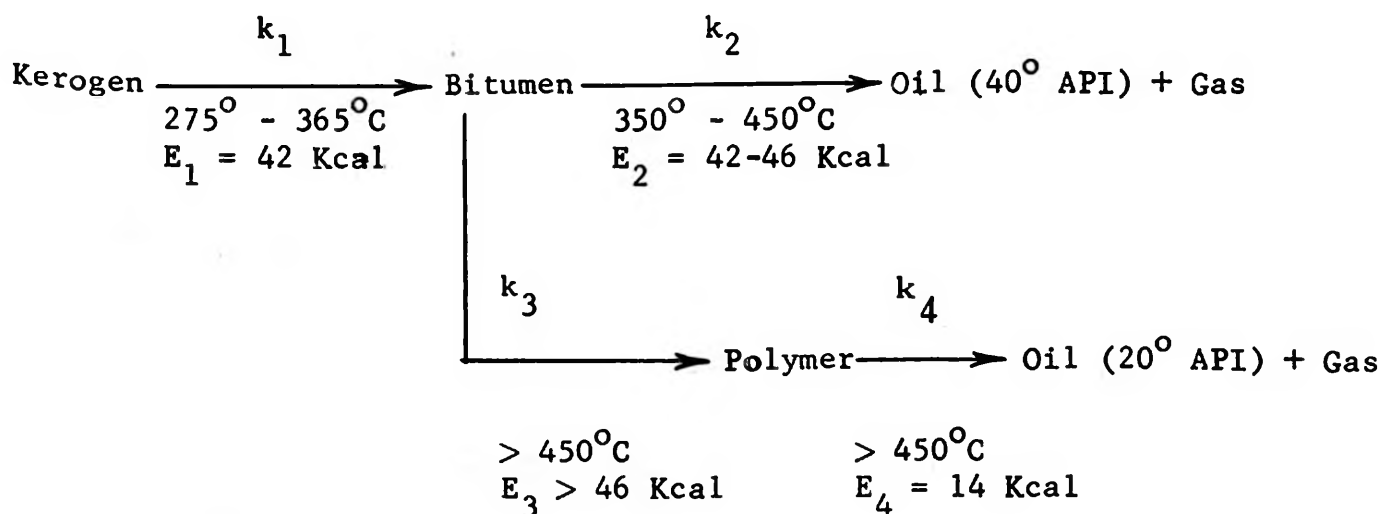
Figure 11 shows a dual path model which more adequately fits all the evidence to date. The rate constants k_1 , k_2 , k_3 , and k_4 are used to designate the various steps and the energy and temperature range of each step are given also.

Table 5 lists the activation energies as determined by the various investigators. They are grouped according to the temperature range involved and the rate constants are given to identify the slow step or rate controlling step in the temperature range given.

In this model k_1 is the rate constant for the initial step, the decomposition of kerogen to bitumen. This occurs through the initial rupture of some cross-linkages accompanied by the loss of hydrogen sulfide and carbon dioxide. The rupture of the first cross-linking units causes the partial fragmentation of the rigid macromolecular kerogen units, with a smaller elastomeric aggregate resulting. As additional energy is applied remaining cross-linkages are broken and the cleavage of some of the weaker bonds in side groups begins. The elastomer formed prior to the production of bitumen would correspond to the rubberoid proposed by Cane and will be discussed in detail later.

Zimmerly's work consisting of the extraction of bitumen from oil shale heated in sealed glass tubes has fairly well fixed the activation energy of step k_1 . The first order treatment of Hubbard's data for bitumen extracted gives good agreement with Zimmerly's work, as shown in Table 5.

Figure 11. Oil Shale Kerogen Decomposition



When additional energy is made available the remaining cross-linkages would be broken and decomposition of the less stable units in the ring clusters and side chains would become important. Also the distillation of significant amounts of low molecular weight hydrocarbons would probably take place. The second step, the bitumen pyrolysis and/or distillation step, is identified in Figure 11 by the rate constant k_2 .

The fact that the bitumen "molecule" is already small enough to be soluble in carbon tetrachloride and benzene suggests that the simple distillation of bitumen to product oil must be more important than was considered in the past.

Table 5
Energies of Decomposition of Oil Shale Kerogen

Author	R	R. D. Step	T. Range	E_a kcal/gm-mole
Zimmerley	B	k_1	275-365°C	41.7
Hubbard & Robinson (U)	B	k_1	400-475	40.0
Hubbard & Robinson (U)	0 + G	k_2	350-450 (52.6 gal/ton)	46.2
Hubbard & Robinson (U)	0 + G	k_2	400-450 (26.7 gal/ton)	42.4
DiRicco & Barrick	0 + G + B	k_1, k_2	250-465	45.5
Cane	0 + G + B	k_2	350-400	48.5
Hubbard & Robinson (A)*	0 + G	k_2	429-477	40.5
Hubbard & Robinson (U)	0 + G	k_2, k_3, k_4	450-525 (52.6 gal/ton)	27.0
Hubbard & Robinson (U)	0 + G	k_3, k_4	475-525 (26.7 gal/ton)	19.0
Allred*	0 + G	k_3, k_4	477-531	25.8
Allred*	0 + G	k_4	531-616	13.6
Johnson	G		331-427	27.0
Hubbard & Robinson (U)	G		400-525	22.0

$$* \ln\left(\frac{l-R}{R}\right) = -kt; \text{ others are all } \ln(1-R) = -kt \text{ where } R = \frac{x}{\text{kerogen}}$$

U = calculation done by U. of Utah study for this paper

A = calculation done by Allred

As long as the temperature is kept low the second step in the decomposition proceeds by the path identified in Figure 11 by the rate constant k_2 . The rate is slightly slower than for step k_1 and the activation energy is thus only slightly higher than for the initial step. The energies of activation for this step are best shown by the treatments in which the oil and gas represent the weight loss in the first order treatment as explained earlier. The resulting values are given in Table 5. The value of 46 kcal/gm-mole might be slightly high due to the low temperature range in which the bitumen has not yet all been formed. However, it is a good approximation.

When the temperature is raised further the decomposition now proceeds by a new path from that postulated up to this point. Either the bitumen itself or the oil produced by step k_2 begins to form a polymer which, when it later decomposes, forms an oil of considerably different properties than the oil produced in step k_2 . The path taken by the reaction to form a polymer is here defined by the rate constant k_3 . It is not possible to define clearly by which path it proceeds, but for the sake of simplicity it is shown here to proceed by the polymerization of the bitumen rather than the oil.

At the lower temperatures there would be sufficient time for the volatile products to pass through the pores of the marlestone matrix and the rate of cracking of the bitumen would determine the rate of appearance of the oil and gas products.

At higher temperatures, the oil would begin to polymerize at the surface of the pores causing a restriction in continued oil evolution. This would have the effect of increasing the internal

pressure, thus increasing the frequency of intra-molecular collisions and enhancing further polymerization.

Once the polymerization had taken place it would be necessary to go to significantly higher temperatures to supply the energy to crack the polymer. When the polymer began to crack the volume of volatile products broken away would be greater than could escape freely through the holes available for their removal. This condition would be especially aggravated by the presence of the polymer mentioned above, which would close off some of the holes. As a result of all this the rate of appearance of product oil outside the sample particles would be controlled by the rate of their diffusion through the vacancies.

If the suggested polymer had begun to form at the crossover point between the k_2 and k_3 paths the decomposition kinetics would come increasingly under diffusion control as the reaction proceeded and would pass over completely to diffusion control at high temperatures. The value of 13.6 kcal/gm-mole, as determined by Allred, indicates that this is the case. The diffusion controlled reaction is here defined by the rate constant k_4 .

Hubbard and Robinson found a break in the slope of their Arrhenius plot at 437°C and Allred found his first break at 477°C. It appears that at about 450°C the crossover from k_2 to k_3 begins.

Paths k_2 and k_3 are parallel and at intermediate temperatures the mechanism would be expected to pass from completely that of thermal cracking, or k_2 , to completely that of diffusion control, or

k_4 . As the transfer takes place the energies would be expected to

fall between the energy values for steps k_2 and k_4 . It is interesting to note that when the oil and gas evolution is in the temperature range of 450-531°C the activation energies are from 19 to 26 kcal/gm-mole, as shown in Table 5.

Considerable experimental evidence for the temperature dependent model proposed in Figure 11 was gathered in the D-OS, B-OS, X-OS, and HP-OS series of experiments.

Table 6 shows for the D-OS series of tests how the specific gravity of the oil increased with temperature and that the gravities all were considerably below the values derived from the Fischer Assay produced oils. The pour points of the oils were also considerably lower than those normally encountered in other, higher-temperature processes. Table 7 gives typical specific gravities and pour points for some oils produced from other common retorts.

If the polymerization-diffusion control model is valid it would be expected that anything which would shorten the time of the oil in the hot zone would decrease the amount of polymerization and thus produce a higher quality oil. The low pressure flow experiments were run at much higher flow rates than were the atmospheric flow tests. At identical temperatures the higher flow rates resulted in an oil of lower gravity. This is illustrated in Table 23, Appendix A, in which oils from the two processes are compared. This is discussed more fully in the section treating the flow studies.

Experiment D-OS-26 was performed in order to determine whether the low gravity of the oil was not in fact due to the non-uniformity of temperature in the retort and not to the above mechanism. As

Table 6

Effect of Temperature on Oil Quality

Test	Temp. °C	Specific Gravity gm/cm ³	Fischer Assay Specific Gravity gm/cm ³	Pour Point °C
D-OS-4	331	.822	.911	-40
D-OS-5	347	.823	.911	-45
D-OS-21	347	.841	.910	-30
D-OS-19	353	.828	.914	-23
D-OS-7	364	.817	.912	-18
D-OS-25	366	.822	.909	-30
D-OS-22	395	.838	.910	-20
D-OS-16	399	.828	.914	-23
D-OS-18	420	.834	.914	-21
D-OS-17	420	.832	.914	-20
D-OS-15	420	.829	.914	-17
D-OS-10	427	.888	.912	- 5
D-OS-23	427	.843	.910	-20
D-OS-1	500	.852	.907	10
D-OS-2	520	.859	.907	0

Table 7

Properties of Crude Shale Oils from Various
Processes

Sample	Retorting Method	Pour Point °F	Specific Gravity gm/cm ³
Green R., Colo.	USBM Fischer	80	.925
Green R., Colo.	USBM Fischer	85	.911
Green R., Colo.	NTU Retort	90	.935
Australia	Pumpherstons	60	
Sweden	Rockesholm	5	
Scotland	Pumpherstons	5	
France	Petit	5	
France	Marceaux	30	
France	Pumpherstons	65	
Clay City, Ky.	USBM Fischer		.924
Scotland	USBM Fischer		.865
Dragon, Utah	USBM Fischer		.904
Elko, Nevada	USBM Fischer		.883

mentioned previously the retort was cooler (by $\approx 50^{\circ}\text{C}$) at the top than at the bottom. Perhaps the reflux action thus initiated would lead to a secondary cracking of the oils if given enough time. In experiment D-OS-26 the bottom of the reflux pot was held at 300°C and the top at 200°C . An oil from HP-OS-19 having a gravity of $.840 \text{ gm/cm}^3$ was refluxed in the pot for 240 hours. The result was seventy per cent recovery of an oil of $.835 \text{ gm/cm}^3$ gravity. Five weight per cent of the initial oil weight remained in the bottom of the pot as a polymer or char. The remaining gas plus losses totaled approximately 25 per cent of the initial sample.

If a reflux action were responsible for the unusually low oil gravity in the earlier experiments the oil in this case should also have been cracked to produce a lighter oil. Actually a small part of the oil was polymerized and a larger fraction was cracked to form gaseous products. The oil which was distilled had the same gravity as the original sample.

An additional experiment was run to determine further the extent of polymerization from high temperature treatment of shale oil. A shale oil sample of specific gravity $.813 \text{ gm/cm}^3$ was sealed in the high pressure bomb for six hours at 485°C . The resultant oil was totally polymerized into a black, flakey, fragile char. Only several milliliters of material would still flow from an initial sample of 200 ml. There was considerable sample weight loss in the form of gas.

An additional test was run in the high pressure retort. The oil from a low pressure flow test (HP-OS-300-21) was heated to 520°C .

and held at that temperature in the open retort. The yield of oil which escaped from the retort was 79 percent, the gas and losses were 11.5 percent, and the residue remaining in the retort was 9.3 percent. The oil gravity was $.93 \text{ gm/cm}^3$ initially and $.86 \text{ gm/cm}^3$ after the distillation. If a simple distillation had taken place at a temperature of 520°C a yield approximating 100 percent should have resulted. In this case, however, the light ends were distilled from the retort but nine percent formed a char due to the high temperature. Part of the char was cracked to produce non-condensable gases but at least nine percent of the initial sample remained as a polymer.

In order to determine if the high oil quality was actually a result of a low temperature mechanism and not a catalytic effect from catalyst traces in the walls of the metal retort, a ground glass liner was designed which prevented any contact of the volatile products with the retort walls. It had no side gas vent and the gases were vented through the cap. It was the same as that shown in Figure 2 except that the side vent was closed off and an exit stem was fused to the top of the ground glass lid. The temperature was raised to 450°C for five hours and the oil collected had a gravity of $.794 \text{ gm/cm}^3$. This very low gravity suggested that the catalytic effect, if any, from the retort walls in the past had acted to increase polymerization, rather than to promote cracking.

Oil Quality and Yields

In addition to the kinetic data the atmospheric batch tests provided significant information concerning the effect of temperature on the yield and quality of the shale oil produced.

The effect of temperature on the yield of oil is shown in Table 8. Because samples of varying initial kerogen concentrations were utilized the experimental weight percentages of oil recovered were divided by the weight percentages of oil recovered in the Fischer Assay tests of the same samples.

It is apparent that satisfactory oil yields (of from 70 to 80 percent of the Fischer Assay yields) can be obtained using temperatures no higher than 375°C. There is every indication that yields approximating that range could be obtained even at the lowest temperature of 331°C if sufficient time were allowed. The gas evolution curves did not reach steady state but continued to increase with time as shown by the zero order gas evolution curve in Figure 12. The gas continued to evolve for 550 hours; and was accompanied by the evolution of oil.

In Table 6 are listed the experimental oil specific gravities, and pour points and for comparative purposes the Fischer Assay oil gravities as determined on the same samples. At all the temperatures involved, from 331°C to 520°C, the oil quality was significantly better than that normally encountered in the crude oils resulting from the various retorting processes. Table 7 illustrates this fact by listing the properties of the product oils of various methods used in retorting oil shales from various parts of the world.

The crude oils recovered in the D-OS- series were separated on the F & M model 720 gas chromatograph using a two foot silicone grease column. A programmed temperature range of about 100 to 300°C and a heating rate of 7.5°C per minute were employed. Figure 13a gives a

Table 8

Effect of Temperature on Oil and Gas Yields

Test	Temperature	Pressure	Duration	Oil Weight Percent U. of U. Fischer Assay	U. of U. % of Fischer Assay	Gas yield ft ³ /ton
D-4	331°C	atm	550 hrs	4.0	11.9	33.6
D-5	347	atm	425	4.8	11.9	496
D-19	353	atm	159	4.3	11.0	477
D-7	364	atm	312	6.0	11.4	884
D-22	395	atm	71	7.6	10.6	71.6
D-16	399	atm	86.5	8.0	11.0	72.8
D-17	420	atm	38.0	8.8	11.0	80.0
D-10	427	atm	37.5	8.9	11.4	73.1
D-14	427	1000 psig	14.7	8.6	11.8	72.9
D-1	500	atm	13.5	7.6	8.2	92.6
						1142

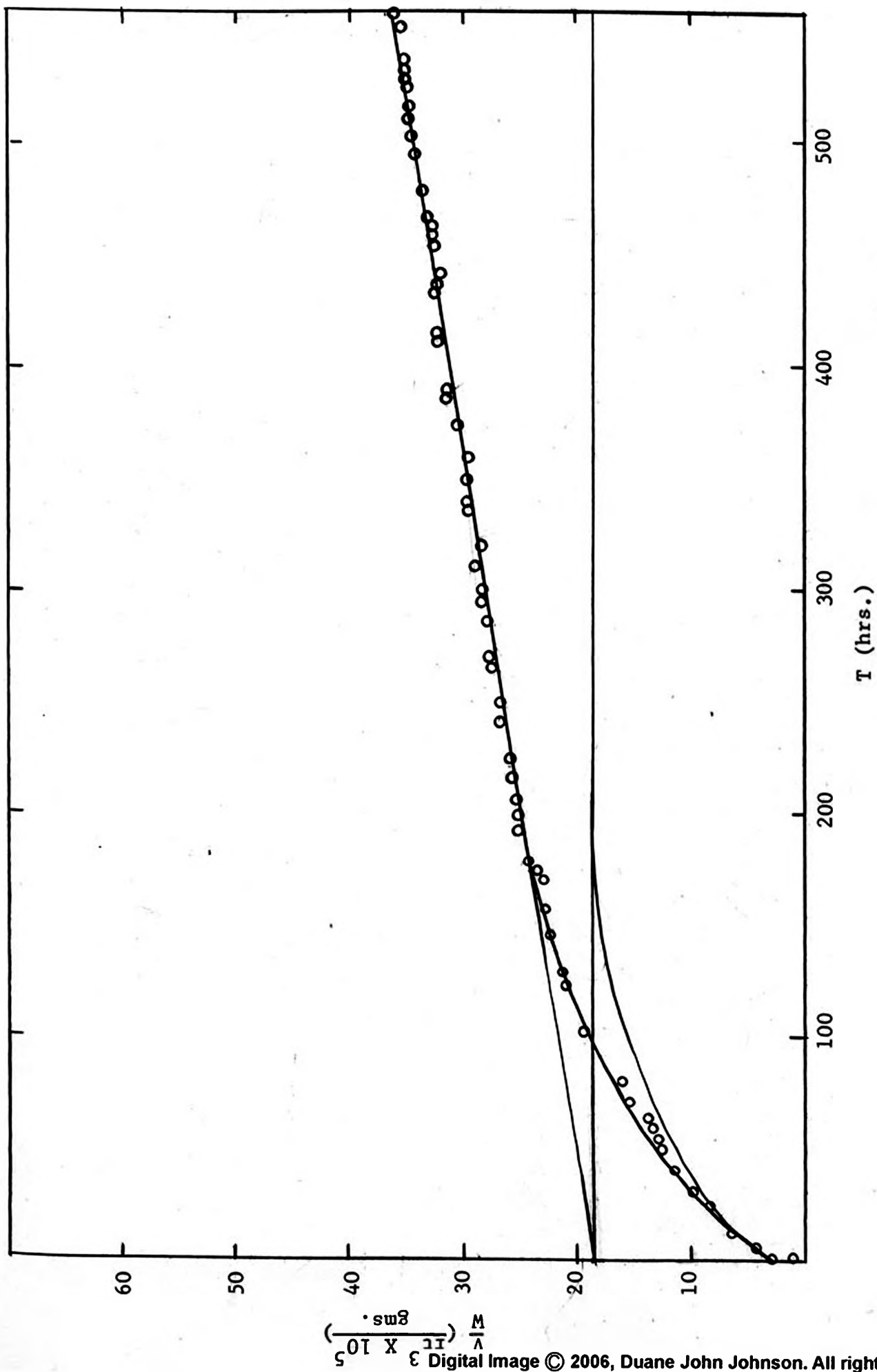


Figure 12. Volume of gas evolved versus time for 331°C .

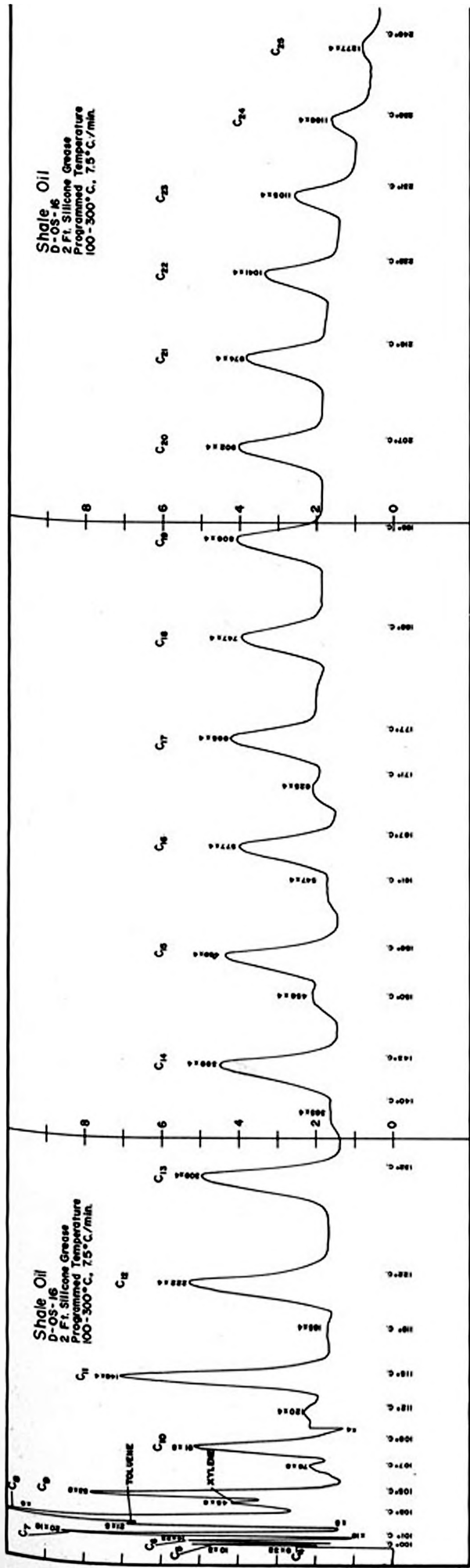
typical chromatographic spectrum, in this case for D-OS-16, which was a decomposition run at 399°C. Figure 13b shows the same oil sample with the addition of the known straight chain paraffins C₁₀, C₁₂, C₁₆, C₂₀. Using these and other internal standards the following compounds were identified; xylene, toluene, analine, cyclopentane, cyclohexane, and the straight chain paraffins C₄, C₅, C₆, C₇, C₈, C₁₀, C₁₂, C₁₆, and C₂₀. These positive identifications make possible further probable identifications, for example the three primary peaks between C₁₂ and C₁₆ are most likely C₁₃, C₁₄, and C₁₅.

The same peaks as those in Figure 13 appeared in all the crude oil samples recovered in the decomposition temperature range of 331 to 427°C. The spectra indicate that the oil is highly paraffinic in nature and that the upper limit of chain length is approximately C₂₅. The peak identified as C₄ or butane was located by bubbling butane through shale oil and noting the subsequent increase in peak height.

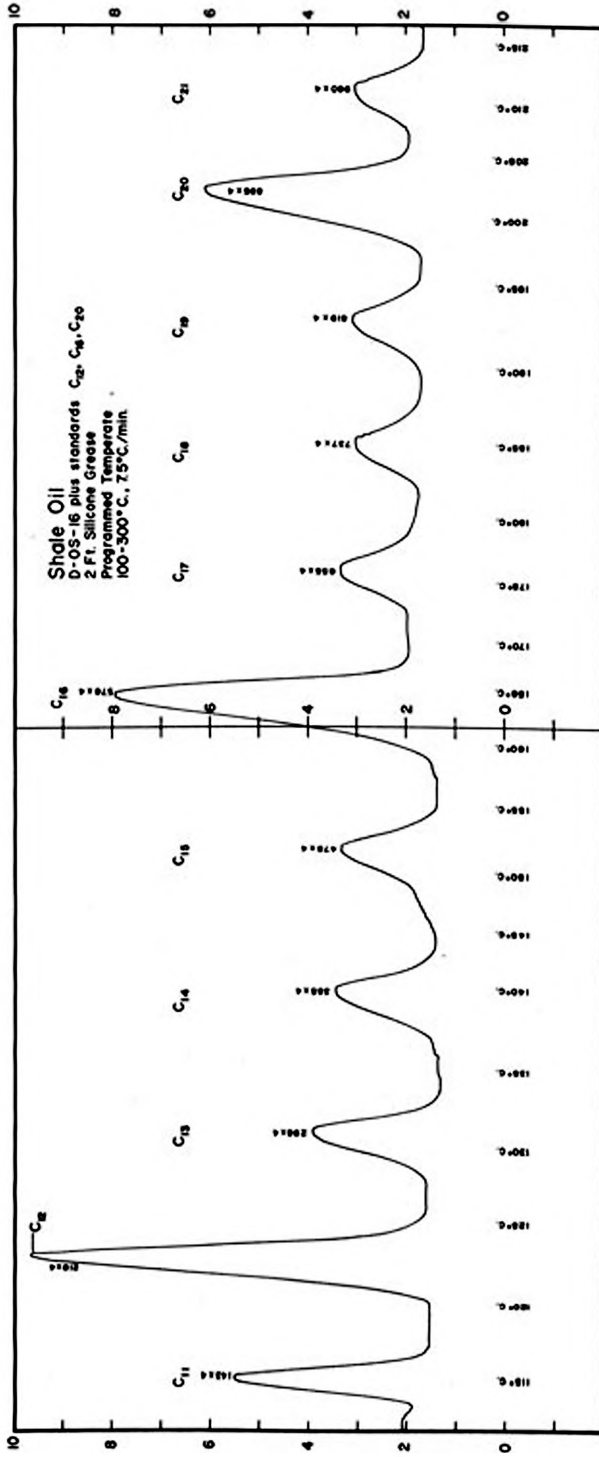
In order to determine if the spectra observed, of which Figure 13 is typical, represented the actual compounds in the oil a simple test was performed.

If the spectra resulting from the injection of the oil samples was not representative of the actual material then either part of the sample had to "pile up" in the column and pass through the detection units at a later time, or some material from each sample had to be irreversibly adsorbed on the silicone grease. Figure 13 reproduces all the peaks which were observed in the chromatograms.

No evidence for the former was found. The sensing units were left on for many hours following a series of analyses without the



a



b

Figure 13. Chromatograms (a) of shale oil (b) of shale oil with standards added.

appearance of any delayed peaks. Also, consecutive analysis of a sample should eventually have given unusual results due to the early or late appearance of the material which had accumulated as each injection was made. This was not the case.

If a fraction of each sample was irreversibly adsorbed on the column the chromatograms for identical samples should have shown considerable changes as the degree of poisoning increased. This was not observed to take place.

During the approximately one year's time that the silicone grease column was used in the analysis of shale oil samples, about 150 oil samples of 10 μ l each were injected into the column. Thus the total amount of sample injected consisted of about 1.5 milliliters. With this in mind 5 ml of oil were injected slowly into the column and the column was held at about 200°C until the detection unit returned to zero. The temperature of the column was then raised to 275°C for several hours and then it was flushed with helium. In a typical analysis the temperature was programmed to rise from 100-300°C at 7.5°C/min after which the column was flushed with helium for several hours at 275°C.

The result of the five ml sample injection was a 50 milligram loss in weight of the column. Irreversible adsorption would have led to a significant increase in the column weight. Also no delayed peaks appeared at a later time.

It appears that other compounds in the oil than those mentioned above must be in such small concentrations that they are masked by the relatively high alkane and low molecular weight aromatic

concentrations. The shift in the chromatogram base line indicates that this is the case.

Osmometer studies in benzene indicated a molecular weight of the oil of 200 to 250.

Pressure Effects

Several static pressure tests were performed with water added to the retort. These were compared with runs in the absence of water. Data for the pressure tests along with similar data from atmospheric tests are given in Table 9.

These data suggest several conclusions. The use of pressure either with or without water present appeared to lower the sulfur content significantly, with the lowest sulfur content resulting when the highest pressure was used. Pressurization also resulted in a lowering of the oil yield, the most significant decrease occurring at the highest pressure. Of course both of these effects could in part have been to the presence of water in the retort. Further investigations of the effects of water are suggested.

The lower temperature tests did not appear to lead to a large amount of oil polymerization, if any, even when at pressures up to 1000 psig. The use of a higher pressure appeared to lead to some polymerization. A temperature of 485°C and a pressure of 3640 psig resulted in essentially complete polymerization of the oil. This suggests that the threshold of the polymerization mechanism discussed earlier must indeed be between 427 and 485°C.

Chromatographic spectra indicated that the effect of water added to the retort was to increase the average molecular weight of the product oils.

Table 9

Effect of Pressure on Oil Yield and Quality

Experiment	Maximum Pressure psig	Temperature °O	H ₂ O Added	Oil Yield % Fischer Assay	Oil Pour Point °C	Oil Specific Gravity gm/cm ³	Sulfur Content Percent
*D-OS-27	3640	485	no	0.0	solid	~ > 1.0	--
D-OS-9	3500	427	yes	42.6	-90	.876	.5
D-OS-12	2560	427	yes	51.0	5	.837	.68
D-OS-13	1000	427	yes	66.3	-20	.814	.75
D-OS-14	1025	427	no	73.0	-22	.814	.82
D-OS-10	atm.	427	no	78.4	- 5	.889	.93
D-OS-23	atm.	427	no	82.4	-20	.834	--
D-OS-15	atm.	420	no		-17	.829	1.1
D-OS-17	atm.	420	no	79.8	-20	.832	1.0
D-OS-18	atm.	420	no	75.4	-21	.834	.93
D-OS-16	atm.	395	no	72.4	-23	.828	.93

* The sample was a crude shale oil with a specific gravity of .813 gm/cm³.

BATCH LOW PRESSURE STUDIES

This series of experiments was designated the B-OS- series and consisted of a number of tests in which heated oil shale was exposed to a pressurized methane gas atmosphere.

Equipment

The retort was the same as that described in the kinetic experiments with the exception that for the B-OS- series the retort was fitted with a pressure gauge and an inlet for admitting the methane.

Experimental Procedure

The sample was crushed and sized in the same manner as in the kinetic experiments. The fragments were then placed in a glass liner which had a ground glass cap and a side vent. In the pressure tests the internal retort pressure was brought up to the desired initial value with the use of pressurized methane.

The retort was sealed and heated at a constant rate. In some cases it remained closed throughout the run and in others gas was bled off to maintain a predetermined value.

Records were kept as to the internal retort pressure, volume of gas evolved, and other experimental conditions.

A material balance was performed, using the following items:

- (1) the weight of the glass liner empty
- (2) the weight of the sample
- (3) the weight of the residue

- (4) the weight of the dry ice/acetone trap empty
- (5) the weight of the dry ice/acetone trap plus recovered liquids
- (6) the gas + loss as determined by difference

All liquids and gases were measured volumetrically and the oils recovered were tested for their specific gravities, pour points, and API gravities by the standard ASTM methods where possible.

Results and Discussion

Table 24, Appendix A, gives the summarized results of the entire series.

The specific gravities of the crude oils recovered and the Fischer Assay specific gravities for the oils recovered from the same oil shale samples are shown in Table 10.

It is apparent that the use of a pressurized methane atmosphere in this batch system resulted in an oil of considerably lower specific gravity than that resulting from the Fischer Assay tests on the same sample material. It is also evident that the use of moderate pressure and a methane atmosphere resulted in significantly lower oil specific gravities than when a retort pressure of one atmosphere was used.

In all of the pressure experiments the oil yield was lowered considerably, with only B-OS-14 providing a yield comparable to the atmospheric pressure runs.

The severely lowered yields of the tests in which the retort was cooled while pressurized and the very low gravity of the oil collected are obviously due to mechanical entrapment of the cooled, liquified heavier oils when the retort

Table 10

Effect of Temperature and Pressure on Oil Yield and Quality

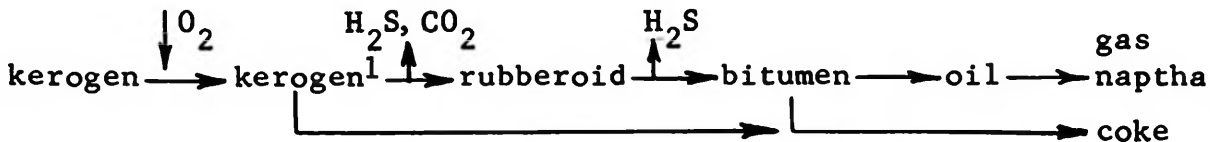
Test	Temp.	Maximum Pressure	Oil Yield % Fischer	Oil Specific Gravity *	Fischer Assay Oil Specific Gravity*
B-OS-5	375	atm.	19.2.	.800	.907
B-OS-2	375	atm.	62.6	.838	.895
B-OS-1	400	atm.			.895
B-OS-10	400	atm.	47.3	.808	.906
B-OS-12	400	atm.	54.5	.816	.906
B-OS-13	440	atm.	85.8	.836	.906
B-OS-16	440	atm.	81.9	.841	.906
B-OS-17	450	atm.		.794	.909
B-OS-8	400	300.	17.0	.782	.906
B-OS-9	400	300	10.3	.779	.906
B-OS-15	400	300	4.24	.777	.906
B-OS-14	440	300	50.2	.774	.906
B-OS-7	375	375	4.73		.907
B-OS-4	430	600		.865	.901
B-OS-6	375	755	3.99		.907
B-OS-11	400	925	21.8	.811	.906
B-OS-3	390	1700	4.72		.895

* gm/cm³

would have the effect of fractionating the oils and only allowing the light oils to be collected outside the retort. The yield was higher in those cases where the gases were continually bled from the retort to keep the pressure down than when the retort was allowed to build to a final pressure, was cooled, and the gases bled off. This indicates the advisability of a flow system of retorting as opposed to static pressure retorting.

Shales Very Rich in Kerogen

In 1948 and 1950 Cane studied the thermal decomposition of torbanite and suggested the following mechanism for its pyrolysis⁽¹¹⁾;



The torbanite studied was unusually rich and assayed at 233 gal/ton or about 91 percent of the initial sample weight converted to oil.

The rubberoid was a dark, soft solid similar to semi-vulcanized rubber. It fractured easily under tension and exhibited swelling tendencies when soaked in benzene.

In the case that the rubberoid is a unique kerogen pyrolysis product it would correspond to the elastomer mentioned in the discussion of the decomposition mechanism. As the breaking of cross-linkages in the parent kerogen aggregate was initiated some rigidity of the kerogen structure would be lost and an elastomer would result.

This would not be a polymerization, but rather a depolymerization to

the point where only a few percent of the "molecular" units are cross-linked as in vulcanized rubber.

The torbanite rubberoid has been shown to exhibit the swelling characteristics of natural rubber when immersed in benzene. This eliminates the possibility that the rubberoid is just a mixture of bitumen and oil shale inasmuch as the elasticity of the mixture would be lost when the bitumen was dissolved by benzene.

Rubberoid must therefore be a unique stage in the decomposition of very rich torbanites to form bitumen.

Some of our tests provided evidence to support Cane's rubberoid stage in kerogen decomposition⁽¹²⁾. Experiments B-OS-5, 6, 10, and 11 produced residues which were rubbery at least in part. In these experiments the sample column in the glass liner yielded a residue which was rubbery at the top, slightly fused in the center, and crumbly or hard at the bottom. This was true at experimental temperatures of 375° and 400°C; no rubberoid was observed at experimental temperatures above 400°C.

As was mentioned in the discussion of the kinetic experiments there was some temperature gradient in the sample column, with the temperature of the experiment representing the temperature of the lower part of the column and the temperature cooling towards the top of the column. When the experimental temperatures were 375°C the bottom of the column was at 375°C and it produced a hard residue while the top yielded a rubbery residue. At temperatures greater than 400°C the entire residue was firm and non-rubberoid. This suggests that somewhere below 375°C, probably in the neighborhood of 325 to 350°C, the rubberoid stage occurs.

The "rubberoid" material was elastic in that it could be easily deformed with the fingers and would return to its original shape. The application of a small shear force, however, would easily tear the material. When the residue was dropped on a hard surface it bounced several times. After standing in the atmosphere at room temperature overnight it lost its elasticity and become rigid and fragile.

The kerogen content of the oil shale producing the elastic residue was the richest of those used, containing approximately 14.8 to 16.5 percent oil by weight. In the lower temperature B-OS series experiments in which a lower oil content oil shale was used (12.3 to 13.4 percent oil by weight) no elasticity was observed in the residue.

The fact that the rubberoid stage only appeared in the decomposition of our oil shale samples which were unusually rich in kerogen can be explained in several ways. One possibility is that the rubberoid is so dispersed in the shale matrix that the characteristics of the shale rather than the characteristics of the mixture of kerogen residue and bitumen determine the properties of the total combined residue. The elastomer resulting from the thermal decomposition of kerogen would show some elasticity but if it were widely dispersed the elastic properties would go unnoticed.

Another possibility is that when the bitumen is present in sufficient quantities it forms a two-phase plastic mixture of shale and bitumen.

The fact that Cane has definitely identified a rubberoid stage in the pyrolysis of rich torbanite would lead one to expect the formation

Digital Image © 2006, Duane John Johnson. All rights reserved.

of the rubberoid in the lean shales also. There is no evidence to date that the kerogen in the rich and lean oil shales differs considerably. This tends to support the first of the above alternatives.

The fact that the elastic residue made its appearance in our lean oil shales containing 85 percent inorganic matter supports the second alternative, namely the two-phase plastic.

It is not clear at this time which is the better explanation for the elasticity of the residues from the lean oil shales. While it would be expected that the lean oil shale kerogen decomposition should proceed by the same path as that of the rich torbanite, it is difficult to explain how the kerogen in the oil shale, making up only 15 percent of the total weight, would determine the physical structure of the entire residue.

At this point it is apparent that additional study is needed to determine if the rubberoid is an actual stage in the decomposition of the kerogen in lean oil shales, or if it is merely a two-phase plastic mixture of bitumen and shale.

STUDY OF THE GAS COMPOSITION

Equipment

The retort and gas monitoring system was the same as that used in the D-OS- series with the exception that at the sample exit shown in Figure 1 a connector was added so that sample tubes could be attached and purged of air while an experiment was in progress. The sample tubes were of uniform length and diameter.

The glass liner with the side-vent was used as a sample holder in the retort.

Procedure

The same numbering system was used, with this series being designated the C-OS- series.

The crushed and sized sample was again placed in the glass liner before being placed in the retort; the retort was sealed and connected to the monitoring system by means of a short tube.

While the temperature was increased at a uniform rate gas samples were taken from the sample exit. This was done by shutting off the normal exit line and forcing the gases through the alternate or sample exit.

The collected gas samples were analyzed by the F & M model 720 gas chromatograph and by the Consolidated model 21-620 mass spectrometer.

A material balance was kept by weighing the following items during each run:

- (1) the glass liner empty
- (2) the glass liner plus sample

- (3) the glass liner plus residue
- (4) the dry ice/acetone trap empty
- (5) the dry ice/acetone trap plus liquids recovered

The volumes of all the liquids and gases recovered were recorded. The oils were tested for their specific gravities, API gravities, and pour points according to standard ASTM methods.

Results and Discussion

A summary of the results is given in Table 25, Appendix A. In Figures 14 through 19 are plotted the percentages of carbon dioxide, hydrogen sulfide, methane, ethane, propane, and hydrogen as a function of the temperature of the oil shale sample at the time when the gas sample was collected. There would be some time lag between the moment a gas species left the sample bed and the time that it was collected; therefore, the temperature truly representing a species collected should be slightly below that recorded. This effect should not be serious, however, as the retort void volume and exit line volume were quite small. The percentage of air in the sample was neglected and the percentages of each gas plotted in Figure 14 through 19 are the percentage of the total gas remaining after the air has been subtracted.

Table 11 shows the temperature effect on the incremental gas yield, the gas product analyses, and the heating value of the total product gas.

An examination of Figures 14 through 19 shows an initial methane peak at 300°C followed by a decrease in concentration and a subsequent

Table 11

Temperature Effect on Gas Yield, Product Gas Analysis, Gas Heating Value

Temperature	Gas Evolved ft ³ x 10 ⁵ /gm	%CO ₂	%CH ₄	%C ₂ H ₆	%C ₃ H ₈	%H ₂ S	%H ₂ + others*	Total Gas Heating Value †
170°C	3.21	.27						
300	1.88	30.5	43.6	2.09	3.55		20.3	570
350	1.7	18.7	15.2	16.3	2.85	.44	46.5	595
380	2.64	3.8	13.1	4.02	3.40	.90	74.8	467
404	3.21	3.5	19.2	6.44	4.54	.61	65.7	560
444	6.61	9.6	28.1	6.92	3.04	.29	52.0	580
485	6.79	26.7	21.2	1.44	.75		49.9	370
500	3.58	41.0	9.94	.85	.90		48.2	258
525	10.7	69.0	4.23	.33			26.4	116
552	33.4	89.6	2.91				7.5	48
575	39.6	77.5	1.34				21.2	70
590	9.25	99.6	.37					3

* Net heating value, not including heat of condensation of water.
 † Btu/ft³

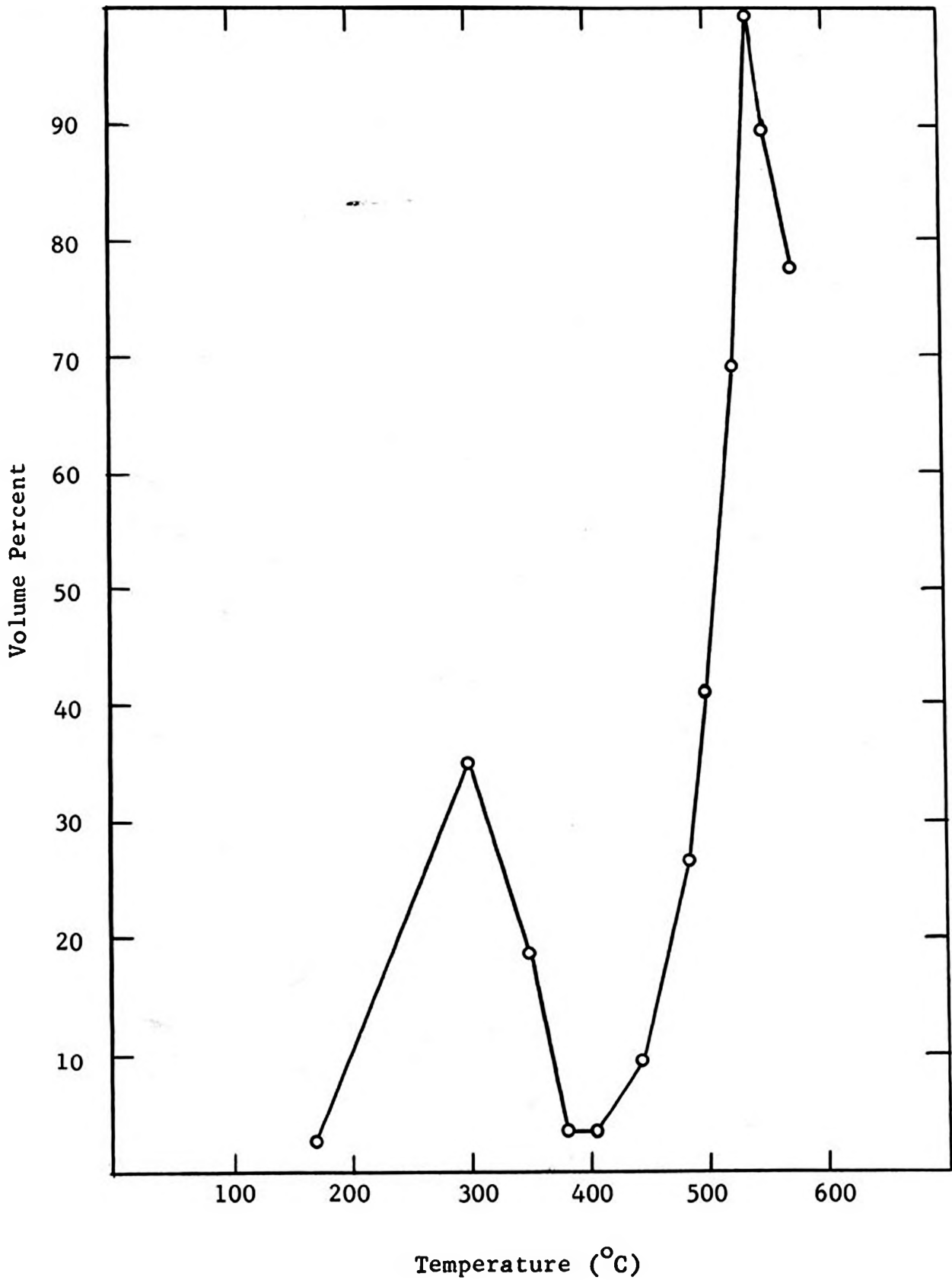


Figure 14. Percent carbon dioxide in product gas versus temperature

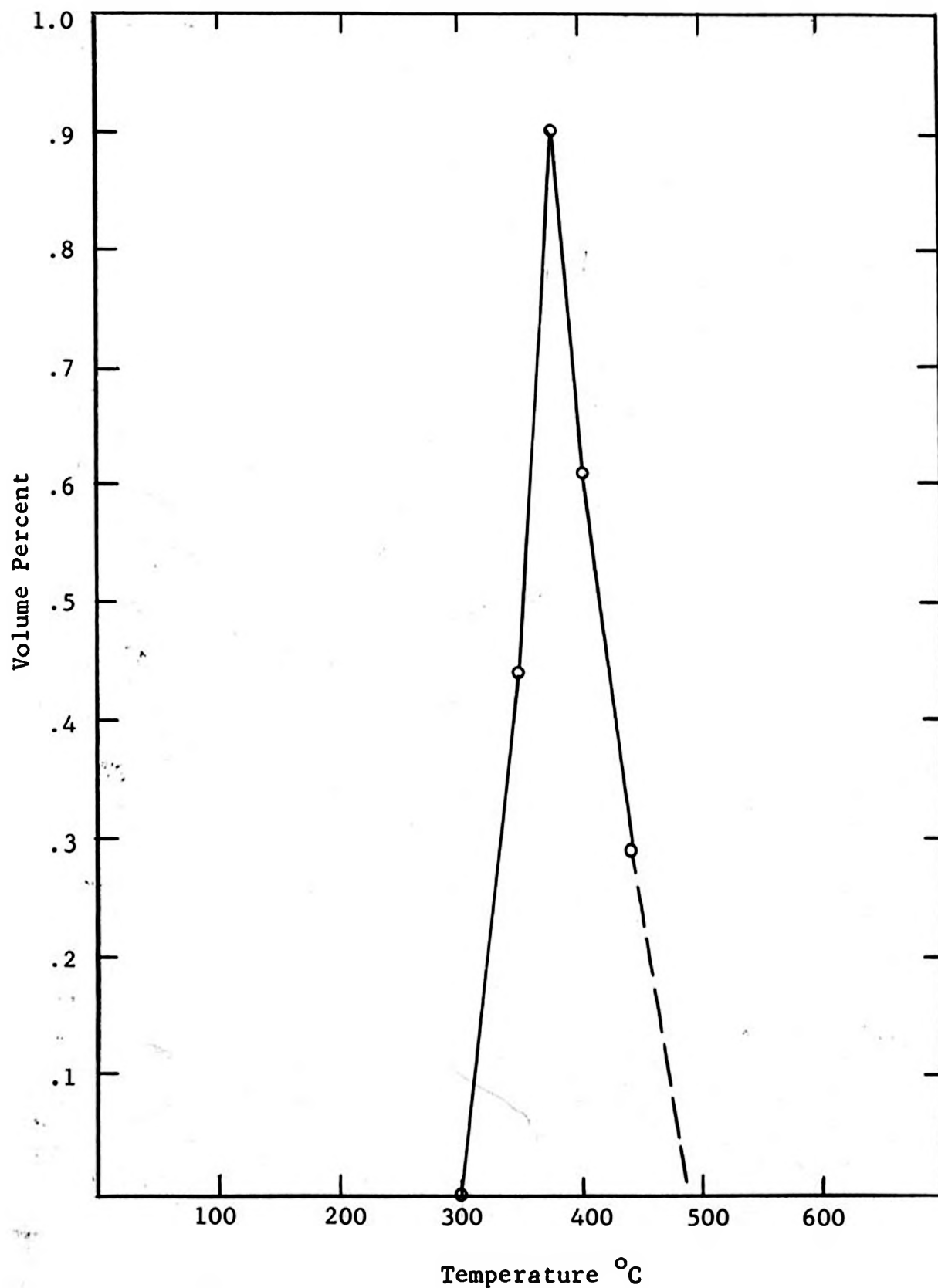


Figure 15. Percent hydrogen sulfide in product gas versus temperature

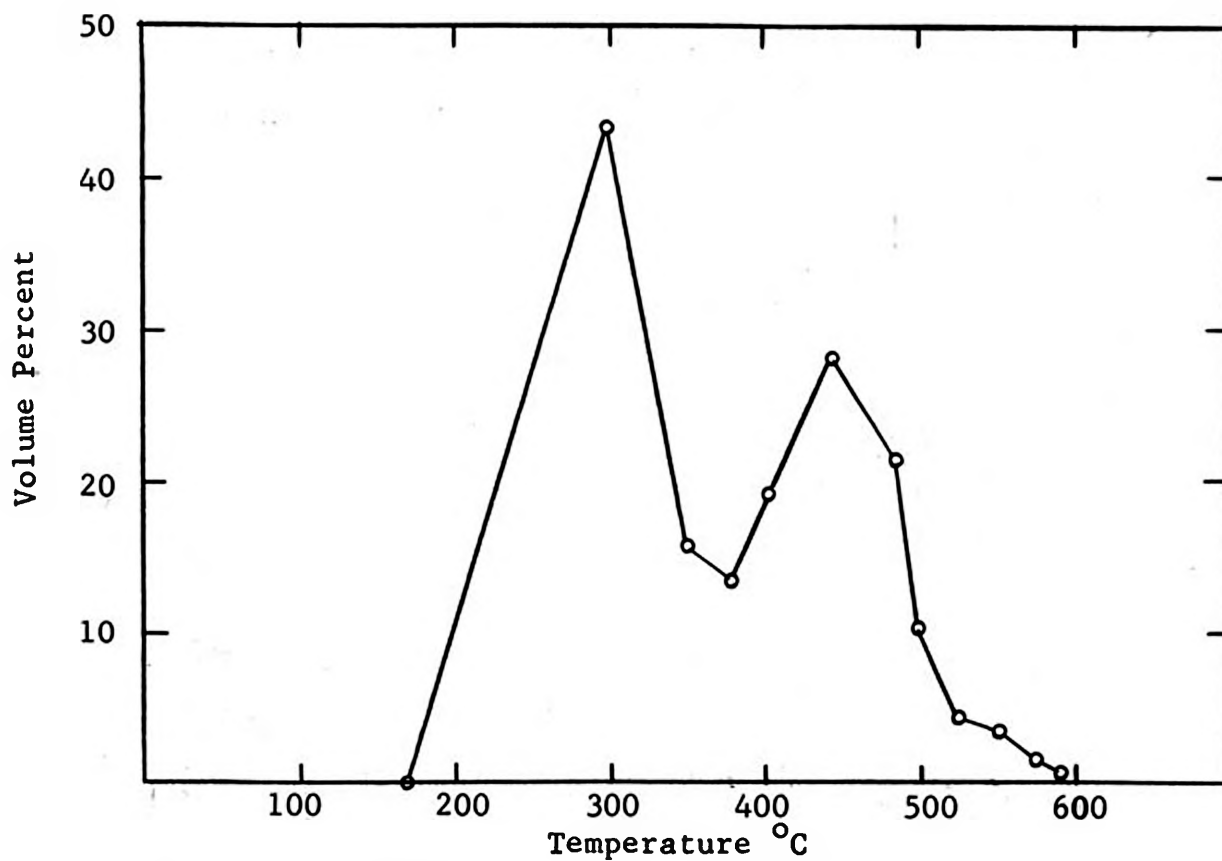


Figure 16. Percent methane in product gas versus temperature

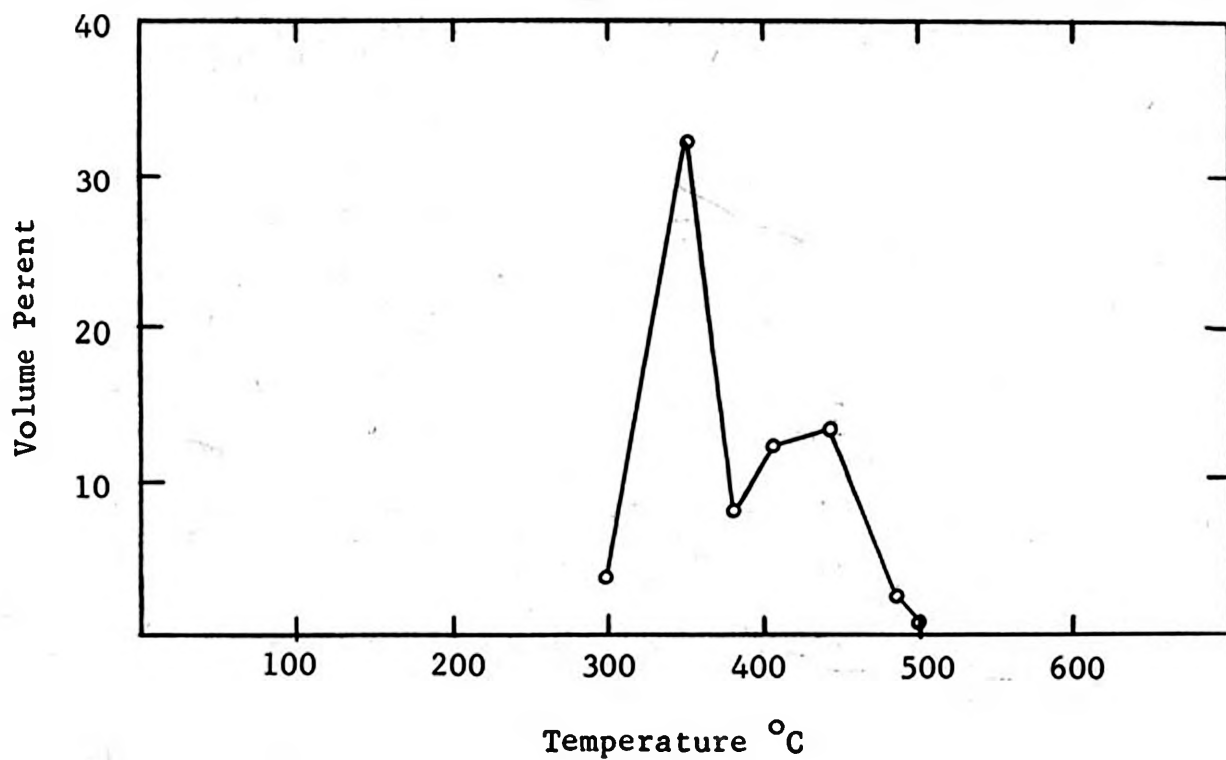


Figure 17. Percent ethane in product gas versus temperature

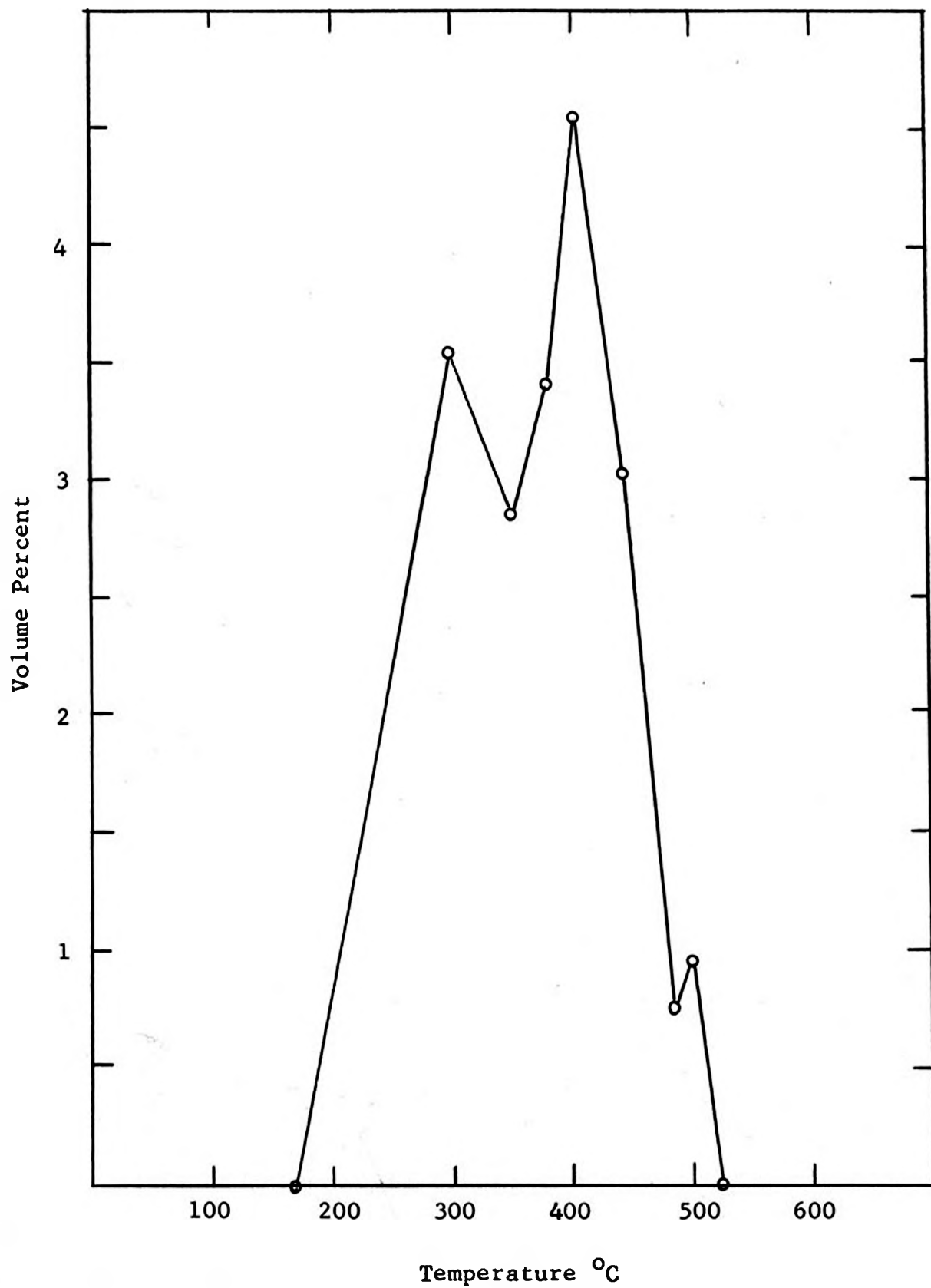


Figure 18. Percent propane in product gas versus temperature

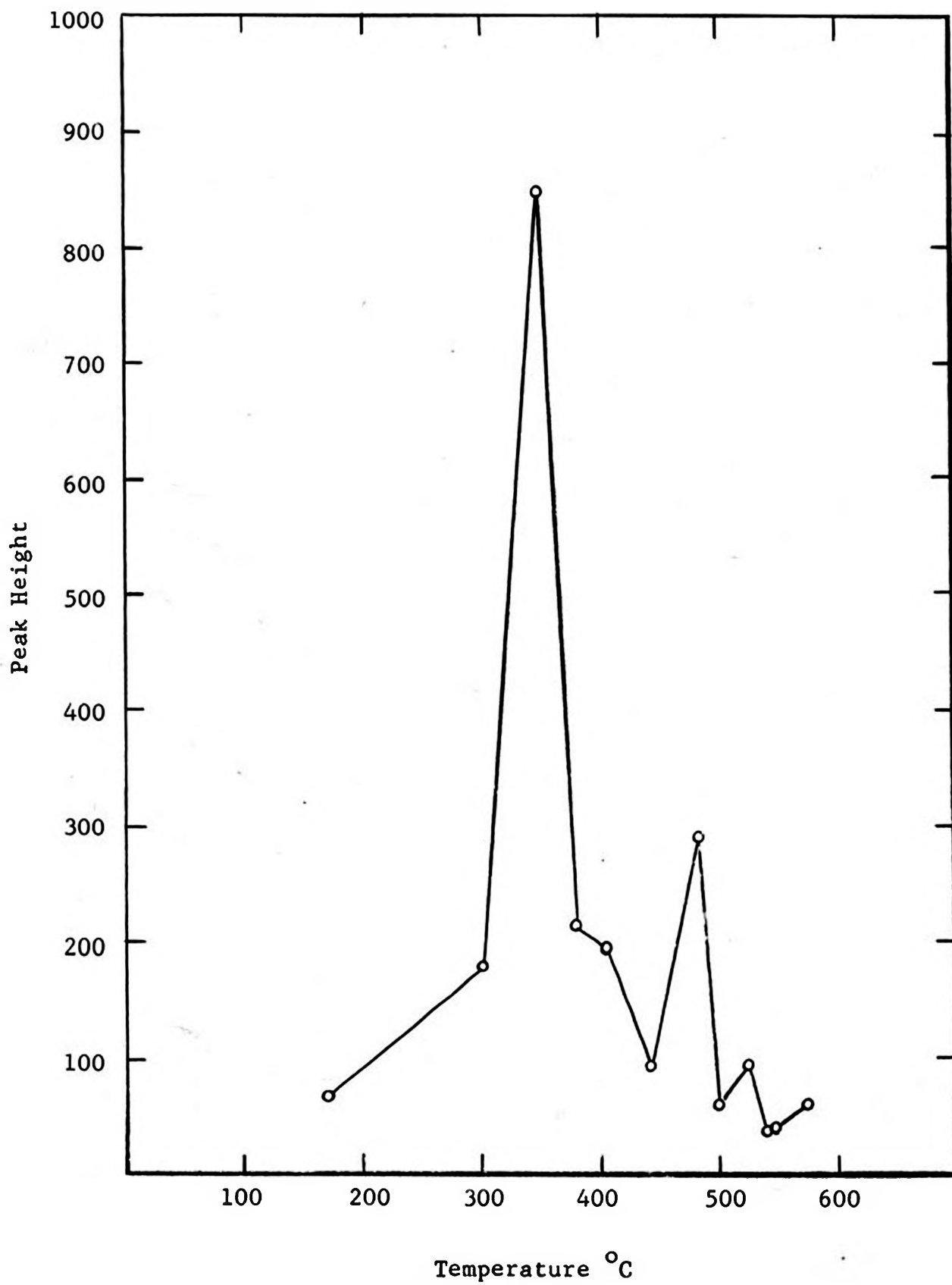


Figure 19. Mass spectrographic peak height for hydrogen versus temperature

peak at 440°C. Ethane has its first peak at 350°C and the second at 444°C. The first propane peak is at 300°C and the second at 404°C. Carbon dioxide reaches a maximum at 300°C, then decreases. At about 444°C the CO₂ concentration again increases, this time continuously as the temperature is raised. The continued rise in CO₂ above 450°C is due to the ever larger decomposition of inorganic carbonates making up part of the shale matrix. The hydrogen sulfide concentration reaches a maximum at about 380°C. Hydrogen peaks occur at 350°C and again at 485°C. In hydrogen the earlier peak is the dominant one.

The location of the maxima indicates that there is an initial gentle cracking or rearrangement of the sample at about 300°C in which only a small number of species which are weakly bonded to the kerogen "molecule" are broken from it, with the accompaniment of the evolution of small amounts of hydrocarbon gases and larger amounts of hydrogen sulfide and carbon dioxide. Significantly, the first oil appeared in the cold finger trap at about 275°C. The small initial quantity of oil suggested that the step in the decomposition of kerogen signalled by the early evolution of gases may be a depolymerization of the type discussed earlier rather than a cracking reaction.

The second group of peaks which occurred from 400 to 475°C would seem to indicate that when that temperature range was reached some new phenomenon was now taking place, thus the rapid gas and oil evolution. Perhaps this was why McKee and Lyder erroneously proposed that the decomposition of kerogen took place within very narrow limits, 400 to 410°C⁽⁴⁷⁾. The early stages of decomposition take place at a much lower temperature but large amounts of oil do not appear until about 400°C.

The data from the C-OS- series, of which C-OS-2 is typical, showed that the carbon dioxide concentration reached a maximum at 300°C at which point the hydrogen sulfide percentage had just become measurable. From that point until 380°C the hydrogen sulfide evolution showed a very rapid increase. Part of the initial carbon dioxide peak was possibly due to the driving out of the carbon dioxide weakly held in the kerogen. For the most part, however, the early carbon dioxide peak should signal the first depolymerization.

The hydrogen sulfide peak reached a maximum at the higher temperature when the kerogen and/or rubberoid was decomposing to form the bitumen. After 380°C the hydrogen sulfide peak was falling off sharply and rapid oil evolution was observed. This corresponded to the distilling and thermal cracking of the bitumen into shale oil, gas, and coke.

Second Stage

The second set of peaks from 400 to 450°C for the hydrocarbon gases in Figures 16 through 19 were a further indication of the decomposition of the bitumen into the oil, gas and coke products.

The location of the secondary hydrocarbon peaks and their sharp decline subsequent to the peaks offer support to the temperature dependent mechanism proposed in Figure 11. The methane, ethane, and hydrogen curves have their secondary peaks at 444, 444 and 485, respectively, and propane at 405°C. The earlier limit of 450°C was chosen as the temperature at which the mechanism changed over from a low temperature bitumen decomposition, to a higher temperature polymerization

of bitumen. This was followed by the diffusion controlled pyrolysis of bitumen and polymer.

The location of the peaks above appears to offer support for the temperature threshold chosen. Significant oil is produced above 450°C but due to the pore constrictions from the polymer formed the rate of its appearance is decreased considerably. This is accompanied by a decrease in the amount of hydrocarbon gases evolved.

The early initial hydrocarbon peaks accompanied by the first oil from about $300\text{-}350^{\circ}\text{C}$ indicate that initial oil evolution proceeds at lower temperatures than is generally considered acceptable for commercial retorting.

FLOW STUDIES

A series of experiments was performed at pressures essentially that of the atmosphere, with only enough positive pressure being used to insure the flow of the natural gas through the oil shale sample in the retort. This series was designated the X-OS- series.

A second series of flow tests were carried out at natural gas pressures of from 200 to 400 psig, also using natural gas as the heating medium. They were designated the HP-OS series.

The HP-OS- series and the X-OS- series were intended to complement one another. For example, HP-OS-300-11 and X-OS-21 were at essentially the same conditions except for the use of higher pressure and higher flow rates in the former.

Due to the comparative nature of the two series the results and discussion for both will be treated together.

Equipment for Low Pressure Flow Study

The equipment was designed so that oil shale could be decomposed using heated natural gas at pressures great enough to insure a positive flow of the gas up through the oil shale bed. Miller has thoroughly described and illustrated the retort and equipment in his Ph.D. dissertation⁽⁵⁰⁾.

The equipment train consisted essentially of the following:

1. A steel reactor surrounded by a steel jacket and a set of heating coils.
2. Several tube furnaces for the purpose of heating the incoming

natural gas. They were filled with soft steel rivets to increase the heating zone surface area.

3. The initial oil receiver, cooled to room temperature.
4. An ice water bath and receiver.
5. A demister filled with glass wool to remove the light uncondensable oils from the gas stream.

A series of thermocouples recorded the temperature in the retort jacket, the sample bed, and in various locations in the gas heaters.

Experimental Procedure

In each test the sample used consisted of two hundred grams of oil shale with particles sized between one-half inch and one-fourth inch.

The system was first flushed with natural gas then the gas heaters were brought up to power. After the flow of hot gas was insured the reactor heater was turned on. By manual control of the powerstats the sample bed was raised to the desired temperature then held there for a period of from thirty to forty-five minutes.

The flow of natural gas was maintained at a constant level during the heating cycle. In several cases this was not possible due to the formation of constrictions in the natural gas tube heaters.

The following items were weighed in order to carry out a material balance:

1. the initial sample
2. the final residue
3. the liquid receivers
4. the liquid receivers plus any liquids recovered

Volumetric measurements were taken on all liquids collected. The oils recovered were tested for the specific gravity, A.P.I. gravity, and pour points according to standard ASTM methods.

Equipment for High Pressure Flow Study

The apparatus utilized was also designed and constructed by Miller in the course of his Ph.D. thesis work at the University of Utah, and it was thoroughly described and illustrated in his dissertation⁽⁵⁰⁾.

The equipment consisted essentially of:

- (1) a natural gas inlet, metering, and ballast system.
- (2) a 300-500 psig, two-stage air-cooled compressor.
- (3) a series of strip heaters to heat the incoming, pressurized natural gas.
- (4) a steel retort fitted with two heating coils and the usual complement of powerstats, controls, etc.
- (5) a series of receivers of various design and intent, and in the following order:
 - (a) the initial receiver, maintained at the same pressure as the retort, water cooled.
 - (b) a step down valve, at the same pressure as the retort on the upstream side and at atmospheric pressure on the downstream side.
 - (c) a water cooled tank heat exchanger.
 - (d) a cyclone separator to remove small suspended oil droplets by centrifugal action.

- (e) a demister of glass wool to remove any remaining oil mist.
 - (f) an exit gas metering system.
- (6) a complete set of thermocouples to measure the temperatures at various locations in the retort and in the inlet gas heaters.

Experimental Procedure.

The procedure used in the experiments was also basically the same as that used by Miller, with the exception of his use of holes drilled in the sample cores in order to record the temperatures in them with thermocouples. This investigator cut notches in the drill cores to accept the sample thermocouples.

Basically the experimental method involved bringing the retort up to the desired internal pressure with natural gas, followed by the heating cycle of the gas heaters and/or retort. While the heat was being applied, liquid and gas samples were taken from the various receivers.

The following measurements were taken in the course of an experiment:

- (1) the sample was weighed prior to the run
- (2) the residue was weighed after each run
- (3) the oil volume and weight were recorded as they were recovered from each receiver
- (4) the flow rate of the gases was recorded prior to their exit.

- (5) the oils recovered were tested for their specific gravities, API gravities, and pour points using the standard ASTM methods where possible. Some of them were analyzed for C, H, N, S, and O.

Results and Discussion for the Flow Experiments

The data are summarized for both the X-OS- and HP-OS- series of experiments in Table 26 - 28, Appendix A.

As shown in Table 12 the high pressure tests yielded 34 to 67 percent of the oil obtained by the United States Bureau of Mines Fisher Assay tests, with the upper figure resulting from a fourteen hour run at a maximum temperature of 350°C. The atmospheric flow tests on the other hand showed yields of from 41.5 to 97.5 percent of the Fischer Assay values, with the upper limit being obtained at 480°C. It is apparent, from these data, that when natural gas is used as a heating medium a sufficient portion of the sensible heat of the natural gas can be delivered to the sample bed to bring about kerogen decomposition and drive out satisfactory amount of oil. Satisfactory in this case includes yields of about sixty to seventy percent of Fischer Assay.

In the high pressure experiments HP-14 through HP-17 the gas flow rate and the power input to the gas heaters were raised sharply and the retort heaters were cut back to determine if higher natural gas flow rates would result in comparable increases in the rate of heat delivery to the oil shale.

Table 13 shows that the heating rate of the sample was, in fact, increased by the increased natural gas flow rate. The time necessary

Table 12

Effect of Temperature on Yield of Oil

High Pressure Flow Experiments							
Test	Temp. (T ^o C)	Pressure psig	Duration at T	Total Duration	Percent Yields by Weight		
					Oil	Fischer Assay	% of Fischer Assay
HP-OS-11	400	300	4.0	14	7.41	12.7	58.3
HP-OS-12	425	300	3.0	12	9.42	16.7	56.4
HP-OS-13	350	300	0.5	15	10.3	22.9	45.0
HP-OS-14	500	300	4.0	12	12.2	18.7	65.0
HP-OS-15	485	300	1.0	20	8.6	14.5	59.3
HP-OS-16	500	200	0.5	16	5.4	15.8	34.2
HP-OS-17	475	400	7.0	16	9.6	14.7	65.3
HP-OS-18	510	300	3.0	9	8.0	12.4	64.5
HP-OS-19	350	300	1.0	14	8.8	13.2	66.7
HP-OS-20	440	300	2.0	18		14.5	
HP-OS-21	420	300	4.0	60	10.0	18.9	52.9
Atmospheric Flow Experiments							
X-OS-22	425	atm.	0.5		13.8	16.7	82.6
X-OS-23	410	atm.	0.5	10	9.5	22.9	41.5
X-OS-24	460	atm.	0.5	4	11.7	18.7	62.6
X-OS-25	500	atm.	0.5	5	13.5	14.5	93.1
X-OS-26	480	atm.	0.5	2.5	15.4	15.8	97.5
X-OS-27	460	atm.	0.5		13.6	14.7	92.5
X-OS-28	510	atm.	0.5				

Table 13

Effect of Natural Gas Flow Rate on Heating Rate

Run	Max. Temp.	Flow Rate ft ³ /min	Time to Reach 400°C (hrs)	Oil Yield % of Fischer Assay	Oil Specific Gravity gm/cm ³	Fischer Assay Oil Specific Gravity gm/cm ³
HP-OS-11	400	0.2	12.	58.3	.870	.896
HP-OS-12	425	0.26	9.5	56.4	.863	.909
HP-OS-14	500	1.0	5.5	62.2	.882	.906
HP-OS-15	485	1.5	7.0	59.3	.885	.899
HP-OS-16	500	1.5-1.6	5.0	34.2	.891	.901
HP-OS-17	475	1.5-1.7	5.0	65.3	.889	.900
HP-OS-18	510	1.6-1.7	2.5	64.5	.887	.909
HP-OS-21	420	0.6-1.0	60.	52.9	.916	.907

to reach 400°C was cut from 12 to 2.5 hours. The slight increase in oil yield and oil gravity appeared to be a temperature effect rather than due to the increased heating rate, although the latter could have been a factor.

Figure 20 shows that heating curves for HP-OS-11 with a natural gas flow rate of about 1.5 to 1.7 cubic feet per minute. Thermocouple number five represents the sample temperature and thermocouple number nine gives the temperature of the bottom of the retort at the point where the natural gas entered. This point was about six inches below the bottom of the sample. In figure 20 is illustrated the wide difference of temperature between thermocouple locations five and nine at the low flow rate. This difference is narrowed considerably by the use of the higher flow rate in HP-OS-18 as shown in Figure 21. A natural gas temperature of 625°C was necessary to attain a sample temperature of 400°C when the low flow rate was used in HP-OS-11, but in HP-OS-18 a sample temperature of 505°C was attained using a natural gas temperature of about 510°C .

The narrowing of the separation between these two curves to the point where they coincide for all practical purposes indicates that the upper limit for the gas flow rate is probably slightly above the flow rate used in HP-OS-18.

Several modifications to the collection equipment were necessary at the higher flow rates because a good deal of fine oil mist was getting past all the receivers and even through the glass wool demister. The flow rate was great enough to mechanically force the glass wool in the demister over to one side of the glass tube in which

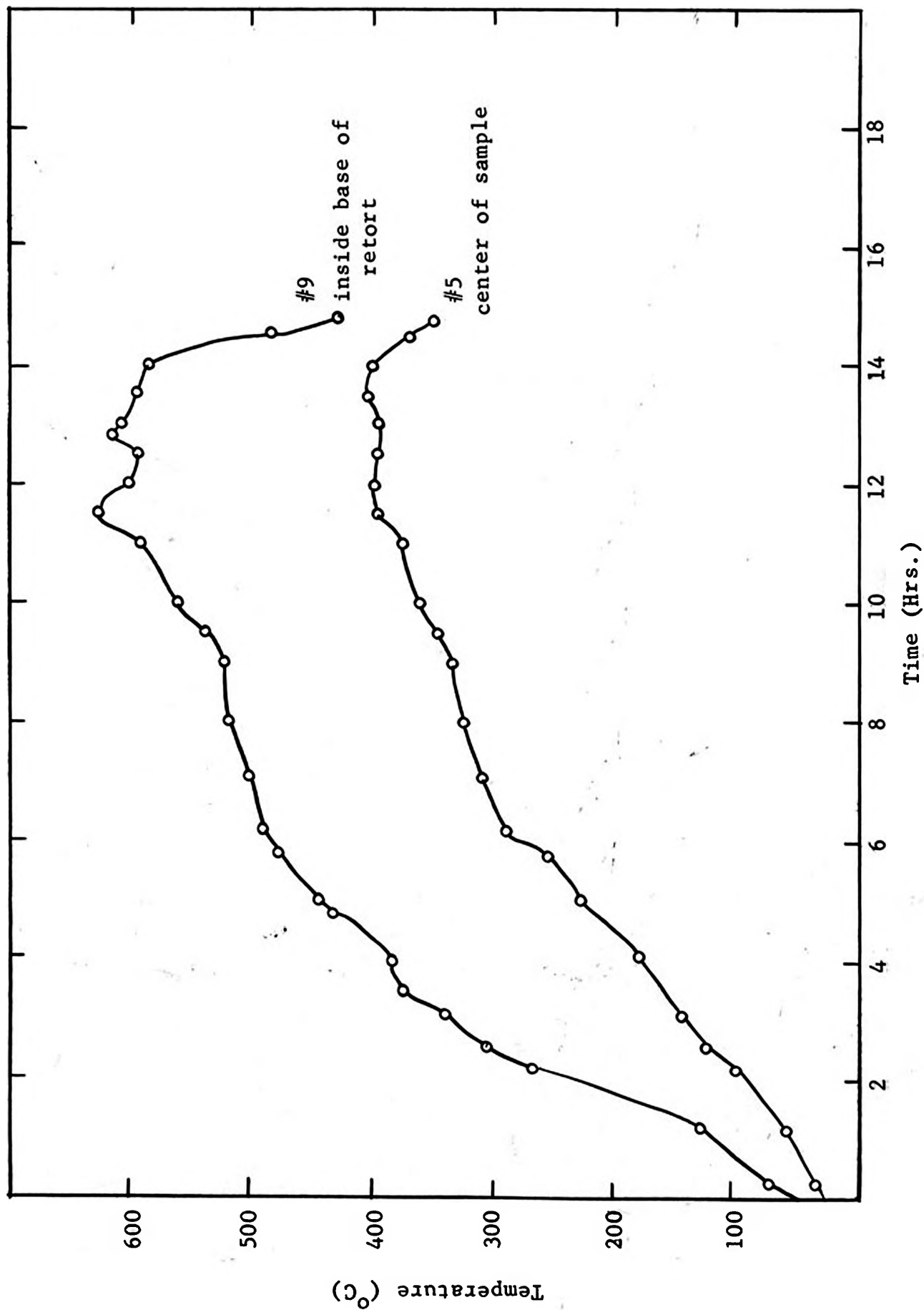


Figure 20. Retort and sample temperature versus time

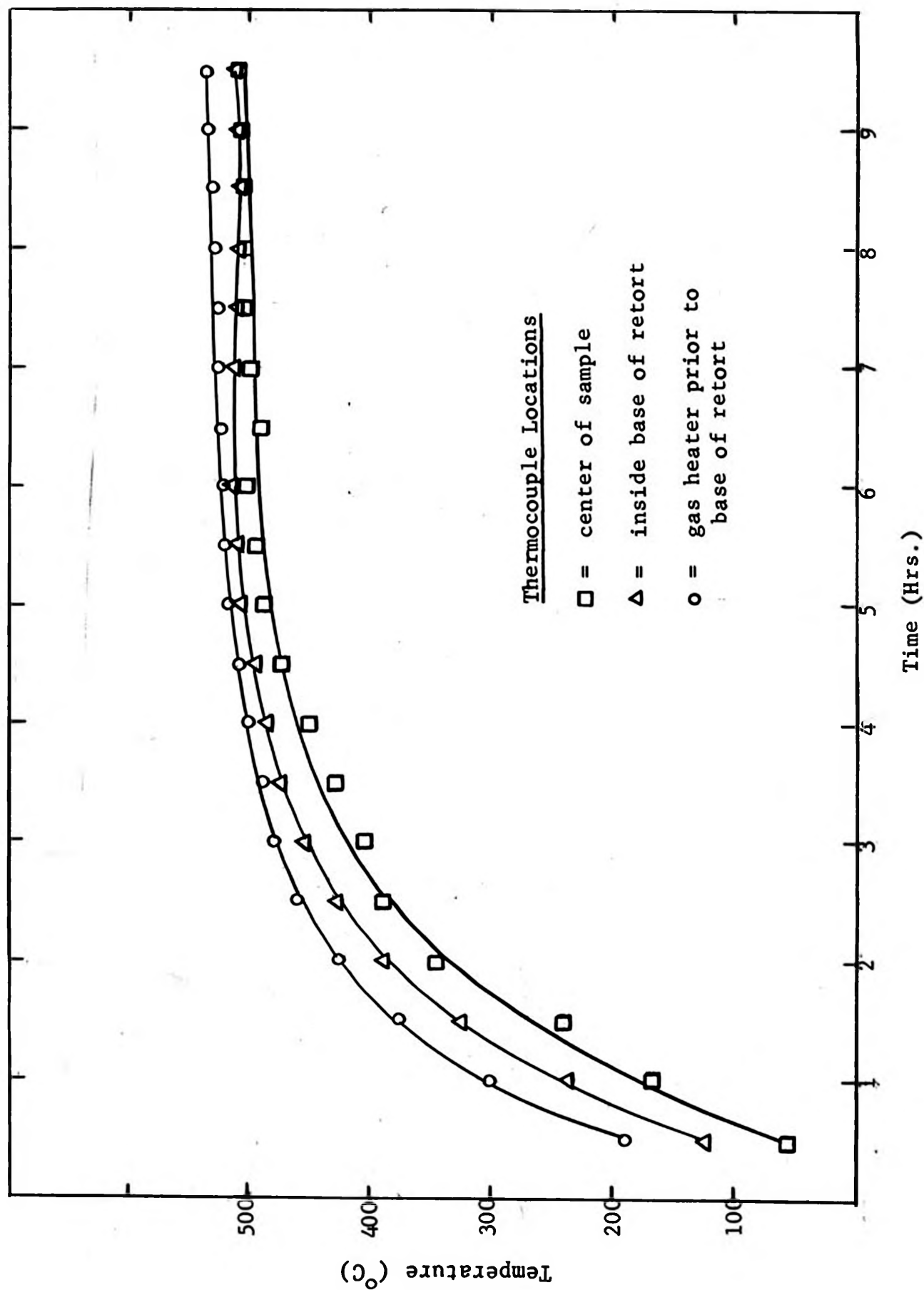


Figure 21. Retort and sample temperatures versus time

the wool was contained. This did not prevent some of the oil from getting past the glass wool, however.

In Figure 22 is shown the effect of the heating rate on the temperature at which the oil appeared. The volume of oil recovered is plotted versus the temperature. This was possible because in the high pressure flow tests the oil was collected in fractions as the temperature increased.

It is apparent that when the slower heating rates were used the oil appeared at lower temperatures. This effect was probably diminished somewhat because the higher heating rates were obtained by greatly increasing the natural gas flow rate. This would have the effect at high flow rates of mechanically sweeping the oil from the retort. The oil in the low flow rate or low heating rate runs probably lingered in the retort for a longer time than in the high temperature runs, thus delaying its appearance until a later time when the temperature was a bit higher.

Table 14 lists the heating rate along with the temperature when $24 \text{ ml/gm} \times 10^{-3}$ of oil recovered in each of the high pressure tests shown. The $24 \text{ ml} \times 10^{-3}/\text{gm}$ of oil was approximately 40 milliliters in each case, and was chosen arbitrarily. The 40 ml. of oil appeared at 352 and 362°C in HP-OS-12 and HP-OS-11 when the lowest heating rates are used and from 405 to 462°C when the higher rates were used in HP-OS-14, 16, 17, and 18. HP-OS-15, with an intermediate heating rate, gave 40 ml. of oil at the intermediate temperature of 395°C.

Karrick, who heated oil shale in the conventional manner also found that the product oils appeared earlier when a lower heating rate was used (36).

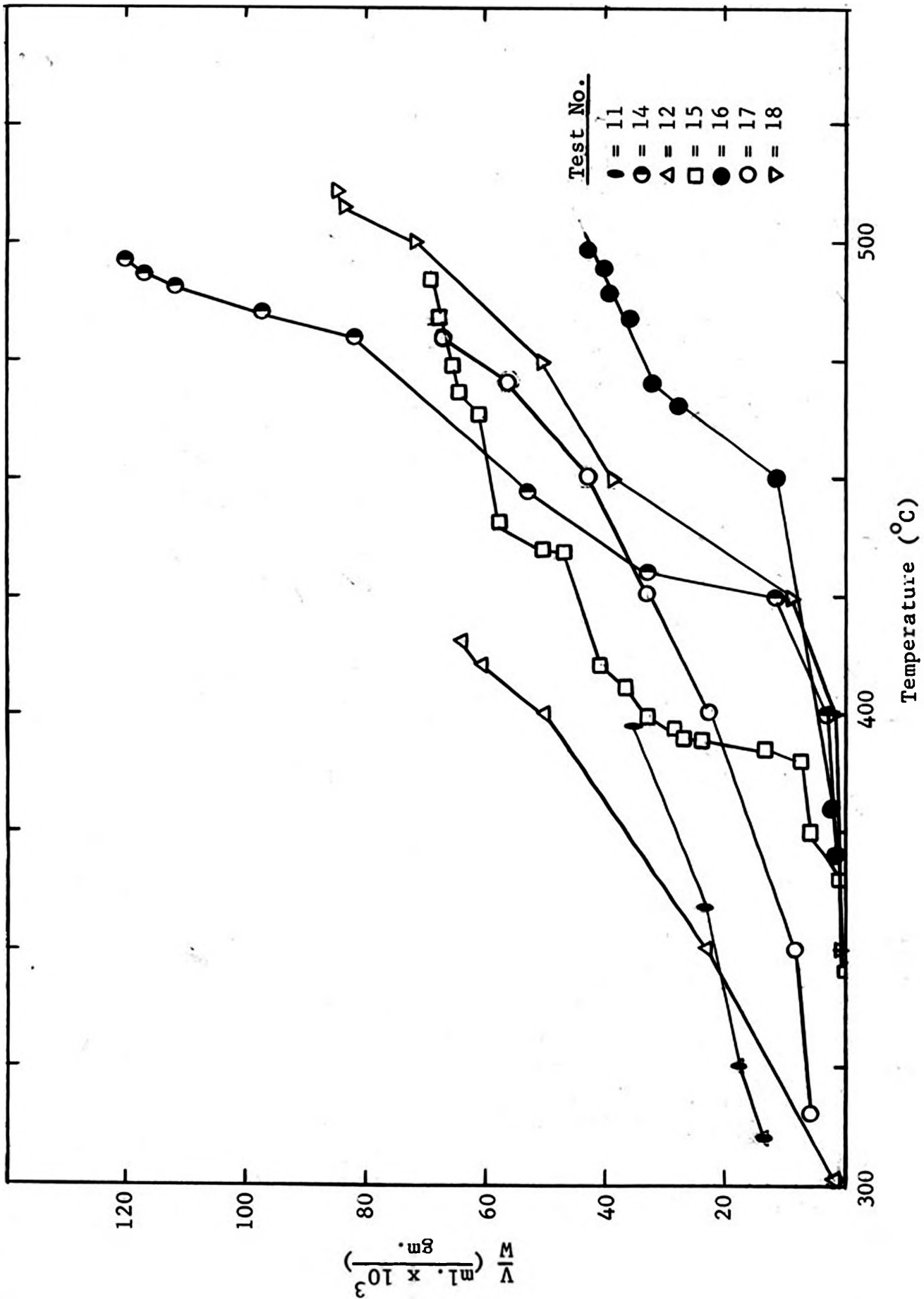


Figure 22. Oil yield versus temperature

Table 14

Effect of Heating Rate on Temperature of Oil Appearance

Run	Time to Reach 400°C. (hrs.)	Temperature when 40 ml. of oil were recovered. (°C)
HP-OS-11	12.	362
HP-OS-12	9.5	352
HP-OS-14	5.5	430
HP-OS-15	7.0	395
HP-OS-16	5.0	462
HP-OS-17	5.0	405
HP-OS-18	2.5	438

Shale Oil Properties

In several of the high pressure flow experiments the liquid samples were collected as fractions. Table 15 lists the samples collected in HP-OS-300-14 along with the oil properties of the fractions and the temperature at which they were collected.

Table 15

Effect of Temperature on Shale Oil Properties

Sample	Temp. °C.	Oil Specific Gravity gm/cm ³	%C	%H	C/H	%S	%N	%O
HP-14-2	370		83.9	12.5	6.71	1.15	.65	1.84
HP-14-3	400		84.0	12.6	6.66	1.16	.6	1.36
HP-14-4	425	.877	84.8	12.3	6.89	1.31	.83	1.08
HP-14-5	430	.873	84.6	12.6	6.71	1.61	.91	1.24
HP-14-6	450	.877	85.0	12.2	6.96	1.30	1.11	1.01
HP-14-7	480	.877	84.5	12.0	7.04	1.27	1.46	1.11
HP-14-8	485	.884	84.5	12.0	7.04	1.04	1.41	1.11
HP-14-9	490	.890	84.6	11.9	7.11	1.24	1.01	1.07
HP-14-10	493		84.2	11.8	7.14	.96	1.08	1.11
HP-14-13	acetone/dry ice trap		84.7	13.7	6.19	1.07	.29	1.09

An examination of the table suggests that the lighter oil was produced early in the experiment, at the lower temperatures. As the

temperature was increased the more stable bonds began to cleave and larger fragments were broken from the kerogen matrix. Also polymerization of the bitumen could have been initiated causing an increase in the gravity of the oil.

The low temperature fractions were low in sulfur and nitrogen. The nitrogen and sulfur contents of the oil increased as the temperature increased and both appeared to go through maxima, sulfur at about 430°C and nitrogen at about 480°C. The oxygen content decreased with increasing temperature. This suggests that most of the nitrogen and sulfur are probably present in the kerogen as components of potentially stable species, for example thiophene, pyridine, and their homologs. Oxygen probably is predominately found in less temperature stable side groups and thus appears earlier in the oil.

Jones and Dickert found that sulfur and nitrogen were present in kerogen mainly as heterocyclics and not as linking agents between ring groups while oxygen was present in two forms; one a heterocyclic material which is relatively stable and the other in side groups which are relatively unstable and which, therefore, appeared in the low temperature oil⁽³⁹⁾.

Thorne⁽⁶⁴⁾ and Dimmen⁽¹⁷⁾ found that with increasing temperature the nitrogen content of the shale oil increased to a maximum and then decreased.

These authors used conventional heating methods and atmospheres, that is their research did not involve the use of methane or natural gas as either a heating medium or as an atmosphere.

The C/H ratio of the oil increased with temperature as shown in Table 15. This indicates that the low temperature oil contained a higher degree of saturation than that collected at later temperatures. This would be the case if the kerogen had a nucleus consisting of aromatic and heterocyclic rings surrounded by less stable paraffinic side chains and heterocyclics.

The liquids taken from the dry ice/acetone trap were high in hydrogen, and low in nitrogen, oxygen, and sulfur. This suggests that the light mist which passed through the receivers was primarily straight chain paraffin in nature, and low in sulfur, nitrogen, and oxygen.

Comparison of Low and High Pressure Flow Studies

A comparison of the low and high temperature material balances points out some important differences. In Table 16 are shown the oil yields, gas yields, and oil specific gravities of the low and high temperature series. It is apparent that where the higher pressure flow system was used there were decreased oil yields, increased amounts of gas production, and lower oil specific gravities.

This suggests that where the high pressure flow system was used there was a greater degree of secondary cracking and/or a lower degree of secondary polymerization of the reactive species produced by the kerogen decomposition than in the low pressure flow equipment. In the high pressure flow retort the natural gas through-put was much higher than in the low pressure flow system and this might have acted to carry the reactive fragments from the hot zone before they could polymerize on the walls. It appears that the tendency for the increased

Table 16

Comparative Oil Yields and Qualities for the Flow Tests

High Pressure Flow Study

Test	Temp. °C.	Percent Yields of Fischer Assay		Oil Specific Gravity gm/cm ³	Fischer Assay Oil Specific Gravity gm/cm ³
		Oil	Gas + Losses		
HP-OS-11	400	58.3	198	.870	.896
HP-OS-12	425	56.4	174	.863	.909
HP-OS-13	350	45.0	429	.857	.903
HP-OS-14	500	65.0	163	.882	.906
HP-OS-15	485	59.3	193	.885	.899
HP-OS-16	500	34.2	288	.891	.901
HP-OS-17	475	65.3	156	.889	.900
HP-OS-18	510	64.5	196	.887	.909
HP-OS-19	350	66.7	123	.844	.895
HP-OS-20	440				.900
HP-OS-21	420	52.9	222	.916	.907

Atmospheric Flow Study

X-OS-22	425	82.6	74.3	.915	.909
X-OS-23	410	41.5		.905	.903
X-OS-24	460	62.6	32.3	.903	.906
X-OS-25	500	93.1	74.3	.914	.899
X-OS-26	480	97.5	132	.915	.901
X-OS-27	460	92.5	119	.889	.900
X-OS-28	510				.909

pressure to initiate polymerization was offset by the high sweep rate of the natural gas. In any case, the pressure used was only a small increase over atmospheric.

It must be noted that the yield of water in the low pressure tests was often several hundred percent larger than expected. When a drier was placed on the natural gas inlet line the percentage yield of water dropped to a reasonable level. The presence of water in the retort, as noted in the high pressure static study in the D-OS series, was accompanied by an increased specific gravity of the oil. In the one low pressure flow study where the drier was used to remove the water from the natural gas line the value of the specific gravity was $.889 \text{ gm/cm}^3$, at 85°F ; the same value as the oil from the high pressure flow run at the same temperature. In the other low pressure flow experiments at the same temperature and where water was present the specific gravity of the oil was $.915$ at 96°F and $.903$ at 82°F . This suggests that the removal of the water may have favorably affected the gravity of the oil, although this is not conclusive.

Penetration of Heated Natural Gas Into Sample

Porosities and permeabilities of the raw oil shale and the residue remaining after an experiment at 480°C are shown in Table 17. Figures 23-26 show photomicrographs of several raw oil shale and several oil shale samples after retorting. The photographs were taken both perpendicular and parallel to the major axis of the sample cores as indicated. The valleys which are visible are vacancies remaining after volatile matter was driven out. The large fissures which were visible

Table 17

Porosity and Permeability of Oil Shale

Test	Sample Description	Temperature °C	Pressure psig	Permeability Horizontal	Permeability Vertical	Porosity %
	Raw Shale			0.0	0.0	0.8
HP-8	Spent Shale Top of Reactor	480	300	125	4.7	44.7
HP-6	Spent Shale Top of Reactor	485	300	5.7	4.3	30.6
	Bottom of Reactor	485	300	14	2.8	41.5

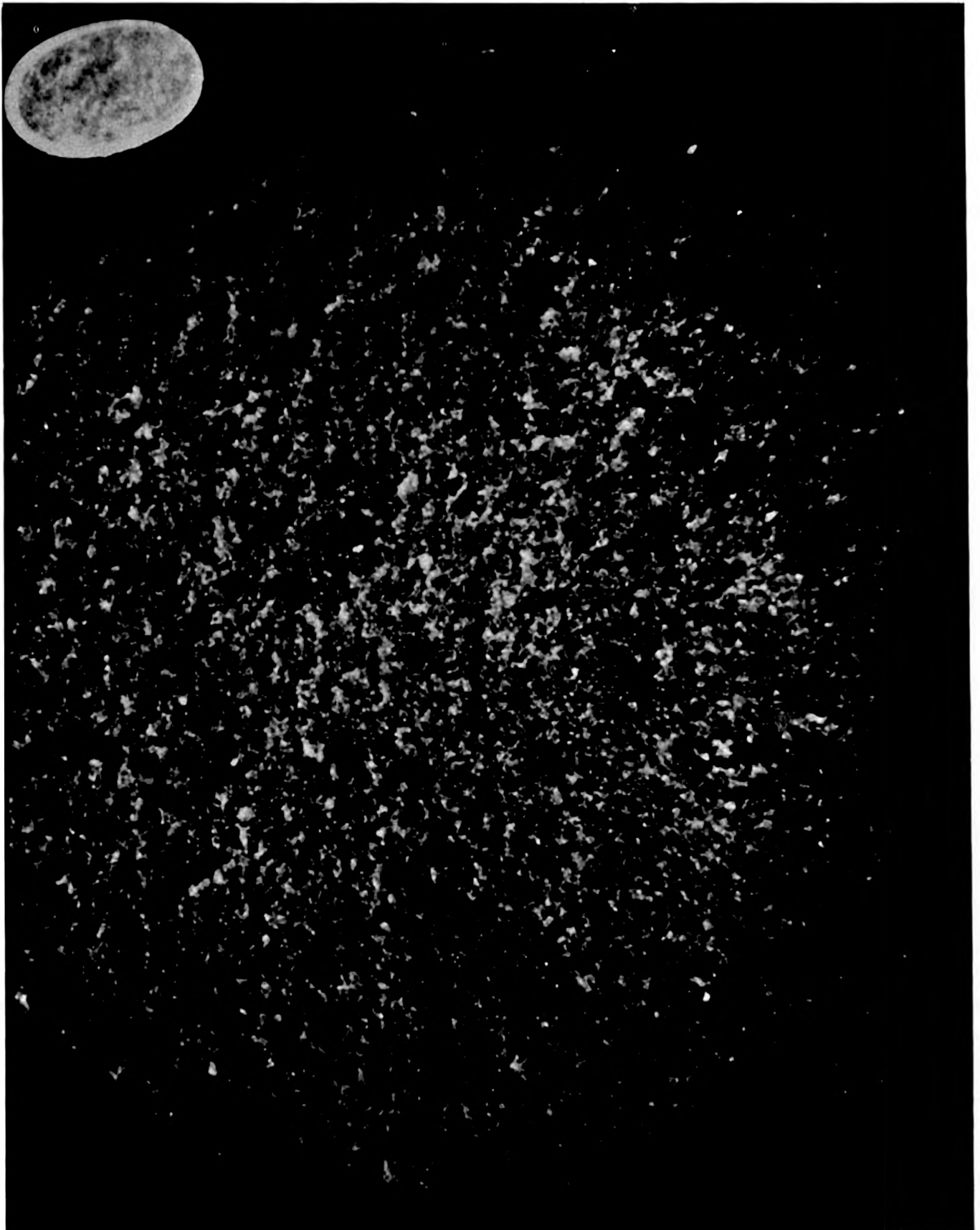


Figure 23. Unheated Oil Shale. Photomicrograph taken parallel

to main drill core axis.



Figure 24. Heated Oil Shale. Photomicrograph taken parallel

to main drill core axis.

Digital Image © 2006, Duane John Johnson. All rights reserved.

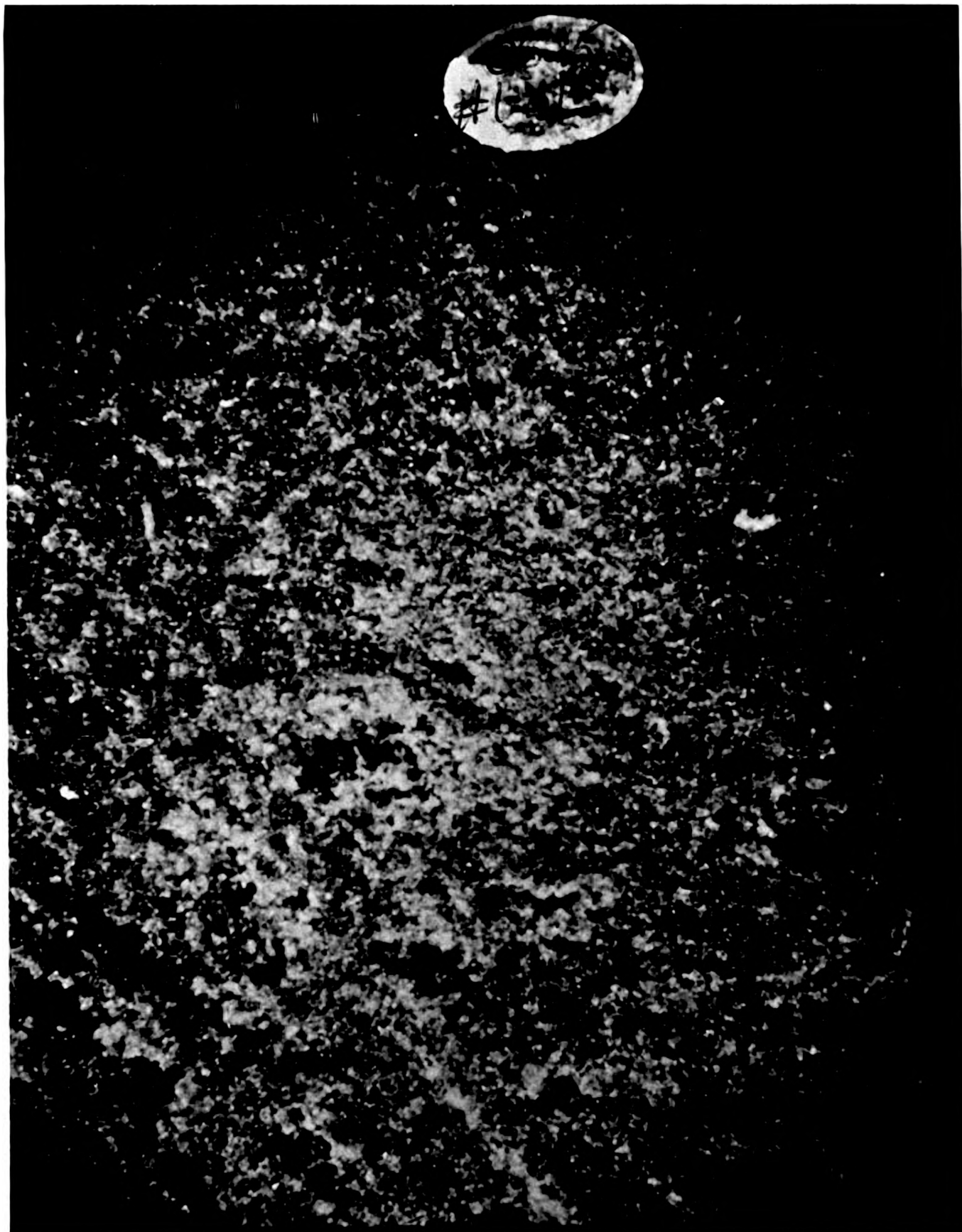


Figure 25. Unheated oil shale. Photomicrograph taken perpendicular to main drill core axis.



Figure 26. Heated oil shale. Photomicrograph taken perpendicular to main drill core axis.

to the naked eye were avoided in making the photomicrographs, and the photographs represent the surface of the spent shale which was smooth to the naked eye. Figures 23 and 24 are taken of the core side view and 25 and 26 are of the core end view.

Table 17 and Figures 23 through 26 indicate that as a result of heating the raw shale with pressurized natural gas the spent shale becomes considerably more pervious to further gas and heat penetration. The photographs show no flowing or fusing of the residue; the increases in porosities and permeabilities also suggest a retention of a rigid skeleton. The residue from the flow experiments had the same visual appearance as the original sample, with the exception that it was considerably blacker, suggesting a carbon residue, and was slightly fractured. In several cases the residue was more fragile and crumbly than the original oil shale sample.

Summary of Flow Tests

In summary, it is apparent that heated natural gas can act as a thermal medium for the decomposition of kerogen at up to 300 psig and 510°C (400 psig at 475°C) retort conditions. These data also suggest that in the range of about .2 to 1.7 cubic feet per minute for the natural gas input flow rate the higher value will increase the heat input greatly with no apparent decrease in oil yield or quality. The value of 1.7 cubic feet per minute produces almost identical temperature-time profiles for the sample and the natural gas inlet, indicating that 1.7 is probably approaching the upper limit where an increase in gas flow rate will result in an equivalent increase in sample heating rate.

The high flow rates necessary to produce the high heating rates resulted in the production of significant amounts of a fine oil mist in the exit gas stream which were very difficult to remove from the carrier gas. The mist, at least in part, passed through cyclone, dry ice/acetone, cold water, and glass wool demister collectors.

Low heating rates brought about the evolution of oil at lower temperatures than when higher heating rates were used. It is not possible to interpret the effect of the heating rate on final oil yields or qualities because the final temperatures of the tests were not the same.

The lower molecular weight oil came over at the lower temperatures, with the specific gravity of the oil increasing with increasing temperature. The C/H ratio increased with temperature, the oxygen decreased, and the nitrogen and sulfur appeared to go through maxima. This suggests certain things about the nature of the kerogen and its decomposition, namely that the oil which came over early and at low temperatures was probably short chain, paraffinic in nature and the saturation of the oil decreased with temperature. The nitrogen and sulfur are probably present in the kerogen primarily as stable heterocyclics such as pyridine, thiophene and their homologs. The oxygen is probably present both as less stable functional groups and as oxygen-containing molecules of high stability, and it therefore appears early in the oil.

The porosity and permeability of the oil shale was increased as the result of the thermal treatment with natural gas at elevated

pressures. No fusing of the residue was noted at sample temperatures of up to 510°C and 300 psig (475°C at 400 psig).

The use of pressure resulted in decreased oil yields, decreased oil specific gravities, and increased amounts of gas production. It is not clear whether this is a pressure effect or an effect of the different retorts and flow rates used.

The low pressure experiments produced higher oil yields and higher oil specific gravities. The high percentage of water in the inlet gas may account in part for these results.

IN SITU STUDY

Subsequent to the bench-scale experiments an in situ pilot study was initiated in the oil shale beds of the Piceance Creek basin of Colorado. Drill holes were bored into the oil shale beds and heated natural gas was introduced, under pressure, into the holes. After a lengthy heating period in which the bed was brought up to temperature a high quality crude oil was recovered in barrel quantities.

Tables 18 and 19 illustrate the high quality of the crude oil recovered as compared to that produced with several conventional retorts. The unusually high API gravities, low pour points, and low sulfur, nitrogen, and oxygen contents are shown.

The gas chromatographic spectra shown in Figures 27 and 28 illustrate the similarity between the in situ crudes and a crude petroleum from Pennsylvania. The latter is unique in that it contains much larger amounts of the gasoline fraction than the average crude petroleum. The gas chromatographic spectra also strongly resemble those of the laboratory experiments. This is apparent when Figures 13 and 27 are compared. The peak distributions and the upper limit of the carbon numbers are nearly identical.

Table 18

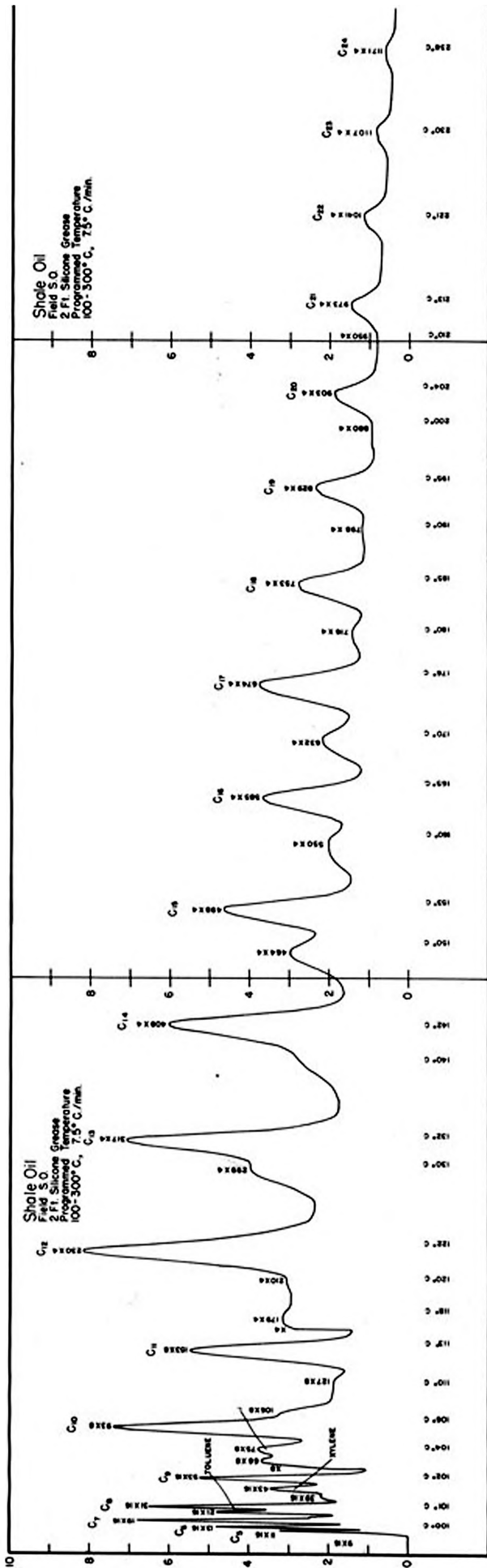
Shale Oil Analyses

Shale Oil	Retort	%C	%H	%N	%S	%O	C/H
Kimmeridge, England	Pumpherstons	80.9	8.6	1.4	6.5	2.6	9.4
Colorado (USBM)	N.T.U.	89.5	11.3	1.77	0.75	1.63	7.48
Colorado (Equity)	U. of U.	83.9	12.5	0.65	1.15	1.84	6.71
Colorado (Equity)	In Situ	85.3	13.4	0.53	0.49	0.55	6.36

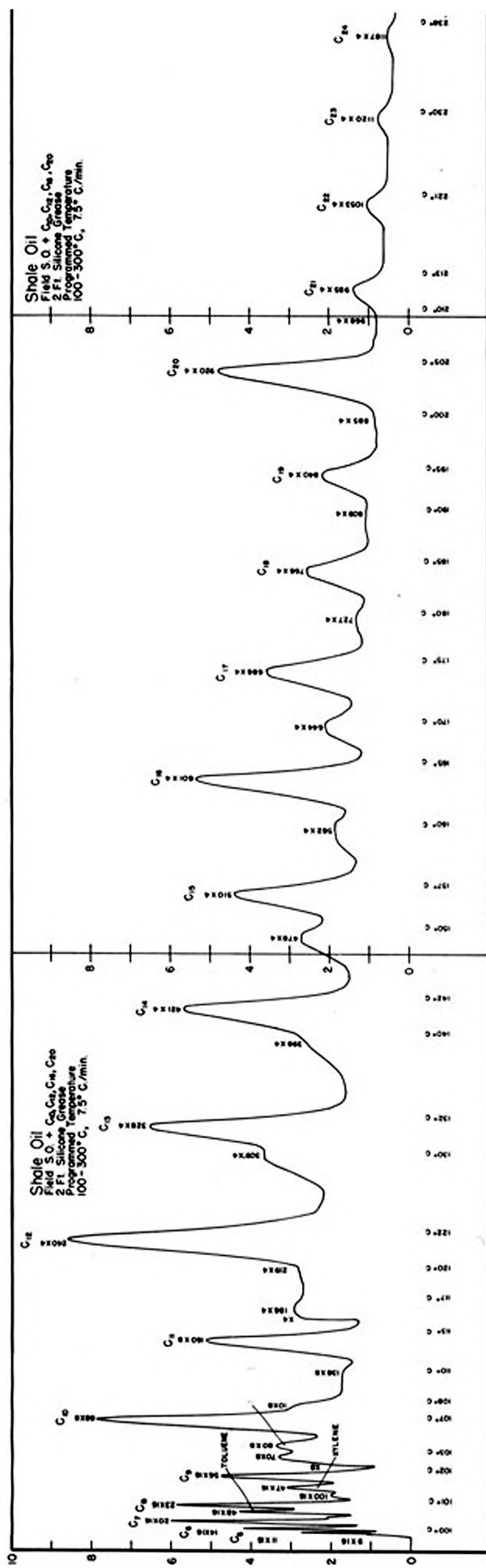
Table 19

Properties of Crude Shale Oils

Location	Retort	Gravities Specific	API Gravities	Pour Points
France	Marceaux	gm/cm ³		30°F
Colorado	Fischer	.925	21.5	80°F
Colorado	NTU			90°F
Colorado	Equity-In Situ	.822	40.6	-20°F
Colorado	Equity-In Situ	.820	41.2	<0°F
Colorado	Equity-In Situ	.813	42.5	

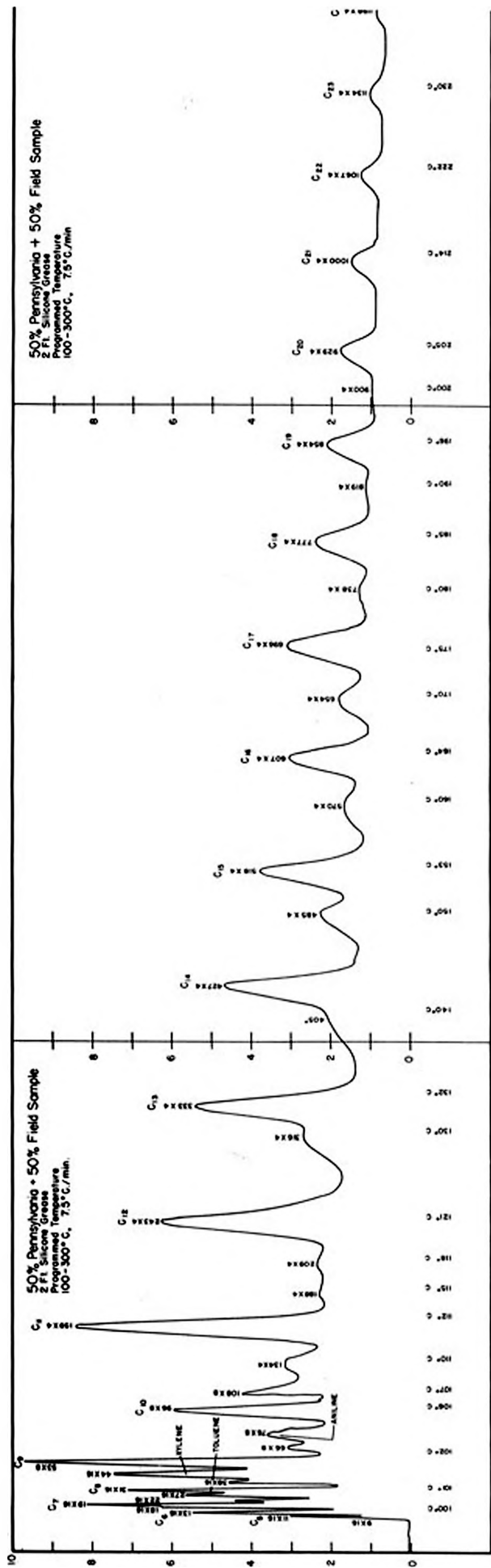


a

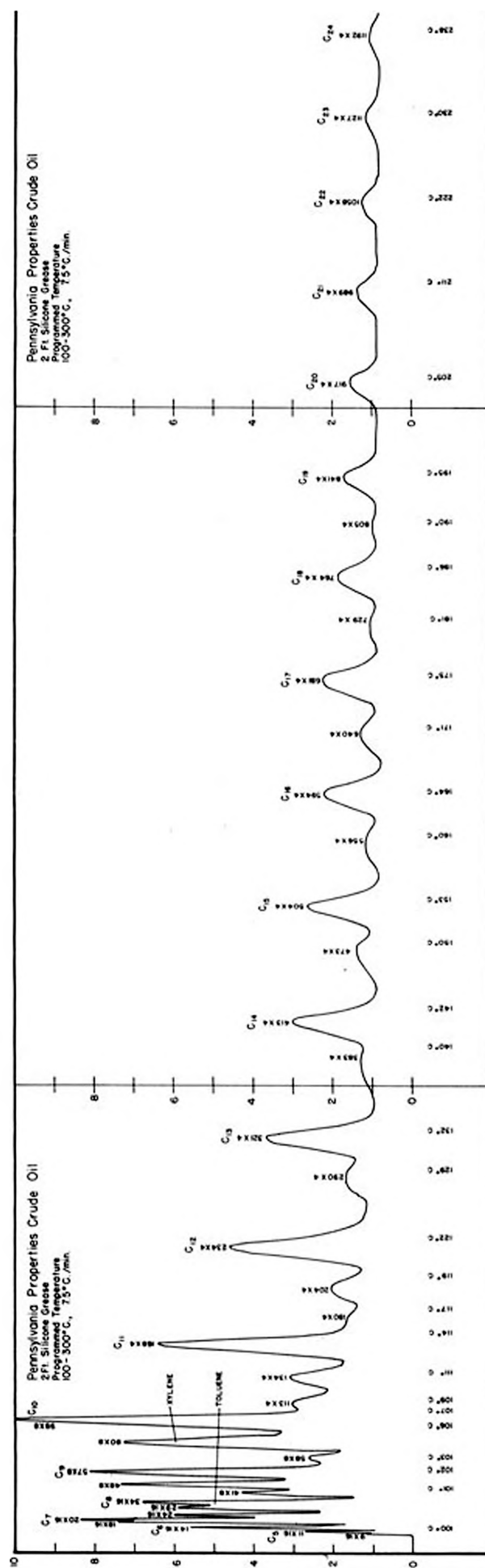


b

Figure 27. Chromatograms (a) of shale oil (b) of shale oil with standards added.



a



b

Figure 28. Chromatograms (a) of Pennsylvania Petroleum and shale oil mixture (b) of Pennsylvania Petroleum.

SUMMARY

This summary will draw from the work of all the various series of experiments D-OS, B-OS, C-OS, X-OS, and HP-OS series, and from the evidence collected in the in situ tests in the field.

Kinetics and Mechanisms

Several important conclusions concerning the kinetics and mechanisms of decomposition of oil shale can be drawn from the data collected and also from the work of previous investigators.

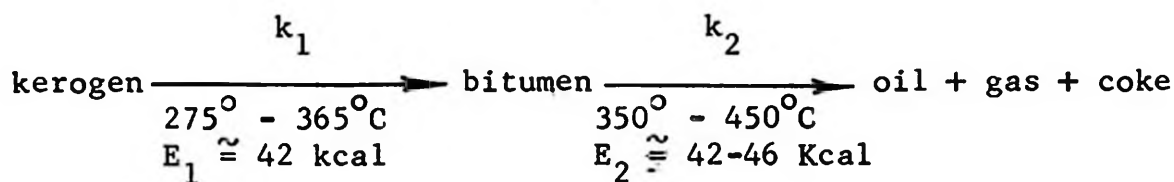
In the past, the investigators of oil shale decomposition kinetics monitored the increase in weight of gas, oil, and bitumen produced in the reaction. This was shown to be in error because the bitumen was not in steady state conditions and they were actually mixing two steps in a consecutive reaction.

Allred found unique activation energies for the high temperature process, indicating a change in mechanism at higher temperatures.

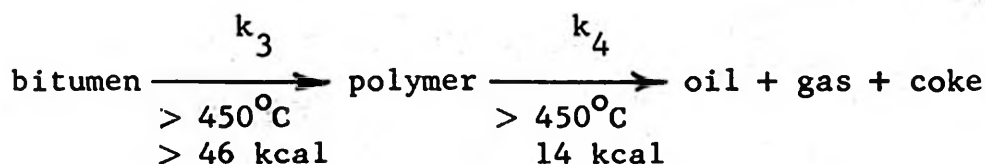
Based on the above considerations it is apparent that the simple two step mechanism proposed by McKee and Lyder is not adequate.

A new kinetics model can be proposed from the data available at this time. This mechanism is discussed in the kinetic section and it consists essentially of the following:

- a. At low temperatures the kerogen decomposition proceeds in the manner suggested by the earlier investigators, that is



b. At higher temperatures a reaction parallel to k_2 is initiated and proceeds as follows:



The crossover point from the low temperature to the high temperature mechanism is about 450°C . At the highest temperatures the reaction is passing predominately through the polymerization path but is under diffusion control. When the boundary of about 450°C is reached a polymer begins to form. When the polymer begins to decompose later the volatile products are too great in number to escape through the available vacancies and as a result the kinetics begin to come under diffusion control. When a high temperature is used it must be sustained in order to supply sufficient energy for the cracking of the polymer. Low temperature decompositions are accompanied by little polymerization as indicated by the unusually low specific gravity and pour point of the oil collected in the research for this paper. A high flow rate resulted in decreased oil specific gravities, suggesting that polymerization was decreased by sweeping the reactive species from the hot zone.

In the kinetic work for this paper a first order treatment of the gas evolved during the pyrolysis runs resulted in a low value of 27 kcal/gm-mole. There was also considerable scatter of the data. Hubbard

and Robinson's data gave acceptable values for the activation energy when the gas + oil was plotted versus time. However, when their data for the gas alone were treated a value of 22 kcal/gm-mole was obtained. Evidently while the kinetic treatment of the data for the gas alone gives good first order plots the energies resulting do not reflect the actual situation. The rate of gas evolution evidently does not follow parallel to that of decomposition, but is dependent upon a varying bitumen concentration. A consistent set of activation energies is obtained from the data of various researchers if they are interpreted in terms of the proposed model.

Natural Gas as a Heating Medium For Oil Shale

Sufficient sensible heat can be delivered from heated natural gas to oil shale to bring about shale oil production in adequate quantities. The yield of oil from the HP-OS and X-OS experiments was from 34 to 97.5 percent of the Fischer assay yields. It was also noted in these tests that increases in the flow rate of the heated natural gas resulted in comparable increases in the sample heating rate. This continued until a threshold of about 510⁰C was reached at which the natural gas and the sample temperatures coincided. At this point the natural gas flow rate was about 1.5 to 1.7 cubic feet per minute. Of course, these values are only valid for the system used.

The use of heated natural gas in the in situ tests in the Piceance Creek Basin resulted in a crude shale oil in barrel quantities.

Effect of Heating Rate on Appearance of Oil

When the higher heating rates were used in the laboratory flow experiments the appearance of the oil was delayed considerably. As shown in detail in the section treating the flow-tests, when heating rates of from 33 to 42°C per hour were used 40 ml. of product oils appeared at from 352 to 362°C. When heating rates of from 80 to 160°C per hour were used the same amount of oil did not appear until from 405 to 462°C.

Oil Quality and Oil Yields

The crude oil produced in these studies was of very high quality as compared to that collected from retorts commonly employed in the destructive distillation of oil shale. In all the series of experiments the quality of oil is favorably compared to that produced in the United States Bureau of Mines Fischer Assays and to the product oils from a number of commercial oil shale retorts such as the Pumpherson, Union, etc.

Periodically oil samples from the Equity Oil Company pilot in situ study were tested according to ASTM methods. The results indicate a very high quality crude oil. Gas chromatographic spectra indicate a strong similarity between the in situ samples and a crude petroleum taken from Pennsylvania. This was a paraffin based crude and was unusually high in the gasoline fractions. The in situ crude oils had a high fluidity and would not be expected to offer any handling problems.

The crude oils from the laboratory and the in situ study were very low in sulfur, oxygen, and nitrogen.

Nature of the Shale Oil

The crude shale oils from the laboratory and the in situ tests were found to be of a low molecular weight, highly paraffinic nature and were low in nitrogen and sulfur. The oil from the flow studies in the laboratory decreased in saturation with temperature, increased in oxygen concentration, and the sulfur and nitrogen concentrations both passed through maxima. Gas chromatographic studies showed an upper chain length of about C₂₅ and osmometer studies in benzene gave an average molecular weight of about 200 to 250.

Effect of Water in the Retort

The presence of water in the retort brought about an increase in the average molecular weight of the oil. This trend was noted in the laboratory static and flow tests. However, the apparent deleterious effect of the water on the quality of oil can only be considered as an observation. There was not sufficient experimentation to warrant drawing a conclusion and a good deal of additional work is needed.

Rubberoid Stage in Kerogen Decomposition

Cane has definitely identified a rubberoid stage in the pyrolysis of rich torbanite kerogen, and there was some evidence of a rubberoid stage in the pyrolysis of the lean oil shale used in this study. However, there is a possibility that it is merely a two-phase plastic mixture of bitumen and shale.

BIBLIOGRAPHY

1. Allred, V. D., "Some Considerations of the Kinetics of Oil Shale Pyrolysis", Marathon Oil Company, 1965.
2. Anon, "Synthetic Liquid Fuels, Annual Report of the Secretary of the Interior for 1949", U. S. Bur. Mines, Rep. Invest. 4652, 1949.
3. Ball, J. O., and Barb, C. F., "Survey of Bitumen Analyses and Extraction Methods", Colo. School Mines Quart. 39 (1), 71, 1944.
4. Bell, H. S., Oil Shale and Shale Oils, "Characteristics of Oil Shale and Shale Oils", Van Nostrand, 1948.
5. Bischoff, F., Radex Riendschar, 8, 1949.
6. Blackburn, C. O., Colo. School Mines Quart. 19 (2), 9, 1924.
7. Bradley, W. H., "Limnology and the Eocene Lakes of the Rocky Mountain Region", Bull. Geol. Soc. Am., 59, 635, 1948.
8. Bradley, W. H., "Origin and Microfossils of the Oil Shale of the Green River Formation of Colorado and Utah", Geol. Surv. Paper 168, 1931.
9. Brantley, F. E., Cox, R. J., Sohns, H. W., Barnet, W. I., and Murphy, W. I. R., "High Temperature Shale Oil", Ind. Eng. Chem., 44, 1952.
10. Cane, R. F., "A Note on the Chemical Constitution of Torbanite Kerogen", J. Soc. Chem. Ind., 65, 412, 1946.
11. Cane, R. F., "The Mechanism of the Pyrolysis of Torbanite", Oil Shale and Cannel Coal, Vol. 2, The Institute of Petroleum, 1950.
12. Cane, R. F., "The Chemistry of the Pyrolysis of Torbanite", Australian Chem. Inst., Jour. Proc., 15, 62, 1948.
13. Carlson, A. J., Inorganic Environment in Kerogen Transformation, Univ. of Calif. (Berkeley) Publ., 295, 1937.
14. Conley, J. E., Am. Inst. Mining Met. Eng., Tech. Publ. 1037, 1939.
15. Craig, E. H. C., Proc. World Eng. Congr., 32, 1, 1929.

16. Dannenberg, R. O., and Matzick, A., "Bureau of Mines Gas-Combustion Report for Oil Shale, A Study of the Effects of Process Variables", U. S. Bur. Mines, Rept. Invest., 5545,
17. Dineen, G. U., Effect of Retorting Temperature on the Composition of Oil Shale", Chemical Engineering Progress Symposium Series 54, 61, 33, Am. Inst. Chem. Eng., 1965.
18. Dineen, G. U., Vanmeter, R. A., Smith, J. R., Bailey, C. W., Cook, G. L., Allbright, C. S., and Ball, J. S., "Composition of Shale Oil Naphtha", U. S. Bur. Mines, Bull. 593, 1953.
19. Diricco, L., and Barrick, P. L., "Pyrolysis of Oil Shale", Ind. Eng. Chem., 48, 1316, 1956.
20. Down, A. L., and Himus, G. W., "A Preliminary Study of the Chemical Constitution of Kerogen", J. Inst. Petrol., 27, 426, 1941.
21. Dulhunty, J. A., "Occurance and Origin of Australian Torbanite", Oil Shale and Cannel Coal, Vol. II., Manson House, London, 155, 1951.
22. Engler, C., Das Erdol, 1913.
23. Esin, O. A., Geld, P. U., and Popel, S. I., J. Appl. Chem. U.S.S.R., 22, 354, 1949.
24. Franks, A. J., and Goodier, B. D., "Preliminary Study of the Organic Matter of Colorado Oil Shales", Colo. School Mines Quart., 17, 4, Supp. A, Oct. 1922.
25. Frost, I. C., and Stanfield, K. E., "Method of Assaying Oil Shale by a Modified Fischer Retort (Revision of U.S.B.M. R.I. 3977)", U. S. Bur. Mines, Rept. Invest. 4477, 1949.
26. Gavin, M. J., "Oil Shale and Historical, Technical, and Economic Study", U. S. Bur. Mines Bull. 210, 1924.
27. Gould, Douglas, "The Destructive Distillation of Oil Shale", Master's Grad. Thesis, Dept. of Metallurgy, Univ. of Utah, 1922.
28. Harding, E. P., "Distribution of Sulfur in Oil Shale III", Ind. Eng. Chem., 21, 9, 818, 1929.
29. Harding, E. P., and Thordarson, W., "Distribution of Sulfur in Oil Shale", Ind. Eng. Chem., 18, 7, 731, 1926.
30. Henderson, "The Origin of the Green River Formation", Bull. Am. Assoc. Petrol. Geologists, 8, 662, 1924.

31. Himus, G. W., "Observations on the Composition of Kerogen Rocks and the Chemical Constitution of Kerogen", Oil Shale and Cannel Coal, Vol. 2, Manson House, London, 592, 1951.
32. Himus, G. W., Petrol., 4, 9, 1941.
33. Hubbard, A. B., "Oil Shale Assay Method for Product Balance Studies", Fuel, 41, L, 49, 1962.
34. Hubbard, A. B., and Robinson, W. E., "A Thermal Decomposition Study of Colorado Oil Shale", U. S. Bur. Mines, Rept. Invest. 4744, 1950.
35. Hubbard, W. E., and Robinson, W. E., "Study of Preheating Colorado Oil Shale", U. S. Bur. Mines, Rept. Invest. 4787, 1951.
36. Hubbard, W. E., Smith, H. N., Heady, W. H., and Robinson, W. E., "Method of Concentrating Kerogen in Colorado Oil Shale by Treatment with Acetic Acid and Gravity Separation", U. S. Bur. Mines Rept. Invest. 4872, 1952.
37. Jensen, H. B., Barnet, W. I., and Murphy, W. I. R., "Thermal Solution and Hydrogenation of Green River Oil Shale", U. S. Bur. Mines, Bull. 533, 1953.
38. Jones, J. C., "Suggestive Evidence on the Origin of Petroleum and Oil Shale", Oil Eng. Finance, 3, 443, 452, 1923.
39. Jones, D. G., and Dickert, J. J., "Composition and Reactions of Oil Shale of the Green River Formation", Chem. Eng. Progr. Symp. Ser. 54, 61, 33, 1965.
40. Jukkola, E. E., Denilauler, A. J., Jensen, H. B., Barnet, W. I., and Murphy, W. I. R., "Thermal Decomposition Rates of Carbonates in Oil Shale", Ind. Eng. Chem., 45, 12, 2713, 1953.
41. Karrick, L. C., "Effects of Temperature and Time of Reaction in Distilling Oil Shales on the Yields and Properties of the Crude Oils", U. S. Bur. Mines, Rept. Invest. 2456, 1923.
42. Karrick, L. C., "Factors Affecting Products from Destructive Distillation of Oil Shales", U. S. Bur. Mines Rept. Invest. 2324, 1922.
43. Kinney, C. R., and Dell, M. B., "Action of Light on Tar Fractions", Ind. Eng. Chem., 45, 4, 809, 1953.
44. Maier, C. G., and Zimmerly, S. R., "The Chemical Dynamics of the Transformation of the Organic Matter to Bitumen in Oil Shale", Univ. of Utah Res. Invest. Bull. 14, 62, 1924.

45. Manning, P. D. U., "The Genesis of Oil Shale and its Relation to Petroleum and Other Fuels", Ph.D. Grad. Thesis, Univ. of Colo., 1927.
46. McKee, R. H., and Goodwin, R. T., "The Organic Matter in Oil Shales, I-Heat Effects", Ind. Eng. Chem. 13, 7, 613, 1921.
47. McKee, R. H., and Lyder, E. E., "The Thermal Decomposition of Oil Shales. II Determination of the Heat of Reaction Involved in Their Thermal Decomposition," J. Ind. Eng. Chem., 13, 8, 1921.
48. McKee, R. H., and Manning, P. D. U., "Shale Oil II, Gases from Oil Shale", Oil Bull. 13, 489, 729, 837, 1927.
49. Meyer, J. E., "Principles of Oil Shale Retorting", Oil Gas. J., 23, 21A, 92, 1924.
50. Miller, L. C., "The Use of Gaseous Thermal Medium In The Thermal Decomposition of Oil Shale," Ph.D. Thesis, Univ. of Utah, 1963.
51. Prien, C. H., "Oil Shale and Shale Oil", Oil Shale and Cannel Coal, Vol. II, Oil Shale Cannel Coal Conf. 2nd, Mansion House, London, 1950.
52. Robinson, W. E., and Lawler, D. L., "Constitution of Hydrocarbon-like Materials Derived from Kerogen Oxidation Products", Fuel, 40, 375, 1961.
53. Robinson, W. E., and Stanfield, K. E., "Constitution of Oil Shale Kerogen", Bibliography and Notes on Bur. Mines Research, U. S. Bur. Mines, Inf. Circ. 7968, 1960.
54. Schnackenberg, W. D., and Prien, C. H., "Effect of Solvent Properties in Thermal Decomposition of Oil Shale Kerogen", Ind. Eng. Chem. 45, 1956.
55. Schwab, Yvan, "Influence of Small Quantities of Impurities on the Thermal Dissociation of Dolomite", Compt. Rendu 224, 47, 1947.
56. Scott, J., "Petroleum Under the Microscope", Petrol. World, 17, 300, 346, 385, 1920.
57. Smith, I. W., "Analytical Method for Study of Thermal Degradation of Oil Shale", U. S. Bur. Mines Rept. Invest. 5932, 1962.
58. Stewart, D. R., "The Oil Shales of the Lothians, III, The Chemistry of Oil Shales", Mem. Geol. Surv. Great Britain, 163, 1912.
59. Stewart, R. G., and Trenchard, J., "The Destructive Distillation of Oil Shale", Colo. School Mines Quart., 18, 3, 6, 1923.

60. Theissen, R., "Origin and Composition of Certain Oil Shales", Econ. Geol., 16, 239, 1921.
61. Tisot, P. R., and Murphy, W. I. R., "Physical Structure of Green River Oil Shale", Chem. Eng. Progr. Symp. Ser. 54, 61, 25, 1965.
62. Tisot, P. R., "Physiochemical Properties of Green River Oil Shale", J. Chem. Eng. Data, 5, 558, 1960.
63. Thomas, G. W., "The Effect of Overburden Pressure on Oil Shale During Underground Retorting", Soc. Petrol. Eng., Preprint SPE 1272, Oct. 1965.
64. Thorne, H. M., Murphy, W. I. R., Stanfield, K. E., Ball, J. S., and Horne, J. W., "Green River Oil Shales and Products; Their Character, Processing Requirements, and Utilization", Oil Shale and Cannel Coal, Vol II, The Institute of Petroleum, 301, 1950.
65. Trager, E. A., "Kerogen and its Relation to the Origin of Oil Shale", Bull. Am. Assoc. Petrol. Geologists, 8, 301, 1924.
66. Wells, W. E., and Ruark, J. R., "Pilot-Plant Batch Retorting of Colorado Oil Shale", U. S. Bur. Mines, Rept. Invest. 4874, 1952.
67. Zimmerly, S. R., "The Chemical Dynamics of the Transformation of Organic Matter to Bitumen in Oil-Shale", Master's Grad. Thesis, Univ. of Utah. 1923.

APPENDIX

Table 20

U. S. Bureau of Mines Fischer Assay Results

Sample Identification	Location-Depth (feet)	yield		weight percent Residue	Gas & Losses	Specific Gravity gm/cm ³	Coking Tendency
		ml. oil	ml. water				
D-OS-1, 2	1122.3-1123.5	7.9	.66	86.3	4.8	.907	None
D-OS-4, 5	1116.3-1117.4	11.9	.4	83.7	4.0	.911	None
D-OS-7, 9, 10	1179.5-1181	11.4	1.1	82.4	5.1	.908	None
D-OS-12	1214 -1215	11.2	1.6	83.3	3.9	.909	None
D-OS-13, 14	1133 -1134.1	11.8	.9	84.4	2.9	.903	None
D-OS-15, 16, 17, 18, 19	1163 -1164.0	11.0	.9	84.8	3.3	.914	None
D-OS-21, 22, 23	1164.3-1165.3	10.6	.8	83.1	5.5	.910	None
D-OS-25	1165.3-1166.9	10.4	.7	82.2	6.7	.909	None
C-OS-1	Old land #2367	2.8	1.6	94.5	1.1	.910	None
C-OS-3	Old land #2341	1.3	1.5	96.3	.9		None
C-OS-2	Old land #2391	4.4	1.4	92.8	1.4	.883	None
B-OS-1	1048 -1048.5	13.4	1.0	80.4	5.2	.895	None
B-OS-2	1038 -1042.1	12.3	.9	81.0	5.5	.895	None
B-OS-3	1038.1-1039.0	12.7	.8	81.5	5.0	.895	None
B-OS-4	1037.1-1037.6	12.3	1.2	81.0	5.5	.901	None
B-OS-5, 6, 7	1175.1-1175.7	14.8	.6	79.7	4.9	.907	Slight
B-OS-8, 9, 10, 11, 12, 13	1162 -1163.7	16.5	.6	78.1	4.8	.906	Slight
B-OS-14, 15, 16	1174 -1175.1	16.5	.6	78.4	4.5	.906	Slight
B-OS-17	1176.4-1177.6	8.3	.3	88.8	2.6	.909	None
HP-OS-11, X-OS-21	1039.0	12.7	.8	81.5	5.0	.896	None
HP-OS-12, X-OS-22	1035.3-1036.1	16.7	1.2	75.1	7.0	.909	None
HP-OS-13, X-OS-23	1024.1-1025.2	22.9	.9	68.3	7.9	.903	Heavy
HP-OS-14, X-OS-24	1547.7-1548.9	18.7	1.2	73.0	7.1	.906	None
HP-OS-15, X-OS-25	1137.0-1135.8	14.5	1.8	76.3	7.4	.899	None
HP-OS-16, X-OS-26	1134.6-1135.8	15.8	.9	77.9	5.25	.901	Slight
HP-OS-17, X-OS-27	1137.0-1138.2	14.7	2.0	74.8	8.5	.900	None
HP-OS-18, X-OS-28	1546.3-1547.5	12.4	1.6	78.4	7.6	.909	None
HP-OS-19	1045.2-1046.5	13.2	1.2	80.5	5.1	.895	None
HP-OS-20	1431.2-1432.3	14.5	1.42	78.6	5.4	.900	None
HP-QS-21	1160.8-1162.0	18.9	.8	75.4	4.9	.907	Slight

Table 21

Data From D-OS Series of Experiments

Experiment	Sample Location	°C	°F	Pressure psig.	Duration Hrs.	Special Conditions	Oil ml.	H ₂ O ml.	Gas ft ³ /ton
D-OS-4	1116.3-1117.4	331	628	atm.	550	kinetic	24.5	3.5	496
D-OS-5	1116.3-1117.4	347	657	atm.	425	kinetic	22.0	7.2	633
D-OS-21	1164 -1165	347	657	atm.	210	kinetic	21.0	5.5	477
D-OS-19	1163 -1164	353	667	atm.	159	kinetic	39.0	8.0	884
D-OS-7	1179.5-1181.0	364	689	atm.	312	kinetic	36.0	7.0	972
D-OS-25	1165.3-1166.9	366	691	atm.	287	kinetic	37.0	8.0	
D-OS-22	1164 -1165	395	743	atm.	71.0	kinetic	44.0	7.0	912
D-OS-16	1163 -1164	399	750	atm.	86.5	kinetic	46.0	7.0	909
D-OS-15	1163 -1164	420	788	atm.	28.0	kinetic	46.0	6.5	971
D-OS-17	1163 -1164	420	788	atm.	38.0	kinetic	42.0	6.0	913
D-OS-18	1163 -1164	420	788	atm.	30.04	kinetic	54.0	7.0	984
D-OS-10	1179.5-1181.0	427	800	atm.	36.0	kinetic	39.0	8.0	1226
D-OS-23	1164 -1165	427	800	atm.	36.0	kinetic			1142
D-OS-1	1122.3-1123.5	500	932	atm.	13.5				1431
D-OS-2	1122.3-1123.5	520	968	atm.	13.0	rivets in retort			
D-OS-3	heavy oil from HP-21	520	968	atm.	9.2	45 ml. oil HP-21	38.0	0	
D-OS-9	1179.5-1181.0	427	800	3500	79.2	H ₂ O in retort	25.0		2184
D-OS-12		427	800	2125	14.6	H ₂ O in retort	29.0		1407
D-OS-13		427	800	1000	14.6	H ₂ O in retort	40.0		917
D-OS-14		427	800	1000	14.7	no H ₂ O	48.0	3.0	717

Table 21 (Continued)

Experiment	Sample Location	Oil 3 gm/cm ³	Oil pour API ^o point	Oil pour point -40 ^o C	% C	% H	% N	% S	% O	ΔH_C Btu/lb.
D-OS-4	1116.3-1117.4	.822	40.7	-40 ^o C	82.8	13.01	.95			
D-OS-5	1116.3-1117.4	.823	40.5	-45	80.7	13.4				
D-OS-21	1164 -1165	.841	36.7	-30	78.7	14.0	1.89			
D-OS-19	1163 -1164	.828	39.4	-23				1.0	.5	19,090
D-OS-7	1179.5-1181.0	.817	41.6	-18						
D-OS-25	1165.3-1166.9	.822	40.6	-30						
D-OS-22	1164 -1165	.838	37.4	-20	84.8	13.4	1.2	.93		
D-OS-16	1163 -1164	.828	39.2	-23						
D-OS-15	1163 -1164	.829	39.2	-17				1.1		
D-OS-17	1163 -1164	.832	38.6	-20	81.0	13.1		1.0	.38	
D-OS-18	1163 -1164	.834	38.1	-21	78.2	13.7	1.3	.93		
D-OS-10	1179.5-1181.0	.889	27.7	-5	84.0	12.6	1.66	.93	1.35	
D-OS-23	1164 -1165	.843	36.3	-20						
D-OS-1	1122.3-1123.5	.852	34.6	10						
D-OS-2	1122.3-1123.5	.859	33.5	0						
D-OS-3	heavy oil from HP-21	.860	33.2	-5						
D-OS-9	1179.5-1181.0	.876	30	-90				.5	.72	
D-OS-12		.837	37.6	5	79.4	13.7	1.77	.68	1.29	
D-OS-13		.814	42.3	-20	84.6	13.5	1.29	.75	1.31	
D-OS-14		.814	42.3	-22	83.7	13.2	1.55	.82	.93	

Table 21 (Continued)

Experiment	Residue			H ₂ O			Gas + Losses		
	A	B	C	A	B	C	A	B	C
	Weight Percent Yields								
D-OS-4	83.7	89.7	107	.4	.67	167	4.0	2.5	62.5
D-OS-5	83.7	92.0	110	.4	.76	190	4.0	2.45	61.2
D-OS-21	83.1	90.2	109	.8	1.71	214	5.5	3.7	67.3
D-OS-19	84.8	91.8	108	.9	1.36	150	3.3	2.54	77.0
D-OS-7	82.4	88.8	108	1.1	1.52	138	5.1	3.64	71.4
D-OS-25	82.2	88.0	107	.7	1.58	226	6.7	3.66	54.6
D-OS-22	83.4	86.0	103	.8	1.84	230	5.5	4.54	82.5
D-OS-16	84.8	87.4	103	.9	1.49	166	3.3	3.18	96.4
D-OS-17	84.8	86.4	101.9	.9	1.43	159	3.3	3.35	101.0
D-OS-18	84.8	86.8	102	.9	1.42	158	3.3	3.51	113.0
D-OS-10	82.4	85.8	104	1.1	1.36	124	5.1	3.87	75.9
D-OS-23	83.1	84.8	102	.8	2.02	252	5.5	4.45	80.9
D-OS-1	86.3	88.5	102	.63	1.13	174	4.8	2.8	58.3
D-OS-2	86.3	90	104	.65	1.2	185	4.8	3.2	66.7
D-OS-3		9.3						11.5	
D-OS-9	82.4	83	101	1.1	0	0	5.1	12.2	239
D-OS-12	83.3	85.7	103	1.6	0	0	3.9	8.57	220
D-OS-13	84.4	85.3	101	.9	0	0	2.9	6.83	235
D-OS-14	84.4	86.6	103	.9	.65	72.2	2.9	4.09	141

A = U.S.B.M. Fischer Assay Weight Percent Yields

B = Experimental Weight Percent Yields

C = Percent B of A

Table 21 (Continued)

Experiment	°C	Temp. °F	Press. psig.	Conditions	Weight Percent Yields		
					A	B	C
D-OS-4	331	628	atm.	kinetic	11.9	7.07	59.4
D-OS-5	347	657	atm.	kinetic	11.9	4.81	40.5
D-OS-21	347	657	atm.	kinetic	10.6	4.34	40.9
D-OS-19	353	667	atm.	kinetic	11.0	4.34	39.5
D-OS-7	364	689	atm.	kinetic	11.4	6.05	53.0
D-OS-25	366	691	atm.	kinetic	10.4	6.77	65.0
D-OS-22	395	743	atm.	kinetic	10.6	7.62	71.9
D-OS-16	399	750	atm.	kinetic	11.0	7.96	72.4
D-OS-17	420	788	atm.	kinetic	11.0	8.78	79.8
D-OS-18	420	788	atm.	kinetic	11.0	8.29	75.4
D-OS-10	427	800	atm.	kinetic	11.4	8.93	78.4
D-OS-23	427	800	atm.	kinetic	10.6	8.74	82.4
D-OS-1	500	932	atm.	kinetic	8.2	7.6	92.3
D-OS-2	520	968	atm.	rivets in retort	8.2	5.8	70.7
D-OS-3	520	968	atm.	oil from HP-21		79.2	
D-OS-9	427	800	3500	H ₂ O	11.4	4.86	42.6
D-OS-12	427	800	2125	H ₂ O	11.2	5.75	51.0
D-OS-13	427	800	1000	H ₂ O	11.8	7.82	66.3
D-OS-14	427	800	1000	no H ₂ O	11.8	8.61	73.0

A = U.S.B.M. Fischer Assay Weight Percent Yields

B = Experimental Weight Percent Yields

C = Percent B of A

Table 22
Gas Sample Analysis

Experiment	%CO	%CO ₂	%CH ₄	%C ₂ H ₆	%C ₂ H ₄	%C ₃ H ₈	%O ₂	%N ₂	%H ₂
D-0S-9	25.6		12.1	5.94		6.21	1.41		
D-0S-10	2.9	80.2	9.7	3.17	.88		.7		
D-0S-11	.56	76.	11.	6.2	0	4.7	1.8	0	
D-0S-12-1	.18	82.	.95	4.3	0	3.4	.57	0	
D-0S-12-2	.65	79.8	10.44	4.97	0	2.80	1.4	0	
D-0S-13-1	.38	88.22	.89	0,	0	0	0	10.51	
D-0S-13-2	.68	85.3	10.60	1.9	0	1.05	.48	0	
D-0S-13-3	.34	54.15	19.04	13.65	0	10.39	2.4	0	
D-0S-14-1	.69	31.3	6.58	28.5	0	22.7	10.3	0	
D-0S-14-2	.86	23.5	36.7	21.5	0	16.3	1.2	0	

Note: O₂ and N₂ are reported as that O₂ or N₂ which is in excess of that contained in air in the sample.

Table 23

Gas Evolution Kinetic Data

D-OS-4, 331°C

Time (hrs.)	$\frac{v}{w} \frac{\text{ft}^3 \times 10^5}{\text{gm}}$	x	$\frac{a}{a-x}$	$\ln\left(\frac{a}{a-x}\right)$
2.5	4.0	3.921	1.265	.2353
5.0	4.7	4.542	1.321	.2782
7.5	5.3	5.063	1.371	.3157
10.0	6.0	5.684	1.437	.3623
12.5	6.7	6.305	1.509	.4112
15.0	7.0	6.526	1.536	.4292
17.5	7.7	7.147	1.619	.4816
20.0	8.0	7.368	1.650	.5009
22.5	8.7	7.989	1.746	.5573
25.0	9.0	8.210	1.783	.5781
30.0	10.0	9.052	1.938	.6618
35.0	11.0	9.894	2.124	.7531
40.0	11.8	10.54	2.291	.8288
45.0	12.5	11.08	2.453	.8975
50.0	13.2	11.62	2.641	.9712
55.0	14.0	12.26	2.905	1.066
60.0	14.7	12.80	3.172	1.154
65.0	15.3	13.25	3.429	1.232
70.0	15.8	13.59	3.658	1.297
75.0	16.3	13.93	3.920	1.366
80.0	17.0	14.47	4.423	1.487
90.0	18.0	15.16	5.277	1.663

$a = 18.7$

$m = \text{slope of zero order portion} = .0316$

$x = v/w \text{ (ft}^3 \times 10^5/\text{gm) for difference curve}$

least squares line $y = .01596x + .1927$

Table 23 (Continued)

D-OS-5, 347°C

Time (hrs.)	$\frac{v}{w} \frac{\text{ft}^3}{\text{gm}} \times 10^5$	x	$\frac{a}{a-x}$	$\ln\left(\frac{a}{a-x}\right)$
1	4.0	4.0	1.129	.1212
10	10.2	10.0	1.401	.1310
20	14.3	13.5	1.630	.4880
30	17.8	16.4	1.886	.634
40	21.0	18.9	2.180	.7790
50	24.0	21.3	2.565	.9420
60	26.7	23.6	3.089	1.128
70	29.0	25.5	3.710	1.310
80	31.0	27.2	4.528	1.510
90	33.0	28.5	5.446	1.690
100	34.7	29.8	6.832	1.920
110	36.1	30.9	8.706	2.163
120	37.6	31.8	11.22	2.410
130	38.2	32.3	13.37	2.595
140	39.8	33.0	18.28	2.905
150	40.8	33.2	20.41	3.015
160	41.6	33.8	31.45	3.450
170	42.4	34.0	38.36	3.650
180	43.1	34.3	57.23	4.040
190	43.8	34.5	85.14	4.440
200	44.4	34.8	317.4	5.750
210	45.0	34.9	349.	8.150

$$a = 34.91$$

$$m = .0491$$

x = v/w (ft³ x 10⁵/gm) for difference curve

least squares line y = .0199x + .01

Table 23 (Continued)

D-OS-21, 347°C

Time (hrs.)	$\frac{v}{w} \frac{\text{ft}^3 \times 10^5}{\text{gm}}$	x	$\frac{a}{a-x}$	$\ln\left(\frac{a}{a-x}\right)$
1.5	6.0	5.867	1.081	.0782
2.0	8.0	7.822	1.111	.1057
4.0	13.5	13.14	1.203	.1845
6.0	18.0	17.47	1.289	.2535
8.0	21.0	20.29	1.352	.3013
10.0	24.0	23.11	1.421	.3514
12.0	27.0	25.93	1.459	.4042
14.0	29.5	28.26	1.568	.4498
16.0	32.0	30.58	1.645	.4976
18.0	34.2	32.6	1.718	.5412
20.0	37.0	35.22	1.823	.6006
24.0	41.0	38.87	1.993	.6897
28.0	44.5	42.0	2.167	.7735
32.0	48.0	45.21	2.375	.8649
36.0	51.0	47.79	2.583	.9489
40.0	54.0	50.44	2.831	1.040
44.0	56.0	52.09	3.010	1.102
52.0	60.5	55.88	3.526	1.260
60.0	64.5	59.17	4.142	1.421
68.0	68.2	62.16	4.923	1.594
76.0	71.0	64.24	5.670	1.735
84.0	74.5	67.03	7.112	1.962
92.0	77.2	69.02	8.688	2.162

a = 78.0

m = .0889

least squares line $y = .0219x + .1318$ x = difference curve v/w ($\text{ft}^3 \times 10^5 / \text{gm}$)

Table 23 (Continued)

D-0S-1a, 353°C

Time (hrs.)	$\frac{v}{w} \frac{\text{ft}^3}{\text{gm}} \times 10^5$	x	$\frac{a}{a-x}$	$\ln\left(\frac{a}{a-x}\right)$
8.0	24.0	23.53	1.612	.4772
10.0	26.5	25.91	1.718	.5412
12.0	29.0	28.29	1.839	.6095
14.0	31.0	30.18	1.948	.6669
16.0	32.7	31.76	2.050	.7179
18.0	34.5	33.44	2.171	.7752
20.0	36.0	34.82	2.281	.8248
24.0	39.0	37.59	2.540	.9321
28.0	42.0	40.35	2.864	1.052
32.0	44.3	42.42	3.166	1.153
36.0	46.5	44.38	3.519	1.258
40.0	48.7	46.35	3.961	1.377
44.0	50.7	48.11	4.464	1.496
48.0	52.5	49.68	5.031	1.616
52.0	54.0	50.94	5.607	1.724
56.0	55.5	52.21	6.331	1.845

$$a = 62.0$$

$$m = .0588$$

$$\text{least squares line } y = .02806x + .2634$$

$$x = \text{difference curve } v/w \text{ (ft}^3 \times 10^5/\text{gm)}$$

Table 23 (Continued)

D-0S-7, 364°C

Time (hrs.)	$\frac{v}{w} \frac{\text{ft}^3 \times 10^5}{\text{gm}}$	x	$\frac{a}{a-x}$	$\ln\left(\frac{a}{a-x}\right)$
5.0	21.5	21.5	1.380	.322
7.5	29.0	29.0	1.625	.485
10.0	33.0	33.0	1.733	.550
12.5	37.0	37.0	1.902	.642
15.0	42.0	40.5	2.080	.732
20.0	48.0	46.0	2.437	.890
25.0	53.0	50.5	2.830	1.04
30.0	57.5	54.5	3.319	1.20
35.0	61.0	58.0	3.90	1.36
40.0	64.0	61.0	4.588	1.52
45.0	66.0	63.5	5.379	1.68
50.0	68.2	65.5	6.24	1.83
55.0	70.2	67.0	7.091	1.96
60.0	72.0	68.3	8.041	2.08
65.0	73.5	69.5	9.176	2.20
70.0	75.0	70.8	10.83	2.38
75.0	76.5	72.0	13.0	2.56
80.0	77.5	72.8	15.0	2.71
85.0	79.0	73.5	17.33	2.85
90.0	80.0	74.5	22.29	3.10
95.0	81.0	75.0	26.0	3.26
100.0	82.0	75.5	31.2	3.44
105.0	83.0	76.0	39.0	3.66

a = 78

m = .0651

x = difference curve v/w ($\text{ft}^3 \times 10^5/\text{gm}$)least squares line $y = .0316x$

Table 23 (Continued)

D-OS-25, 366°C

Time (hrs.)	$\frac{v}{w} \frac{\text{ft}^3 \times 10^5}{\text{gm}}$	x	$\frac{a}{a-x}$	$\ln\left(\frac{a}{a-x}\right)$
15.0	49.0	48.0	2.131	.7566
17.5	53.0	51.9	2.343	.8514
20.0	56.0	54.7	2.529	.9277
22.5	59.0	57.6	2.747	1.010
25.0	61.0	59.4	2.909	1.068
30.0	65.0	63.1	3.30	1.194
35.0	68.5	66.2	3.731	1.317
40.0	72.0	69.4	4.293	1.457
45.0	74.5	71.6	4.788	1.566
50.0	77.0	73.8	5.412	1.689
55.0	79.5	75.0	6.222	1.828
60.0	81.5	77.6	7.033	1.951
65.0	83.0	78.8	7.742	2.047
70.0	85.0	80.5	9.039	2.202
75.0	86.5	81.7	10.24	2.327
80.0	88.0	82.8	11.82	2.470
85.0	89.0	83.5	12.97	2.562
90.0	90.0	84.2	14.36	2.665
95.0	91.0	84.9	16.09	2.778
100.0	92.0	85.6	18.30	2.907
105.0	93.0	86.2	21.20	3.054
110.0	94.0	86.9	25.20	3.227
115.5	95.0	87.6	31.07	3.436
120.0	95.5	87.8	33.09	3.499

$$a = 90.5$$

$$m = .06446$$

x = v/w (ft³ x 10⁵/gm) for difference curve

$$\text{least squares lines } y = .02545v + .156$$

Table 23 (Continued)

D-0S-22, 395°C

Time (hrs.)	$\frac{v}{w} \frac{\text{ft}^3 \times 10^5}{\text{gm}}$	x	$\frac{x}{a-x}$	$\ln\left(\frac{a}{a-x}\right)$
8.0	82.5	80.33	3.351	1.209
8.5	85.0	82.69	3.60	1.281
9.0	86.5	84.06	3.761	1.325
10.0	90.0	87.29	4.207	1.437
11.0	93.0	90.01	4.676	1.542
12.0	95.7	92.44	5.191	1.647
13.0	98.0	94.47	5.717	1.743
14.0	99.8	96.00	6.189	1.823
15.0	101.5	97.43	6.707	1.903
16.0	103.0	98.65	7.227	1.978
17.0	104.7	100.1	7.944	2.072
18.0	106.0	101.1	8.554	2.146
19.0	107.3	102.1	9.266	2.226
20.0	108.5	103.1	10.02	2.304
22.0	110.8	104.8	11.84	2.471
24.0	112.7	106.2	13.77	2.622
26.0	114.2	107.1	15.56	2.745
28.0	116.0	108.4	18.77	2.932
30.0	117.5	109.3	22.27	3.103
34.0	120.0	110.8	30.72	3.425
38.0	122.2	111.9	43.82	3.78
42.0	124.2	112.8	67.40	4.211

$$a = 114.5$$

$$m = .2714$$

x = v/w (ft³ x 10⁵/gm) for difference curve

less squares line y = .08412x + .6064

Table 23

D-OS-16, 395°C

Time (hrs)	$\frac{v}{w} \frac{\text{ft}^3 \times 10^5}{\text{gm}}$	x	$\frac{a}{a-x}$	$\ln\left(\frac{a}{a-x}\right)$
11.0	63.0	60.87	3.610	1.284
12.0	65.5	63.18	4.006	1.388
14.0	69.0	66.29	4.702	1.548
16.0	71.5	68.41	5.332	1.674
18.0	74.0	70.52	6.155	1.817
20.0	76.1	72.23	7.037	1.951
22.0	77.9	73.65	7.979	2.077
24.0	79.5	74.86	9.016	2.199
26.0	80.5	75.47	9.650	2.267
28.0	82.0	76.59	11.06	2.403
30.0	83.5	77.70	12.96	2.562
32.0	85.0	78.81	15.63	2.749
34.0	86.0	79.43	17.64	2.870
36.0	87.0	80.04	20.25	3.008

$$a = 84.2$$

$$m = .1933$$

$$x = v/w \left(\text{ft}^3 \times 10^5 / \text{gm} \right) \text{ for difference curve}$$

$$\text{least squares line } y = .06657x + .5925$$

Table 23 (Continued)

D-OS-18, 420°C

Time (hrs.)	$\frac{v}{w} \frac{\text{ft}^3}{\text{gm}} \times 10^5$	x	$\frac{a}{a-x}$	$\ln\left(\frac{a}{a-x}\right)$
3.0	46.5	45.37	2.028	.7071
3.5	52.7	51.38	2.348	.8535
4.0	58.0	56.49	2.711	.9975
4.5	62.0	60.30	3.065	1.120
5.0	66.0	64.11	3.526	1.260
5.5	69.0	66.93	3.965	1.377
6.0	71.5	69.24	4.417	1.485
7.0	76.0	73.36	5.546	1.713
8.0	79.5	76.48	6.876	1.928
9.0	82.0	78.61	8.216	2.106
10.0	84.5	80.73	10.21	2.323
11.0	86.5	82.35	12.52	2.528
12.0	88.5	83.98	16.20	2.785
13.0	90.0	85.10	20.33	3.012
14.0	91.4	86.12	26.49	3.277
15.0	92.6	86.94	35.03	3.556
16.0	93.5	87.47	44.05	3.785
17.0	94.5	88.09	63.52	4.151
18.0	95.0	88.21	69.50	4.243

$$a = 89.50$$

$$m = .3770$$

$x = v/w (\text{ft}^3 \times 10^5/\text{gm})$ for the difference curve

$$\text{least squares line } y = .2330x + .0483$$

Table 23 (Continued)

D-OS-17, 420°C

Time (hrs.)	$\frac{v}{w} \frac{\text{ft}^3 \times 10^5}{\text{gm}}$	x	$\frac{a}{a-x}$	$\ln\left(\frac{a}{a-x}\right)$
3.0	48.0	46.8	2.035	.7107
3.5	53.6	52.2	2.312	.8379
4.0	58.0	56.4	2.584	.9494
4.5	62.0	60.2	2.893	1.062
5.0	65.0	63.0	3.172	1.154
6.0	70.4	68.0	3.833	1.344
7.0	75.0	72.2	4.646	1.536
8.0	79.0	75.8	5.679	1.737
9.0	82.0	78.4	6.765	1.912
10.0	84.8	80.8	8.214	2.106
11.0	87.0	82.6	9.787	2.281
12.0	89.0	84.2	11.79	2.468
13.0	90.5	85.3	13.73	2.620
14.0	92.0	86.4	16.42	2.799
15.0	93.5	87.5	20.44	3.018
16.0	94.8	88.4	25.56	3.241
17.0	96.0	89.2	32.86	3.492
18.0	96.8	89.6	38.33	3.646

$$a = 92.0$$

$$m = .400$$

$$x = v/w (\text{ft}^3 \times 10^5 / \text{gm}) \text{ for difference curve}$$

$$\text{least squares line } y = .1913x + .1799$$

Table 23 (Continued)

D-OS-15, 420°C

Time (hrs.)	$\frac{v}{w} \frac{\text{ft}^3 \times 10^5}{\text{gm}}$	x	$\frac{a}{a-x}$	$\ln\left(\frac{a}{a-x}\right)$
2.0	30.5	29.79	1.555	.4412
2.25	35.0	34.20	1.694	.5269
2.50	39.0	38.11	1.840	.6095
3.0	46.0	44.93	2.165	.7723
3.5	51.0	49.75	2.474	.9059
4.0	56.0	54.57	2.886	1.060
4.5	60.0	58.39	3.326	1.202
5.0	63.2	61.41	3.781	1.330
5.5	66.1	64.14	4.312	1.461
6.0	69.0	66.86	5.017	1.613
6.5	71.5	69.18	5.831	1.763
7.0	73.5	71.00	6.681	1.899
7.5	75.5	72.82	7.820	2.057
8.0	77.3	74.44	9.220	2.221
8.5	78.7	75.67	10.66	2.366
9.0	80.0	76.79	12.44	2.521
10.0	82.0	78.43	16.47	2.801
11.0	83.5	79.57	21.26	3.057

$$a = 83.5$$

$$m = .357$$

$x = v/w (\text{ft}^3 \times 10^5 / \text{gm})$ for difference curve

$$\text{least squares line } y = .2911x - .1209$$

Table 23 (Continued)

D-OS-10, 427°C

Time (hrs.)	$\frac{v}{w} \frac{\text{ft}^3 \times 10^5}{\text{gm}}$	x	$\frac{a}{a-x}$	$\ln\left(\frac{a}{a-x}\right)$
4.0	66.0	64.73	3.084	1.126
4.5	71.5	70.07	3.724	1.315
5.0	75.5	73.92	4.378	1.477
5.5	78.5	76.76	5.031	1.616
6.0	81.0	79.10	5.736	1.747
6.5	83.3	81.24	6.580	1.884
7.0	85.3	83.08	7.533	2.019
7.5	87.0	84.62	8.573	2.149
8.0	88.3	85.77	9.548	2.256
9.0	91.0	88.15	12.52	2.528
10.0	93.0	89.83	16.05	2.776
11.0	94.7	91.22	20.90	3.040
12.0	96.3	92.50	29.03	3.368
13.0	97.5	93.38	39.63	3.680

$$a = 95.8$$

$$m = .3167$$

$$x = v/w (\text{ft}^3 \times 10^5 / \text{gm}) \text{ for difference curve}$$

$$\text{least squares line } y = .2726x + .09043$$

Table 23 (Continued)

D-OS-23, 427°C

Time (hrs.)	$\frac{v}{w} \frac{\text{ft}^3}{\text{gm}} \times 10^5$	x	$\frac{a}{a-x}$	$\ln\left(\frac{a}{a-x}\right)$
5.0	92.5	91.36	3.600	1.281
5.5	96.5	95.24	4.047	1.398
6.0	100.0	98.63	4.539	1.513
6.5	102.8	101.3	5.023	1.614
7.0	105.2	103.6	5.524	1.709
7.5	107.5	105.8	6.107	1.809
8.0	109.2	107.4	6.613	1.889
8.5	111.0	109.1	7.252	1.981
9.0	111.5	109.4	7.416	2.004
9.5	114.0	111.8	8.622	2.154
10.0	115.5	113.2	9.521	2.254
11.0	117.5	115.0	10.99	2.397
12.0	119.7	117.0	13.26	2.584
13.0	121.5	118.5	15.87	2.764
14.0	123.0	119.8	18.88	2.938
15.0	124.5	121.1	23.30	3.148
16.0	125.8	122.1	29.03	3.368
17.0	127.0	123.1	37.36	3.621

$$a = 126.5$$

$$m = .2286$$

$$x = v/w (\text{ft}^3 \times 10^5 / \text{gm}) \text{ for difference curve}$$

$$\text{least squares line } y = .1859x + .3821$$

Table 24

Data for B-OS Series of Experiments

run	Temp °C	Min.	Max.	Final	Duration (hrs.)	Used CH ₄	ml. oil	ml. H ₂ O	oil specific gravity	oil API gravity	oil pour point	Gas yield
									gm/cm ³			ft ³ /ton
B-OS-1	400		atm.			No						
B-OS-2	375		atm.			No	35	5	.838	36	41°F	
B-OS-3	390	300	- 1700	- 500		Yes	<2					
B-OS-4	430	300	-	- 594		Yes	9	0	.865	31.3		
B-OS-5	375		atm.		12	No	15	4	.800	43.8		
B-OS-6	375	300	- 755	- atm.	12	Yes	3	2.2				
B-OS-7	375	300	- 375	- atm.	12	Yes	3	2.5				
B-OS-8	400	300	- 300	- 300	12	Yes	5.3	2.3	.782			
B-OS-9	400	300	- 300	- 300	12	Yes	6.4	3.0	.779			
B-OS-10	400		atm.		12	No	39.0	5.0	.808	41.8		
B-OS-11	400	300	- 925	- 300	12	Yes	15.8	2.2	.811	42.0		1020
B-OS-12	400		atm.		12	No	49.0	5.0	.816	40.6	<0°F	1353
B-OS-13	440		atm.		12	No	50.2	4.4	.836	36.6	<0	1880
B-OS-14	440	300	- 300	- 300	12	Yes	45.0	4.0	.774	49.6		1894
B-OS-15	400	300	- 300	- 300	12	Yes	3.7	2.0	.77			634
B-OS-16	440		atm.		12	No	70.0	6.0	.841			1772
B-OS-17	450		atm.		7.5		47.0	5.0	.794	45.0	18-20	1502

Table 24 (Continued)

Test	Temp.	% oil			% residue			% H ₂ O			% Gas + Losses			USBM specific gravity gm/cm ³
		A	B	C	A	B	C	A	B	C	A	B	C	
B-OS-1	400 ^o	13.4			83									.895
B-OS-2	375	12.7	7.7	62	84			1.3				6.5		.895
B-OS-3	390	12.7	.6	4.72	91.7									.895
B-OS-4	430		2.1		88.8			.2				8.9		.901
B-OS-5	375	14.8	2.85	19.2	79.7	92.9	116	.6	1.0	167.	4.9	3.2	65.4	.907
B-OS-6	375	14.8	.59	3.99	79.7	97.6	122	.6	.53	88.4	4.9	1.2	24.5	.907
B-OS-7	375	14.8	.7	4.73	79.7	97.7	123	.6	.6	100	4.9	1.0	20.4	.907
B-OS-8	400	16.5	2.8	17.0	78.1			.6	.6	100	4.8			.906
B-OS-9	400	16.5	1.7	10.3	78.1	94.8	121	.6	.7	117	4.8	2.7	56.3	.906
B-OS-10	400	16.5	7.8	47.3	78.1	87.6	112	.6	1.3	216	4.8	3.4	70.8	.906
B-OS-11	400	16.5	3.6	21.8	78.1	91.9	118	.6	.6	100	4.8	3.9	81.3	.906
B-OS-12	400	16.5	9.0	54.5	78.1	85.7	110	.6	1.2	200	4.8	4.0	83.3	.906
B-OS-13	440	16.5	14.1	85.5	78.1	79.2	101	.6	1.5	250	4.8	5.2	108	.906
B-OS-14	440	16.5	8.29	50.2	78.4	84.9	108	.6	.96	160	4.5	5.88	131	.906
B-OS-15	400	16.5	.7	4.24	78.4	96.8	123	.6	.4	66.7	4.5	1.9	42.2	.906
B-OS-16	440	16.5	13.5	81.9	78.4	80.7	103	.6	1.36	22.6	4.5	4.4	97.8	.906
B-OS-17	450	8.3	9.1	110	88.8	85.6	104	.3	1.22	407	2.6	4.10	158	.909

A = percent yield by Fischer Assay

B = percent yield

C = yield, percent of Fischer Assay

Table 25

Gas Analysis Data For C-OS Experiments

Exp. #	Sample #	Temp. °C.	% CH ₄	% C ₂ H ₆	% C ₂ H ₈	% CO ₂	% H ₂ *	% H ₂ S
C-OS-1	1	295	35.5	2.3	4.3	25	32.8	
	2	343	24	3.25	3.8	21.5	30.5	
	3	373	17	4.35	2.1	4.0	56.5	15.75
	4	388	22.5	6.1	1.7	3.5	59	7.2
	5	395	23	7.2	2.25	3.0	55	9.3
	6	426	17.5	5.15	1.65	6.0	70	
	7	459	46.5	4.0	3.3	15.0	31	
	8	480	30.5	8.5	0.35	27.0	33	
	9	532	20.8	0	0.05	37.0	42	
	10	561	13.7	0	0	62.0	24.1	
	11	576	10.4	0	0	58.5	31	
C-OS-2	1	140				.27	99.73	
	2	170						
	3	230						
	4	300	43.56	2.09	3.55	30.52	20.28	
	5	340						
	6	350	15.21	16.27	2.85	18.72	46.51	.44
	7	380	13.07	4.02	3.4	3.84	74.77	.90
	8	402						
	9	404	19.19	6.44	4.54	3.54	65.67	.61
	10	440	28.10	6.92	3.04	9.6	52.04	.29
	11	444						
	12	480	21.25	1.44	.75	26.66	49.89	
13	485	9.94	.85	.9	40.97	48.16		
14	500	4.23	.33		69.03	26.41		
15	525							
16	550	2.91			89.58	7.51		
17	552	1.34			77.48	21.18		
18	575	.37			99.63			
19	540							

Table 25 (Continued)

Exp. #	Sample #	Temp. °C.	% CH ₄	% C ₂ H ₆	% C ₂ H ₈	% CO ₂	% H ₂ *	% H ₂ S
C-OS-3	1	150						
	190		.91	.03	.04	.24	98.78	
	260							
	310		31.10	2.63	5.08	9.16	52.04	
	400							
	405		42.84	8.60	5.89	1.68	40.99	
	451							
	455		81.59	8.24	3.30	1.98	10.97	
	502		24.76	.99	.53	56.19	17.53	
	555							
	560		16.90	.26	.30	34.73	47.82	
	590							
	594		8.67	.16	.36	54.99	37.25	

* H₂ + unknowns by difference

Table 26

Data For Flow Studies

Experiment	Sample Location	Maximum Temp. (T) °C	Time at T (hours)	Pressure Psig	Duration Hours	Flow Rate Small Meter Units	Flow ft ³ /min
HP-OS-300-10	1036.6-1049.0	500	.5	300		15-18	.34-.42
HP-OS-300-11	1039.0	400	4	300	14	10	.2
HP-OS-300-12	1035.3-1036.1	425	3	300	12	12	.26
HP-OS-300-13	1024.1-1025.2	350	.5	300	15	10	.2
HP-OS-300-14	1547.7-1548.9	500	4	300	12	40	~1
HP-OS-300-15	1137.0-1135.8	485	1	300	20	60	1.5
HP-OS-200-16	1134.6-1135.8	500	.5	200	16	60-66	1.5-1.6
HP-OS-400-17	1137.0-1138.2	475	7	400	16	60-75	1.5-1.7
HP-OS-300-18	1546.3-1547.5	510	3	300	9	68-75	1.6-1.7
HP-OS-300-19	1045.2-1046.5	350	1	300	14		
HP-OS-300-20	1431.2-1432.3	440	2	300	18	35	~.8
HP-OS-300-21	1160.8-1162.0	420	4	300	60	25-40	.6-1
* X-OS-22	1035.3-1036.1	425?		atmos.			
X-OS-23	1024.1-1025.2	410	.5	atmos.	10	7?	
X-OS-24	1547.7-1548.9	460	.5	atmos.	4	7?	
X-OS-25	1135.8-1137.0	500	.5	atmos.	5	7	
X-OS-26	1134.6-1135.8	480	.5	atmos.	2.5	7	
X-OS-27	1137.0-1138.2	460?	.5?	atmos.		7?	
X-OS-28	1546.3-1547.5	510?	.5?	atmos.		7?	

different flow
from above units

* Each atmospheric experiment was designed to complement its corresponding high pressure experiment. For example: X-OS-22 and HP-OS-300-12; X-OS-23 and HP-OS-300-13; etc.

Table 27

Yield Data For Flow Studies

Experiment	Amounts (ml)			Yield Weight Percents											
	Oil	Water	A	Oil			Water			Residue			C		
				A	B	C	A	B	C	A	B	C			
HP-OS-300-10	178	14	8.65	13.4	64.5	.76	1.0	76.0	80.2	80.4	99.7				
HP-OS-300-11	148	17.5	7.41	12.7	58.3	1.0	.8	125.0	81.7	81.5	100				
HP-OS-300-12	188	26	9.42	16.7	56.4	1.4	1.2	117	78.4	75.1	104				
X-OS-22	30		13.8	16.7	82.6	6.5	1.2	542	73.1	75.1	97.3				
HP-OS-300-13	170		10.3	22.9	45.0	.3	.9	33.3	55.4	68.3	81.1				
X-OS-23	20	41	9.5	22.9	41.5	20.5	.9	228	83.1	68.3	122				
HP-OS-300-14	199	2.0	12.2	18.7	65.2	.1	1.2	83	76.1	73.0	104				
X-OS-24			11.7	18.7	62.6	10	1.2	833	75.9	73.0	104				
HP-OS-300-15	147	2.0	8.6	14.5	59.3	.06	1.8	3.3	77.1	76.3	101				
X-OS-25	30		13.5	14.5	93.1	8.5	1.8	472	72.5	76.3	95.0				
HP-OS-200-16	96		5.4	15.8	34.2	0	.9	0	79.3	77.9	102				
X-OS-26	31	3.6	15.4	15.8	97.5	1.8	.9	200	75.8	77.9	97.3				
HP-OS-400-17	171	3.0	9.6	14.7	65.3	.2	2.0	10.0	76.8	74.8	103				
X-OS-27	30		13.6	14.7	92.5	1.0	2.0	50.0	75.3	74.8	101				
HP-OS-300-18	157		8.0	12.4	64.5	.2	1.6	12.5	78.3	78.4	100				
X-OS-28	18			12.4			1.6		79.9	78.4	102				
HP-OS-300-19	144		8.8	13.2	66.7	.7	1.2	58.3	84.2	80.5	105				
X-OS-29				13.2			1.2		80.5	80.5					
HP-OS-300-20	153			14.5		.35	1.42	24.6	82.7	78.6	105				
X-OS-30															
HP-OS-300-21	138		10.0	18.9	52.9	0	.8	0	79.0	75.4	105				

A = % at University of Utah

B = % by U.S.B.M. (Fischer Assay)

C = U. of U. percent of U.S.B.M.

Table 27 (Continued)

Experiment	Amounts (ml)		Yield Weight Percents			Average specific gravity gm/cm ³	U.S.B.M. specific gravity gm/cm ³
	Oil	Water	A	Gas + Losses B	C		
HP-OS-300-10	178	14	10.4	5.2	200	.870	.895
HP-OS-300-11	148	17.5	9.9	5.0	198	.863	.896
HP-OS-300-12	188	26	12.2	7.0	174	.915	.909
X-OS-22	30		5.2	7.0	74.3	.857	.909
HP-OS-300-13	170		33.9	7.9	429	.905	.903
X-OS-23	20	41		7.9		.882	.903
HP-OS-300-14	199	2.0	11.6	7.1	163	.903	.906
X-OS-24			2.3	7.1	32.3	.885	.906
HP-OS-300-15	147	2.0	14.3	7.4	193	.914	.899
X-OS-25	30		5.5	7.4	74.3	.891	.899
HP-OS-200-16	96		15.1	5.25	288	.915	.901
X-OS-26	31	3.6	6.95	5.25	132	.889	.901
HP-OS-400-17	171	3.0	13.3	8.5	156	.889	.900
X-OS-27	30		10.1	8.5	119	.887	.900
HP-OS-300-18	157		14.9	7.6	196	.844	.909
X-OS-28	18			7.6			.909
HP-OS-300-19	144		6.3	5.1	123	.895	.895
X-OS-29				5.1			.900
HP-OS-300-20	153			5.4			.900
X-OS-30							.900
HP-OS-300-21	138		10.9	4.9	222	.916	.907

A = % at University of Utah
 B = % by U.S.B.M. (Fischer Assay)
 C = U. of U. percent of U.S.B.M.

Properties of Oil Samples

Experiment	Sample#	Temp. #5	Condensor Sample Taken From	ml. oil	ml. H ₂ O	oil specific gravity gm/cm ³	oil API
HP-OS-300-10	1	all	all rec's.	178	14		
HP-OS-300-11	1	310	1 & 2	23.7	0	.837	37.6
	2	325	1 & 2	6.2	0	.854	34.2
	3	360	1 & 2	10.1	0		
	4	400	1 & 2	21.0	4.5	.867	31.7
	5	0-400	1 & 2 W	48.0	6.0	.884	28.6
	6	exit tube	exit tube	7.0	0		
	7	mixture	mixture	32.0	7.0	.873	30.6
HP-OS-300-12	1	1-5	1-5				
	2	300	#1	3.3	1.0	.844	36.1
	3	350	#1	32.5	2.5	.854	34.2
	4	400	#1	53.0	10.0	.867	31.7
	5	410	#1	18.0	5.0	.841	36.7
	6	415	#1	6.0	2.0	.877	29.8
	7	0-425	#2	23.0	0	.900	25.7
HP-OS-300-13 HP-OS-300-14	1	0-425	1 & 2 W	52.0	7.0		
	2			170			
	3	345	all	0.7	1.3		
	4	370	all	1.0	0		
	5	400	all	1.8	0		
	6	425	all	8.6	0	.877	28.8
	7	430	all	36.0	0	.873	29.1
	8	450	all	30.0	0	.877	28.8
	480	all	39.0	0	.877	28.8	
	485	all	23.0	0	.884	27.5	

W means after receivers were warmed. Therefore, it is the heavy oil from entire temperature range. °F.
All pour points are in °F.

Table 28 (Continued)

Experiment	Sample#	oil pour point	%C	%H	%N	%S	%O
HP-OS-300-10 HP-OS-300-11	1	55°F	84.8	12.3	1.42	.80	1.55
	1				1.10	1.48	1.18
	2				1.32	1.12	1.14
	3						
	4						
	5				1.25	.95	1.17
	6				1.22	1.18	1.32
HP-OS-300-12	7						
	1		83.98	12.13	.66	1.87	1.57
	2	51	84.15	12.35	.74	.93	1.46
	3	58-59	84.8	12.0	1.14	1.13	1.23
	4		83-84	12.0	1.64	.95	.91
	5						
	6	66	84.86	11.8	1.42	.91	1.40
7	76	84.94	11.5	2.06	.79	1.64	
HP-OS-300-13 HP-OS-300-14	1						
	2		83.9	12.5	.65	1.15	1.84
	3		84.0	12.6	.6	1.16	1.36
	4		84.8	12.3	.83	1.31	1.08
	5	60	84.6	12.6	.91	1.61	1.24
	6		85.0	12.2	1.11	1.30	1.01
	7	62	84.5	12.0	1.46	1.27	1.11
	8		84.5	12.0	1.41	1.04	1.11

Table 28 (Continued)

Experiment	Sample#	Temp. #5	Condensor Sample Taken From	ml. oil	ml. H ₂ O	oil specific gravity gm/cm ³	oil API ^o
HP-OS-300-14	9	400	all	21.0	0	.890	26.4
	10	493	all	7.0	0		
	11	496	all	5.5	0		
0-500	12	0-500	W all	23.0	0	.903	24.2
	13	0-500	acetone trap	2.2	.6		
HP-OS-300-15	1	350	all	several drops	1.0		
	2	365	all	1.4 ml.	0		
	3	375	all	8.0	0	.887	28.0
	4	390	all	5.8	0		
	5	393	all	6.0	0		
	6	394	all	6.1	0	.888	27.8
	7	394	all	9.7	0	.885	28.4
	8	395	all	5.0	0		
	9	397	all	3.4	0		
	10	400	all	5.9	0		
	11	406	all	6.0	0		
	12	411	all	6.6	0		
	13	434	all	8.3	0	.889	27.7
	14	435	all	6.6	0	.890	27.5
	15	422	all	7.2	trace	.891	27.3
	16	441	all	4.6	0		
	17	463	all	4.0	0		
	18	468	all	5.5	0		
	19	480	all	4.7	0		
	20	492	all	2.7	0		
	21	425	all	2.0	0	89°F	60°F
	22	0-490	W all	27.3	0	:901	24.1

Table 28 (Continued)

Experiment	Sample#	oil pour point OF	%C	%H	%N	%S	%O
HP-OS-300-14 con't	9	67	84.6	11.9	1.01	1.24	1.07
	10		84.2	11.8	1.08	.96	1.11
	11		83.0	11.4	1.11	1.32	1.24
	12	73	83.8	11.5	1.43	1.20	1.27
	13		84.7	13.7	.29	1.07	1.09
HP-OS-300-15	1						
	2						
	3	69-70					
	4						
	5						
	6						
	7						
	8						
	9						
	10						
	11	70-71					
	12						
	13						
	14	71-73					
15							
16							
17							
18	73						
19							
20							
21							
22							

Table 28 (Continued)

Experiment	Sample#	Temp. #5	Condensor Sample Taken From	ml. oil	ml. H ₂ O	oil specific gravity gm/cm ³	oil API ^o
HP-OS-300-15 con't	23	0-490	acetone trap	.7 gm.	trace		
	24	0-490	demister	1.2 gm.	0		
	1	381	all	3.4	0	.881	29.1
	2	450	all	25.0		.884	28.6
	3	466	all	15.0		.886	28.2
	4	470	all	6.7			
	5	484	all	6.0			
	6	489	all	4.8			
	7	490	all	1.8			
	8	495	all	2.0	0		
	9	498	all	1.0	0		
	10	498	all	1.0	0		
HP-OS-400-17	11	0-498	W all	24.0	0	.897	24.5
	12	0-498	demister	2.3 gm.	0		
	13	0-498	acetone trap	2.7 gm.	0		
	1	315	all	10.0	trace	95°F .907	
	2	350	all	2.8	0		
	3	400	all	22.9	0	.881	28.1
	4	425	all	16.0	0	.879	28.5
	5	450	all	16.0	0	.885	27.5
	6	471	all	21.0	0	.885	27.5
	7	473	all	13.9	0	.890	26.6
	8	465	all	8.4	0	.892	26.2
	9	465	all	7.0	0		
10	0-476	W all	47.0	0	95°F .897	24.4	
11	0-475	demister	1.6 gm.	0			
12	0-475	acetone trap	4.6 gm.	1.1			

Table 28 (Continued)

Experiment	Sample#	oil pour point OF	%C	%H	%N	%S	%O	
HP-OS-300-15 con't	23							
	24							
HP-OS-300-16	1	61-63						
	2							
	3							
	4	61-63						
	5							
	6	65-66						
	7							
HP-OS-400-17	8							
	9							
	10							
	11	84-85						
	12							
	13							
	1							
	2							
	3		71	84.9	12.0	1.32	1.04	1.13
	4							
	5		68	85.2	11.9	1.74	.90	1.22
	6							
	7		73	84.9	12.0	1.81	.91	1.39
8								
9			84.8	11.8	1.81	.79	1.08	
10		75	85.3	11.9	1.86	.74	1.11	
11								
12			84.8	13.8	.11	.60	.63	

Table 28 (Continued)

Experiment	Sample#	Temp. #5	Condensor Sample Taken From	ml. oil	ml. H ₂ O	oil specific gravity gm/cm ³	oil API ^o
HP-OS-300-18	1	350	all	2.1	0		
	2	400	all	.8	trace	.877	28.8
	3	425	all	8.0	trace	.880	28.3
	4	450	all	57.0	0	.889	26.8
	5	475	all	22.0	0	.893	26.0
	6	500	all	37.0	0	.898	25.2
	7	493	all	12.8	0		
	8	507	all	5.2	0		
	9	507	all	2.5	0		
	10	510	all	.7	0	85°F	
	11	0-510	W all		0	.907	23.3
	12	0-510	acetone trap		4.8		
	HP-OS-300-19	13	0-510	demister	2.1 gm.	0	69°F
1		0-350	W all	121	11.0	.836	37.1
2		0-350	scraped (solid) from all	23.0	2.0	.891	25.1
1		0-440	warm #1	35.0	0		
HP-OS-300-20	2	0-440	warm #2	110	0		
	3	0-440	acetone trap	6.0	6.0		
	4	0-440	demister	2.6 gm.	0		
	5	0-440	small flow meter	.4 gm.	0		
	1	0-420	warm #1	30.0	0	60°F	25.9
HP-OS-300-21	1	0-420	2&3 (new) warm	117	0	895 1000°F .992	20.3

Table 28 (Continued)

Experiment	Sample#	oil pour point OF	%C	%H	%N	%S	%O
HP-OS-300-18	1						
	2						
	3						
	4	65-66	*84.3	12.4	1.21	.82	1.60
	5	65-66					
	6						
	7	69-70					
	8						
	9						
	10						
	11	77-78	*85.1	11.6	1.76	.67	1.10
	12						
	13						
HP-OS-300-19	1	42-43					
	2						
HP-OS-300-20	1						
	2						
	3						
	4						
	5						
HP-OS-300-21	1	.51					
	1	70-72					

* Only 2 samples were analyzed for C,H,N,S,O, not sure if they were #4 & #11 as listed here. They were numbered 1 & 2 but were placed here by their values for C,H,N,S,O.

Table 28 (Continued)

Experiment	Sample#	Temp. #5	Condensor Sample Taken From	ml. oil	ml. H ₂ O	oil specific gravity gm/cm ³	oil API ^o
X-OS-20							
X-OS-21							
X-OS-22	1	0-425	all	30.2	13.0	.915 110°F .905	
X-OS-23	1	0-410	all	20.0	41.0		
X-OS-24	1	0-460	all	23.4 gm.	20.0		
X-OS-25	1	0-500	all	30.0	17.0	98°F .914 96°F .915	21.4
X-OS-26	1	0-480	all	31.0	3.6		
X-OS-27	1	0-460	all	30.6	2.0	85°F .889 88°F .902	26.3
X-OS-28	1	0-510	all	18.0			24.0

Table 28 (Continued)

Experiment	Sample#	oil pour point OF	%C	%H	%N	%S	%O
X-OS-20							
X-02-21							
X-02-22	1		84.3	11.4	1.69	.96	1.73
X-0S-23	1						
X-0S-24	1		84.5	11.9	1.21	1.14	1.90
X-0S-25	1						
X-0S-26	1						
X-0S-27	1	75					
X-0S-28	1	77					

bad-system plugged during run

RESEARCH PROPOSALS

1. A rubbery elastic residue resulted from the pyrolysis of an unusually rich oil shale. Cane heated a 200 gal/ton torbanite and also identified a rubberoid stage prior to the formation of the bitumen.

It is possible that the rubberoid is not a unique decomposition product of kerogen but merely a two-phase mixture of bitumen and oil shale.

If the rubberoid is a unique decomposition product of kerogen why has it only been identified in the rich oil shales?

A study must be made to determine whether the rubberoid is an actual decomposition product or merely the two-phase plastic. It must also be determined if it only makes an appearance in the rich oil shales.

A lean oil shale could be heated to temperatures at which the bitumen just begins to form. The sample would then be quenched rapidly and the inorganics acid leached to free the organic material. The remaining material could then be examined for the presence of the rubberoid.

As an alternate method the inorganic carbonates could be acid leached prior to heating the sample.

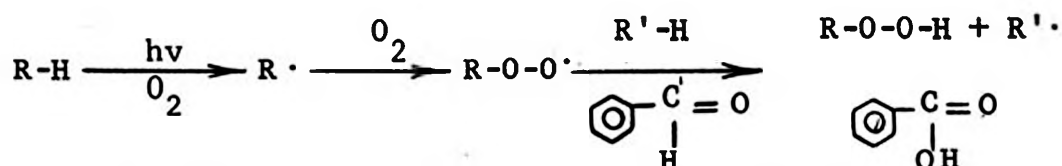
2. For some time it has been apparent that when fresh shale oils were allowed to stand exposed to the atmosphere significant changes in

the oils resulted. They became darker, their fluidity was decreased, and solid tar-like material formed.

Preliminary studies of shale oil indicated that oxygen and light acted to bring about these changes. This was determined by irradiating the oils with a mercury vapor lamp under controlled helium and oxygen atmospheres.

It needs to be determined to what extent oxygen and light each contribute to the observed changes, i.e. to what extent the changes would have occurred in their absence.

The most significant changes observed in the preliminary tests were in the carbonyl region of the infrared adsorption spectra. Electron spin resonance determinations indicated that free radicals were not present in either the raw shale oil or radiated oil. These observations suggest that a mechanism of the general type:



was responsible for the observed changes in the irradiated oxygenated oils.

Further infrared studies of the oils need to be carried out in order to determine if this is the case. The amounts of solid material formed as a function of time could also be determined by solvent extraction. A solvent could be used in which the solid material was insoluble.

The effect of the addition of known gum inhibitors on the reaction should be studied.

3. The effect of the presence of water during the retorting of oil shales should be studied. When water was added to the retort during several of the thermal distillations the yield of shale oil increased and gas chromatographic analyses of the oils indicated that the average molecular weight increased. This needs to be examined in further detail and under varying conditions of temperatures and pressure.

Water would be added to a batch pressure retort and a series of oil shale decompositions performed at various temperatures and pressures. Gas chromatographic analyses of the product oils would be compared with those from the pyrolysis of oil shale in the absence of water. Standard ASTM tests could also be performed on the oil to determine its quality.

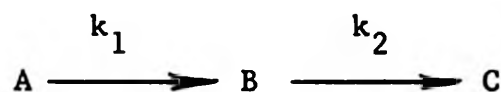
Steam could also be injected into the heated methane inlet system of a flow retort to determine how the presence of water effects the yield and quality of the product oils from the thermal treatment of oil shale in a flow system.

4. It must be determined to what extent the mesh size of the sample influences the pyrolysis of oil shale.

If the two-step mechanism proposed is correct it would be expected that at high temperatures considerable sample internal pressures would develop leading to increased polymerization. In that case a fine ground sample would, to some extent, relieve these pressures and decrease the extent of polymerization. The result

would probably be the earlier appearance of the oil and a higher quality oil.

5. For the general first order series reaction: ⁽³⁾



the differentials expressing the rate of appearance of A, B, and C are:

$$\frac{dA}{dt} = -k_1 A \qquad \frac{dC}{dt} = k_2 B$$

$$\frac{dB}{dt} = k_1 A - k_2 B$$

and the integrated forms of the equations are:

$$A = A_0 e^{-k_1 t}$$

$$B = \frac{A_0 k_1}{k_2 k_1} (e^{-k_1 t} - e^{-k_2 t})$$

$$C = A_0 \left[1 + \frac{1}{k_1 - k_2} (k_2 e^{-k_1 t} - k_1 e^{-k_2 t}) \right]$$

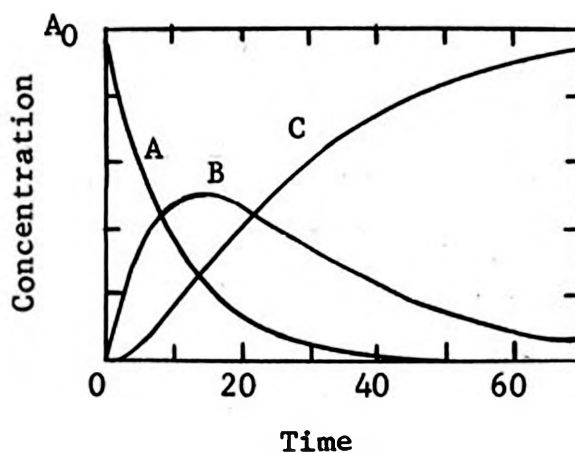
There is very good evidence that the pyrolysis of oil, shale kerogen is a series reaction of this type. The values of k_1 and k_2 have been determined by assuming that either k_1 or k_2 is negligible or in the steady state and then solving for the other.

A more correct approach would be to use the differential or integral forms of the equations shown above and also make use of the

experimental concentration curves for A, B, and C.

The analog computer could be used to solve the problem in the following manner. The three differentials would be used to set up the correct computer circuit using an integrating circuit in each case. Values for k_1 and k_2 and the time would be chosen arbitrarily and fed into the integrators. The resultant voltage from the integrators would correspond to A, B, and C for the time chosen.

The experimental curves for concentrations of A, B, and C for oil shale pyrolysis are:



The three experimental curves for A, B, and C are placed on an oscilloscope screen and the calculated curves for A, B, and C placed over them. The values of k_1 and k_2 are then changed in the necessary direction until the calculated and observed curves overlap perfectly or as closely as possible.

As mentioned above the approach in the past has been to assume that either k_1 or k_2 was in the steady state and solve for the other. Based on these studies it is to be expected that k_1 and k_2 are of nearly the same order of magnitude, with k_1 being slightly larger.

The numerical analysis of the equations above should strengthen or refute these conclusions.

6. In the last decade a process has been developed whereby powdered coal is hydrogenated at from 600 to 1000°C and 500 to 6000 psig. The retention time above 350°C for the sample is from one to ten minutes. After this heating cycle the material is quenched as rapidly as possible. About 90 percent of the moisture and ash-free material is converted to liquid and gas. Of that amount from 30 to 60 percent is light liquid hydrocarbons (benzene, toluene, xylene, naphthalene, etc.) and 32 to 40 percent is gas (mainly methane).⁽⁸⁾

In conventional coal hydrogenation processes in which the sample is held in the hot zone for an hour or longer a very heavy oil usually results due to the extensive polymerization of the volatile matter driven from the coal. As compared to the light oil above, this heavy oil is in lower yields, is harder to separate from the coke, and must be further treated to make it suitable for most uses.

It would be interesting to perform a series of tests of the nature described above but substituting powdered oil shale as the sample. This might lead to increased yields of light oil as experienced with coal. Because the shale oil from conventional oil shale retorts is primarily paraffinic it would be expected that the light paraffins would be optimized.

7. Studies made by Jones and Dickert⁽⁴⁾ suggested that there is a significant amount of organic-inorganic bonding present in oil shale. It was concluded that this was in the form of bonding of acid groups in the kerogen to the inorganic materials in the shale.

It should be determined to what extent this bonding effects the kinetics of decomposition of oil shale kerogen. This could be done by acid leaching a portion of the oil shale to free the inorganic carbonates.

The kinetics and mechanisms of decomposition of the free kerogen could then be compared to those of the intact oil shale. The early evolution of CO_2 and H_2S marks the initial rearrangement of kerogen to form bitumen. It would be expected that the heat treatment of the free kerogen should be accompanied by an earlier evolution of the carbon dioxide or at least its appearance in higher concentrations than with the untreated oil shale.

Because the decomposition of kerogen to product oil involves primarily the removal of unstable paraffinic side chains and naphthenic groups the acid treatment of the oil shale would not be expected to effect the kinetics of decomposition to any marked degree.

8. McIntosh⁽⁵⁾ sealed powdered coal in glass tubes with various hydrocarbon and non-hydrocarbon gases. He then irradiated the tubes with a high intensity light and ran mass spectrographic analyses of the gaseous products in the tubes. He observed that the presence of heavy hydrocarbon gases such as isobutane and butene-1 resulted in an increase in total gas remaining in the tube after flashing and also

a heavier average molecular weight of the gas. Product gases as large as C_7 were detected. He suggested that possibly the atmospheric gas used was thermally decomposed and polymerized with free radicals or reactive gases from the coal. O_2 and SO_2 when used as atmospheres gave no hydrocarbon gases as products but CO_2 did.

It should be determined if there are interactions between the atmosphere and the powdered coal in the above system. This could effectively be accomplished by using radioactively labeled tracer gases as the atmospheres. All the gases used by McIntosh are available in quite high levels of activity which would be necessary for such an experiment. The tagged gases would be sealed in the glass tubes with the coal and flashed as before but in this case the tubes could be connected to a pusher gas and a flow through gas counter. The loss in activity of the gas atmospheres would be determined prior to their mass spectrographic analyses. The powdered coal would also be examined to determine the amount of activity it had picked up in the process.

9. There is some question as to whether the formation of oil, gas, and coke from the bitumen is primarily decomposition of the bitumen or primarily a simple distillation of the bitumen.

By impregnating the residue from an oil shale decomposition with the product oil collected this question can partially be resolved. By following the thermal decomposition of the original oil shale as compared to the oil treated residue the similarity of the kinetics of decomposition of the two can be determined.

A simple distillation model should give essentially the same kinetic results as the treated residue while a thermal decomposition model should show kinetics differing from those of the treated residue.

10. It has been shown that when diphenyl triketone rearranges in the presence of acids, bases, copper acetate, and aluminum chloride the products are benzil, carbon monoxide, and carbon dioxide. Intermediate products can be expected in some cases. It has been shown further that the decarbonylation takes place at the center carbonyl group. (1,6,7)

It is also known that sunlight promotes the rearrangement but it is not known if the center carbonyl is lost during the radiation of diphenyl triketone. This can be determined by building diphenyl triketone tagged with C^{14} in the side carbonyl position. If the center carbonyl is lost as expected the activity should remain with the benzil.

RESEARCH PROPOSAL REFERENCES

1. Calvin, J., and Lemmon, R. M., "The Decarbonylation of Ethyl Pyruvate," J. Am. Chem. Soc., 69, 1232, 1947.
2. Cane, R. F., "The Mechanism of Pyrolysis of Torbanite," Oil Shale and Cannel Coal, Vol. 2, The Institute of Petroleum, 1950.
3. Frost, A. A., and Pearson, R. G., Kinetics and Mechanism, Wiley and Sons, Inc., 166, 1953.
4. Jones, D. G., and Dickert, J. J., "Composition and Reactions of Oil Shale of the Green River Formation," Chem. Eng. Progr. Symp., Ser. 54, 61, 33, 1965.
5. McIntosh, M., "Flash Heating of Coal," Ph.D. Thesis, Department of Fuels Engineering, University of Utah, 1965.
6. Roberts, J. D., Smith, D. R., and Lee, C. C., "The Decarbonylation of Diphenyl Triketone," J. Am. Chem. Soc., 73, 618-25, 1951.
7. Schonberg, A., and Mustafa, A., "Photochemical Reactions in Sunlight. Part XII. Reactions with Phenanthraquinone, 9-Arylxanthenes, and Diphenyl Triketone," J. Chem. Soc., 997, 1947.
8. Schroeder, W. C., "Hydrogenation of Coal," United States Patent Number 3,030,297, April 17, 1962.